SPATIAL VARIATIONS OF SEAFLOOR IRON CYCLE IN CILICIAN BASIN (EASTERN MEDITERRANEAN)

A THESIS SUBMITTED TO

THE GRADUATE SCHOOL OF MARINE SCIENCES

OF

MIDDLE EAST TECHNICAL UNIVERSITY

BY

ESRA ERMİŞ

IN PARTIAL FULFILLMENT OF THE REQUIREMENTS

FOR

THE DEGREE OF MASTER OF SCIENCE

IN

OCEANOGRAPHY DEPARTMENT

JANUARY 2017

SPATIAL VARIATIONS OF SEAFLOOR IRON CYCLE IN CILICIAN BASIN (EASTERN MEDITERRANEAN)

submitted by **ESRA ERMİŞ** in partial fulfillment of the requirements for the degree of **Master of Science in Oceanography Department, Middle East Technical University** by,

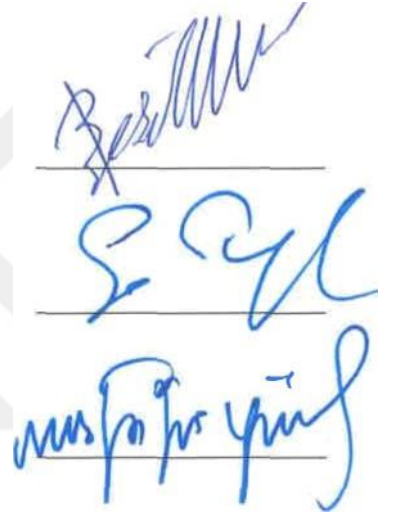Associate Prof. Dr. Barış Salihoğlu

Director, **Graduate School of Marine Sciences**

Prof. Dr. Süleyman Tuğrul

Head of Department, **Oceanography**

Assistant Prof. Dr. Mustafa Yücel

Supervisor, **Graduate School of Marine Sciences**

Examining Committee Members:

Assistant Prof. Dr. Mustafa Yücel

Supervisor, Graduate School of Marine Sciences, METU

Prof. Dr. Namık Çağatay

Faculty of Mines, Istanbul Technical University

Assistant Prof. Dr. Mustafa Koçak

Graduate School of Marine Sciences, METU

Date: 30.01.2017

I hereby declare that all information in this document has been obtained and presented in accordance with academic rules and ethical conduct. I also declare that, as required by these rules and conduct, I have fully cited and referenced all material and results that are not original to this work.

ERMİŞ ESRA

ABSTRACT

SPATIAL VARIATIONS OF SEAFLOOR IRON CYCLE IN CILICIAN BASIN (EASTERN MEDITERRANEAN)

ERMİŞ, Esra

M.Sc., Department of Oceanography

Supervisor: Assistant Prof. Dr. Mustafa YÜCEL

Middle East Technical University

January 2017, 104 PAGES

The biogeochemical cycling of iron (Fe) can play a potentially important role in the oligotrophic Mediterranean Sea. This importance stems from: (i) iron is an essential micronutrient for the new production, and (ii) it is associated with other essential redox-sensitive elements including carbon, nitrogen, oxygen and trace metals. Organic carbon burial in seafloor promotes the formation of gradients of iron and manganese species due to their role as electron acceptor for microbial respiration. The fraction of Fe and Mn species that is readily available for microbes is referred as reactive Fe and Mn, which comprise various labile forms of oxyhyroxides that could be extracted by a citrate-buffered dithionite solution. This thesis reports the first geochemical distribution of reactive iron and manganese, accompanied by other total metal distributions and their reactive-total partitioning in 25 surface sediment samples taken from four transects in Mersin Bay from Seyhan River to the Aydıncık. The coastal samples are taken from 10-100 m depth of a transect affected mainly by Seyhan and Berdan rivers in the Mersin Bay, and two transects along Göksu River. The deep-seafloor samples are obtained from a depth between 100-500 m in two transects offshore Erdemli and Göksu. The reactive iron in Cilician basin surface sediments is diversely distributed. Reactive iron enrichment decreases with depth whereas Mn enrichment significantly increases towards the open sea. Fe_R has significant correlation with organic carbon in Aydıncık transect. There is significant positive

correlation between organic carbon and % mud fraction in Aydıncık transect. Each transect differs in biogeochemical properties of seawater and seafloor. The spatial biogeochemical gradient from coastal to deep seafloor could be seen more clear in Aydıncık and Göksu transects, hinting at coast to offshore transport of riverine reactive iron and manganese.

Key words: seafloor iron biogeochemistry, reactive iron, reactive manganese, organic carbon, trace metals, Cilician Basin, seafloor microbial activity.

ÖZ

KİLİKYA BASENİ'NDE (DOĞU AKDENİZ) BENTİK JEOKİMYASAL DEMİR DÖNGÜSÜ

ERMİŞ, Esra

Yüksek Lisans Tezi, Oşinografi Anabilim Dalı

Tez Danışmanı: Yard. Doç. Dr. Mustafa YÜCEL

Orta Doğu Teknik Üniversitesi

Ocak 2017,104 SAYFA

Demir (Fe) biyojeokimyasal döngüsü oligotrofik Doğu Akdeniz'de önemli rollere sahip olabilmektedir. Bu önemin nedenleri (i) demirin yeni üretim için temel bir mikro besin tuzu olması, ve (ii) Deniz sistemi için gerekli olan oksijen, nitrojen ve iz metaller gibi redoksa duyarlı temel elementlerle bağlantısıdır. Deniz tabanında mikrobial solunumda elektron kaynağı olarak görev alan demir ve mangan bileşiklerinin gradyan oluşumu organik karbon akümülasyonu tarafından yönlendirilmektedir. Organizma tarafından kullanılabilen reaktif Fe ve Mn olarak da adlandırılan, sitrat-dithionite tampon çözeltisi tarafından extracte edilebilen bu fraksiyon oksik çevrede oksihidroksit formları şeklinde bulunmaktadır. Bu tez, Mersin Körfezi'nin Seyhan Nehri ile Aydıncık arasında 4 ana transekten toplanan 25 yüzey sediman örneklerinde reaktif demir ve mangan biyojeokimyasal dağılımın, diğer iz metallerle olan ilişkisi ve reaktif-toplam metal dağılımını ilk kaydını oluşturmaktadır. Kıyı örnekleri 10-100m derinlik aralığından toplanmış olup transeklerden birisi Seyhan ve Berdan nehirlerinden, diğer ikisi ise Göksu nehri açıklarından alınmıştır. Derin deniz örnekleri ise 100-500m derinlik aralığında Erdemli ve Göksu açıklarından toplanmıştır. Kilikya Baseni yüzey sedimanında reaktif

demir farklı dağılımlar göstermektedir. Reaktif demir zenginleşmesi derinlikle azalırken, Mn zenginleşmesi açığa doğru artmaktadır. Fe_R ve organik karbon Aydıncık transektinde önemli pozitif korelasyon göstermektedir. Aydıncık transekti organik karbon ve çamur tane boyu arasında dikkate değer bir korelasyon görülmektedir. Her bir transekt kendine özgü deniz suyu ve deniz tabanı biyojeokimyasal özellikleri göstermektedir. Kıyıdan açık denize doğru nehir-orijinli reaktif demir ve mangan taşınmasını ima eden, kıyıdan açık denize doğru biyojeokimyasal geçiş Aydıncık ve Göksu transektlerinde daha net bir şekilde gözlemlenebilmektedir.

Key words: deniz tabanı demir biyojeokimyası, reaktif demir, reaktif mangan, organic karbon, iz metaller, Kilikya Baseni, deniz tabanı mikrobiyal aktivitesi.

'Gökyüzüdür zarı beynimizin, kuşlar bulutlar dolanır içinde.' M. C. Anday

ACKNOWLEDGEMENTS

TABLE OF CONTENTS

LIST OF TABLES

LIST OF FIGURES

CHAPTER I

INTRODUCTION

Iron is one of the most important micronutrients with a diverse biogeochemistry in the marine environment. The biogeochemical cycling of iron has great influence on marine ecosystems both in the water column as well as sediments (Achterberg, 2001). Iron's vitality stems from being a limiting nutrient for new production in euphotic zones, taking part in electron transfer reactions via rapidly changing redox state and having the capacity to closely couple with the biogeochemical cycling of redox-related carbon, sulfur, nitrogen, phosphorous and other trace metals (Hyacinthe, 2006). Occurring in two valence states as oxidized ferric iron, Fe(III), and reduced ferrous iron, Fe(II), iron plays a key role in redox reactions both in water column and sediment with biotic and abiotic activities. Two main roles in biological processes are the uptake of iron as a prerequisite for cell growth (assimilation) by organisms such as phytoplankton, and providing energy from reduction of iron(III) to maintain heterotrophic metabolic activities of cells (dissimilation). (Haese, 2006). Further, changes in thermodynamic and kinetic conditions and reactions shape the oxidation state of iron. The results of those reactions and conditions causes precipitation or dissolution of iron-bound minerals and other essential redox-sensitive elements such as carbon, phosphorous and trace metals (Slomp, 2013). Apart from roles in biological and abiotic processes, the amount and type of these minerals in sediments supports the microbial communities and iron-derived reaction pathways (Schmidt, 2010).

The overall objective of this thesis is to understand the distribution of the most important and biogeochemically active fraction of iron in marine sediments, so called 'reactive iron', in the Cilician basin seafloor. The findings of this thesis will shed light on the early diagenetic pathways and coast-to-open water transport of iron and manganese phases which directly influence the carbon cycle in the region. Below, I first introduce various

aspects of iron biogeochemical cycles, and the oceanography of the study sites, and then continue with presenting my methodology and results.

1. IRON IN MARINE ECOSYSTEM

Despite being one of the most abundant elements in the Earth's crust, dissolved iron is present in sub-nanomolar levels (very low, trace) in the oceans (Achterberg et al, 2001; Scholz et al, 2014). The sources iron in marine ecosystem is atmospheric deposition, river, and hydrothermal vents (Martin and Fitzwater, 1988, Martin et al., 1990, Yucel et al., 2011). The speciation of iron in marine ecosystem varies in size, chemistry, and reactivity as well as the possible sources and depositional conditions even in existing in trace levels. These low levels however do not minimize the role of iron biogeochemical cycle that leads the keystone processes of entire marine ecosystem (Johnson, 1997; Maldonado, 2001; Liu, 2002). The shelf to basin shuttle of iron influence its fate as in reactivity, concentration, mobilization and transportation and bioavailability for organisms for both as a micronutrient and electron source for survival (Figure 1.1).

Despite decades of studies, seafloor of iron biogeochemistry is poorly defined especially at regional scales and at the intersection of land-ocean and sediment-water boundaries.
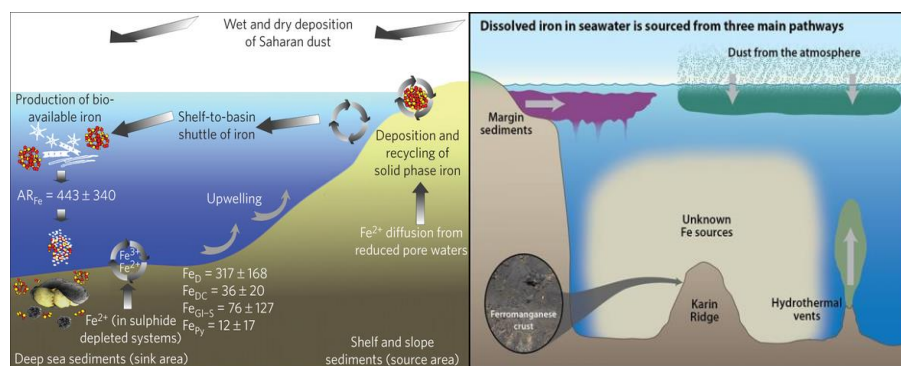
Figure 2.1. Iron sources in shelf and slope sediments(left,Boyd and Elwood, 2010) and open seawater;right;Baldermann et al.,2015)

The most recent studies investigate speciation, size fractionation and isotope fractionation of iron even in low concentration levels in seawater and sediments with the state of the art methods and technology to understand global oceanic processes, past and future predictions of climate events (Clough et al., 2016; Kleint et al., 2016, Raiswell et al., 2016, Fitzsimmons et al., 2016). In Figure 1.2, iron inputs and bioavailability is
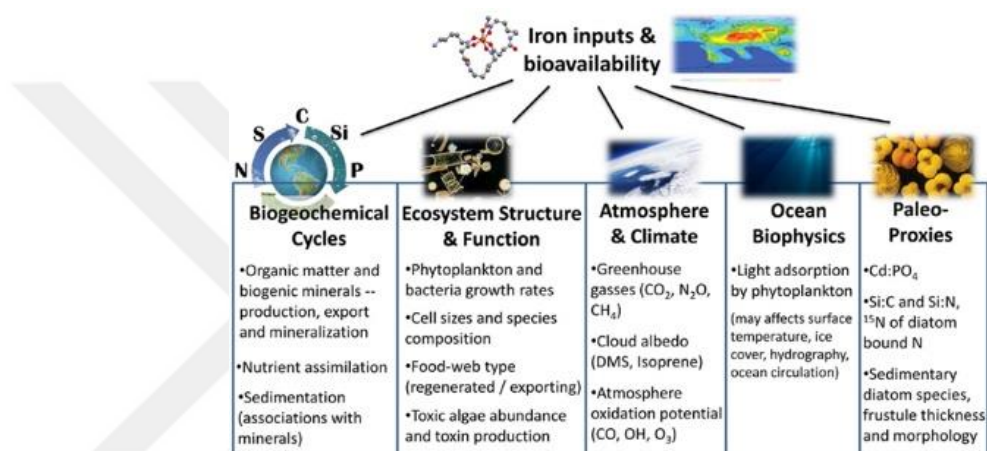
Figure 1.2. Iron inputs and bioavailability from Shaked and Lis, 2012.

summarized retrieved from Shaked and Lis 2012.

Iron minerals enter the sea via atmospheric deposition, rivers and hydrothermal vents, as in particulate Fe(III), colloidal, organically complexed, or particulate Fe(II) forms (such as pyrite) (Yücel, 2011, Gartman et al., 2014). Each source shapes the fate of iron particle in seawater and accumulation in sediments with iron-associated particles. Thus, the environmental conditions impinged on its speciation is a hot topic to shed light on the iron biogeochemistry in seawater. Iron speciation based on size fractionation is defined as particulate form (>0.45 µm), colloidal (0.45-0.02 µm) and soluble (<0.02 µm). In each size fraction iron exist in a diversity of forms such as Fe-oxyhydroxides, organic ligand bound-Fe, Fe(II) or Fe(III) oxidation state for both biota and detritus with inter-transition in those forms driven by external conditions (i.e. light, oxygen). The colloidal or truly dissolved fraction of iron in marine environment has complex composition, reactivity,

behavior and effect on the new production. The size and isotopic fractionation of iron to link the its origin in marine environment is still a mystery (Toner et al., 2016). To illustrate, partitioning between colloidal iron and the smaller soluble Fe size fraction is found to show a significant variability in the surface ocean caused by the number of factors affecting size fractionation (e.g., Fe sources, ligand controls, thermodynamic controls, biological utilization) claiming that seasonal component (e.g., seasonal biological growth, seasonal changes in Fe supply) causes a proportion of the observed surface ocean variability. Apart from the crucial roles in new production, the iron bound in seafloor sediments is important due to its role as an electron source for microbial respiration aroused from its reactivity. The size, particle chemistry, and morphology are crucial to assess whether particles are reactive with dissolved constituents, provide substrates for respiration and growth, and are delivered to marine sediments or dispersed by deep-ocean currents. Thus, iron mobilization from the shelf to open seafloor, its link with vital organic matter, phosphorus, sulfur cycles, its effects of continental sources on seafloor needs to be investigated for further future estimations of these crucial cycles for both ocean and global cycles.

New knowledge of iron cycle could also help fighting global warming. Natural iron fertilization triggers increase in new production via extra-intracellular activities in euphotic zone, therefore, a decrease in atmospheric CO_2 emitted by ocean, in other words carbon sequestration, is observed. To find the solution of anthropogenic CO_2 increase, the iron fertilization experiments in ocean were performed in the last decade, both natural and artificial fertilization in distinct parts of ocean (Breitbart E., 2010). In this manner, the continental margins were found to be a key source of Fe (Elrod, 2004; Breitbart E., 2010). For example, in the high nutrient low chlorophyll (HNLC) North Pacific Ocean, the continental margin was a source of Fe via winter mixing making lateral source of Fe available for organisms and Fe can be transported over 900 km (Lam, 2008).

Besides being a limiting nutrient and playing a key role for new production, seafloor iron shuttle across benthic redox zones has further significance in addition to fueling primary production. The iron and manganese rich shelf sediments may also enhance organic carbon (OC) preservation (e.g., Kaiser and Guggenberger, 2000; Poulton and Raiswell, 2005; Lalonde et al., 2012, Roy et al., 2013, Homoky et al., 2013). The mechanistic perspective

4

offered by Lalonde et al. (2012) was that co-precipitation, or chelation between organic carbon and iron, or both of these processes form macromolecular domains of complexes that can be resistant to dissolution (Slomp, 2013). These authors estimated that about 22% of global sedimentary OC could be preserved by reactive Fe phases (Lalonde et al., 2012). Thus, the iron minerals gain importance in terms of their chemical and physical properties such as particulate forms, residence time, accumulation through sediment, reactivity, solubility, bioavailability, adsorption of elements on their surface. These properties affect the fate of essential redox sensitive elements especially in redox fronts either in sediments or water columns.

1.1 Reactivity of iron compounds and their bioavailability in marine sediments

Iron is present in seawater and seafloor as two oxidation states: Fe(II) and Fe(III). Fe(II) is referred as relatively bioavailable and soluble form. It is produced naturally in chemically reducing conditions. Fe(III) is the major form stable in oxic conditions and tends to precipitate as particles. Iron is mainly present in marine environment as iron oxides forms that vary in reactivity (Sunda and Huntsman, 1995). The chemistry and minerology of iron oxyhydroxides in sediment, therefore, is a main determinant for their further utilization in the environment.

Fe(III) in seawater and sediment environment tends to be in particulate form and accumulate mostly as ferric hydroxides (Murray, 1979), Fe-bound alumino-silicates (Raiswell and Canfield, 1998), and ferric phosphate phases (Hyacinthe and Van Cappellen, 2006). Particulate iron in sediments is generally determined by chemical extraction techniques that target phases that may differ in speciation and reactivity (Canfield, 1988; Slomp et al., 1996).

Poulton and Raiswell (2002) defines that a highly reactive iron fraction is the fraction of iron dissolvable by a citrate–dithionite extraction (Kostka and Luther (1994), Raiswell et al., 1994; Poulton and Canfield, 2005). This technique formed the basis of this thesis work. All the main iron oxy(hyrd)oxides (ferrihydrite, goethite, lepidocrocite and hematite)

referred as reactive iron are quantified by this technique with little effects on iron-bound silicates and magnetite. The reactivity of various iron minerals towards dissolved sulfide are given in Table 1.1.

Table 1.1. Reactivity of iron minerals towards sulfide (pH 7.5, 25°C) according to 1: Poulton et al. (2004), 2: Canfield et al. (1992), and 3: Raiswell and Canfield (1996). The 'poorly-reactive silicate fraction' was determined operationally as (FeHCl boiling - FeDithionite) / Fetotal (Achterberg et al.,2001, Shulz and Zabel,2016).

Iron mineral / Fraction	Half Life, $t_{1/2}$
Hydrous Ferric Oxide[1]	5 min
2-Line Ferrihydrite[1]	12.3 hours
Lepidocrocite[1]	10.9 hours
Goethite[1]	63 days
Magnetitie[1]	72 days
Hematite[1]	182 years
Sheet Silicate[2]	10 000 years
Poorly-reactive silicate fraction[3]	2.4×10^6 years

The reactivity of iron minerals in Table 1.1 shows half life of minerals towards sulfide. Under reducing conditions, in the presence of excess sulfate, hydrogen sulfide and pyrite (FeS_2) iron sulfides (amorphous and crystalline forms such as mackinawite) are formed. Regarding this, highly reactive iron is defined as the sum of extracted iron by citrate-dithionite plus that present as iron sulfides (Poulton and Raiswell, 2005). Pyrite (FeS_2), on the other hand, is a stable end product of iron-sulfide geochemical reactions which is not extractable by citrate-dithionite leach. Therefore pyrite-iron is not a part of the reactive iron pool in sediments.

Reactivity of iron mostly depends on the surficial reactions occurred at the interface of
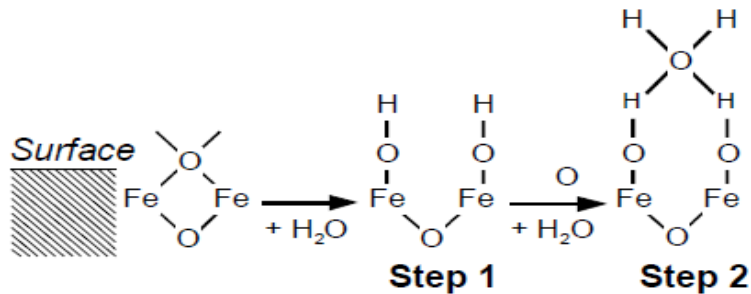
Figure 1.3. In the presence of water the iron oxide surface is hydroxylated (step 1) and followed by H_2O adsorbed (Step 2) (Shulz and Zabel, 2016, redrawn from Schwertmann and Taylor 1989.)

transport regime and the marine environment. In oxic waters surface of iron oxide is hydroxylated and subsequently H_2O is adsorbed (Shulz and Zabel, 2016). The iron oxide has a very high affinity for adsorption of anions and also cations under natural conditions especially for the adsorption of trace metals, phosphorus and organic acids. The reactions involve either protonation or deprotonation depending upon pH of the environment. In the presence of excess anion or cation such as trace metals, anions or organic ligands the adsorption onto iron oxides balances the negatively or positively charged surfaces. The examples of these reactions are shown as below;

$S\text{-}OH + H^+ \Leftrightarrow S\text{-}OH_2^+$ (Eqn. 1)

$S\text{-}OH + OH^- \Leftrightarrow S\text{-}O^- + H_2O$ (Eqn. 2)

7

$$-\text{S-OH} \quad +\text{C}_2\text{O}_4^- \quad \Longleftrightarrow \quad \begin{array}{c} -\text{S-O-C=O}^- \\ | \quad\quad | \\ -\text{S-O-C=O}^- \end{array} \quad + \text{H}_2\text{O}$$
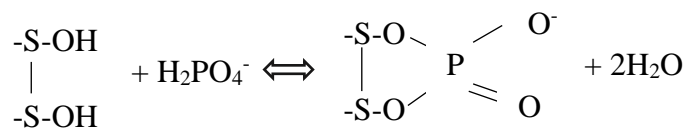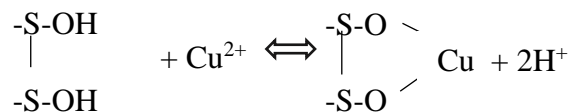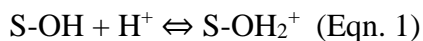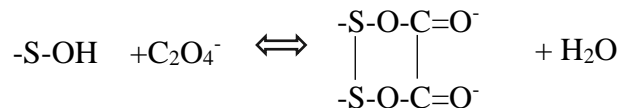
Figure 1.4. The equations of surface adsoption of cation, anion and organic compounds (Retrieved from Shulz and Zabel, 2016).

1.2 Redox reactions of Iron compounds in thermodynamic ladder

Biogeochemical processes in global sedimentary cycle are key controllers of the Earth's surface and climate in geological timescales (Aller, 2006, ref. therein). These processes shape the fate of organic material arriving at the seafloor and the dynamic interactions of deposits and buildup with overlying water and the atmosphere. The seafloor environment is led by a broad range of reactions, such as precipitation, dissolution, redox reactions, recrystallization and biogenic processes. Since the life processes entails far-from-equilibrium conditions, biology drives rapid reactions in thermodynamically unstable conditions. That is called early diagenesis which is the combination of physical, chemical and biological processes changing the composition and abundance of organic matter in the upper part of marine sediments. Henrichs (1987) stated that between 30% to 99% of the organic matter accumulated in the sediment is remineralized by organisms.

As the seafloor environment acts as open systems, in other words strongly tied with the overlying water and the marine ecosystem, its behavior impacts the bounded marine environment in short and long term scales. These impacts are observed relatively obvious in shallow waters due to release of regenerated nutrients for new production for phytoplankton (Aller, 2006). However, the impacts of these multi-elemental cycles in diverse seafloor types through global ocean and atmosphere is a challenge and still being quantified for the accurate global budget estimations, biogeochemical models (Scholz,2014, Aller, 2006, Liu et al., 2015, Severmann et al., 2010).

Fe speciation and its bioavailability depends on its governing factors and mediators. Figure 1.5 is a simplified diagram of reactions for distinct iron species (retrieved from Shaked and Lis, 2012) that shows the reactions and mediators of redox reactions. Iron in dissolved organic, inorganic and colloidal/particulate forms are selected by environmental
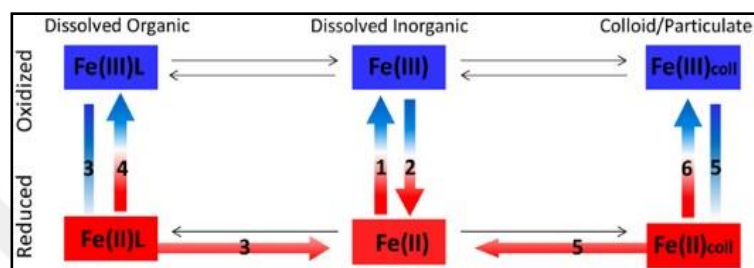
Mediators and governing factors	Effects on speciation and bioavailability	References
1. Fe(II)' OXIDATION		
• O_2, O_2^-, H_2O_2 • Regulated by pH, temp, salinity	• Fe(III) formation and subsequent hydrolysis and precipitation, decreases bioavailability	a–c
2. Fe(III)' REDUCTION		
• Enzymatic– phytoplankton (assimilatory) & bacteria (dissimilatory – low oxygen) • Direct photolysis or reduction by photo-produced reactive transients • O_2^- (photochemical/biological origin) • Humic and fulvic acids	• Elevated [Fe(II)s.s] and maintenance of active redox cycle, both of which slow down Fe(III) hydrolysis and precipitation • Availability is enhanced when [Fe'] increases (as Fe(III) and Fe(II) are equally bioavailable)	d–g
3. Fe(III)L REDUCTION AND DISSOCIATION		
• Enzymatic (as above) • Photochemical (as above) • Superoxide (as above)	• Weaker ligand binding to Fe(II) (compared to Fe(III)L) may favor dissociation of free Fe(II) and increase in [Fe'] and bioavailability • If Fe(II) remains complexed – its oxidation may be stalled/accelerated compared to Fe(II). Bioavailability of Fe(II)L – unknown	h–i
4. Fe(II)L OXIDATION		
• O_2, O_2^-, H_2O_2 • Ligands (L)– some stabilize the complex as Fe(II)L, some accelerate its oxidation	• Rates are slower/faster than Fe(II) oxidation resulting in elevated/lowered [Fe(II)Ls.s] • Bioavailability of Fe(II)L – unknown	j–k
5. REDUCTIVE DISSOLUTION OF SOLID PHASE IRON		
• Bacterial dissimilatory reduction in aggregates • Ingested colloids (zooplankton) • Direct photolysis and light enhanced siderophore mediated dissolution	• Elevated [Fe'] due to increased Fe(II) flux • Elevated FeL (when ligands are at play) • Dissolution enhances bioavailability as solid phase iron is largely inaccessible	l–m
6. OXIDATION OF SURFACE ADSORBED Fe(II)		
• O_2 and mineral surfaces (O_2 oxidizes surface bound Fe(II) much faster than dissolved Fe(II))	• If oxidation precedes detachment of Fe(II): decreased flux of Fe(II) • Following oxidation, the newly precipitated Fe is more reactive than the original mineral	n

[Fe(II)s.s] , steady state Fe(II) concentrations.
References: a. Santana-Casiano et al. (2005), b. Gonzalez-Davila et al. (2005), c. King et al. (1995), d. Shaked et al. (2002), e. Kustka et al. (2005), f. Voelker and Sedlak (1995), g. Miller et al. (1995), h. Barbeau et al. (2001), i. Rijkenberg et al. (2006), j. Rose and Waite (2002), k. Rose and Waite (2003), l. Balzano et al. (2009), m. Barbeau et al. (1996), n. Stumm and Sulzberger (1992).

Figure 1.5. Redox reactions of various Fe species; the major factors and their effects on speciation and bioavailability (Retrieved from Shaked and Lis, 2012).

conditions; such as redox potential. Figure 1.5 summarizes the leading factors and effects on iron speciation; each form could be transferred into other form and oxidation state via photosynthetic activities, physical and kinetic conditions and microbial activity. Dissolved reduced inorganic iron decreases its bioavailability with oxidation. The particulate and colloidal forms appear in bacterial dissimilatory reactions and adsorption of ligands, trace metals, organic matter onto dissolved mineral surfaces to final precipitate in colloidal form. However, the reactivity and distribution of iron in seafloor, how the iron species transport in seafloor, in what degree it is bound to organic carbon, sediment type and conditions is little known specifically in terms of inter-linked organic matter degradation, nitrate, sulfur, phosphorus traps, and microbial pathways.

The seafloor environment varies in diagenetic processes and cycles due to diverse depositional conditions and biology. Diagenetic processes mainly effect the availability of sedimentary reactants, products and their deposition conditions with depth due to close relationship between organisms and lithogenic fractions. In this manner, one of the main drivers of early diagenesis is organic matter burial. Figure 1.6 shows the major type of diagenetic organic matter cycle in vertical cross section. Deposition of reactive organic matter is followed by decomposition and oxidation by organisms. The consumption of organic substrate depends on reactivity and burial conditions of matter, biomass of organisms with time and depth resulted variations in amount and preservation of organic matter. Microorganisms and benthic community consumes organic matter for survival, hence, directly and indirectly influences the amount of available oxidants (O_2, NO_3^-, Mn oxides, Fe oxides, SO_4^{2-}, and CO_2) and authigenic minerals. Other importance comes from its impacts on the principal reaction variables pH, redox potential, the CO_2 cycle, coupling of recycling of nutrients to the overlying waters and the atmosphere (Shulz and Zabel, 2016).

The thermodynamic ladder, in other words the redox-controlled cascade of organic matter degradation pathways is a function of free energy gain for oxidation of organic matter. Organisms accepts terminal electrons for energy in order of O_2, NO_3^-, Mn oxides, Fe oxides, SO_4^{2-} and CO_2 from methanogenesis. The transition from oxic to anoxic
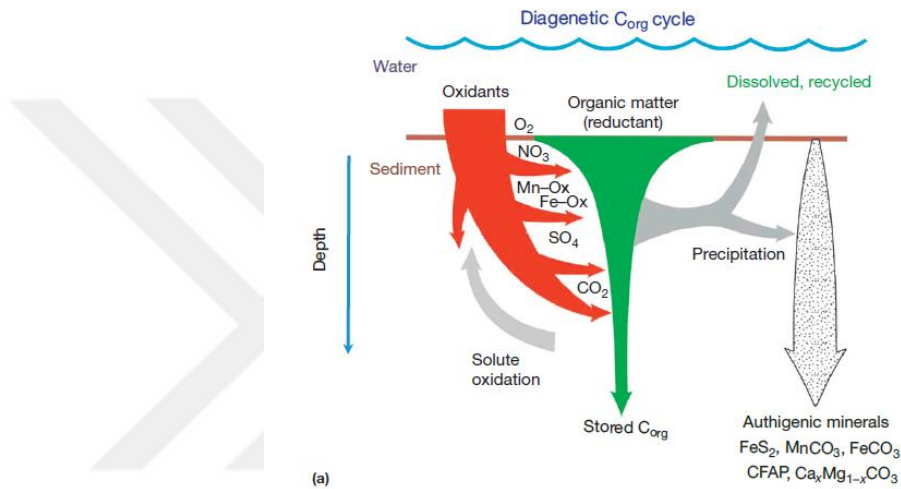
Figure 1.6. The organic matter burial drives redox zonation and mineral mobilization in seafloor.

conditions, called redox front, can vary in seafloor or water column. The redox state and diagenetic zonation in marine environment can be mm to meters in seafloor surface, subseafloor, or water column. The organic carbon accumulation rates, abundance of each oxidants and diversity, benthic organisms (bioturbation) control the redox zonation and the pathways. Pathways of organic matter degradation and reactions are showed in Figure 1.6. Towards methanogenesis available free energy decreases for organisms. Each pathway results in changes of chemical environment such as release of N_2, Mn^{2+}, Fe^{2+}, or H_2S. Manganese and iron reduction takes place among the remineralization of associated particulate minerals, therefore, impacts the fate of mineral-bound elements. The high organic matter accumulation drives the redox shuttle and release of its associated forms described in Figure 1.6. The redox zonation in distinct environment comes into

prominence as its association with carbon, sulfur and nitrogen and metal mobilization in seafloor. The abundance of these oxidants drives the respiration pathways and microbial communities. To illustrate, Mogollón et al. (2016) has investigated the suboxic sediments in three stations of Eastern Equatorial Pacific with low organic carbon content (<0.5 dry wt %) and low sedimentation rates (10^{-1}–100mm ky^{-1}) and were quantified using a reaction-transport model with reactions involving the Mn and N cycles. This and other studies focuses on the transportation and mobilization of iron and manganese cycles in seafloor. Another factor in early diagenesis is the type and origin of organic matter. Labile, i.e. easy to degrade organic matter includes small organic molecules (such as acetate, formate). Larger organic molecules may be more refractory to degradation. C/N ratio also plays a role: typically marine-origin organic matter has lower C/N ratios (rich in N) and is more labile whereas terrestrial organic matter has higher C/N ratios and typically more refractory.

It is found that microbial cultures can use all kind of iron oxides for the dissimilation with different rates and various degrees (Lovley 1991; Kostka and Nealson 1995). The reaction pathways of iron oxides for energy mainly depends on the lifetime, surface area and composition of the iron oxide. Reactive iron as defined by Koska and Luther (1994) is the bioavailable and preferred fraction of iron minerals for cells.

Another key controller of redox zonation is the sediment diagenetic regimes. Sedimentation processes can affect the redox reaction succession of oxidants. To illustrate, unsteady regimes, such as highly mobile surface of seafloor may not have vertical redox ladder likewise steady accumulation. Even in steady accumulation regimes may differ in redox reaction distribution shaped by grains size, organic matter burial, permeability, sediment bioturbation (Aller, 2006).

1.3 Influences on iron-bound essential elements: carbon, sulfur and phosphorus

Lifetime of iron oxides particulates designates the crystallinity which means order of crystal lattice. As the aging increases, highly reactive iron oxide fraction with distance to
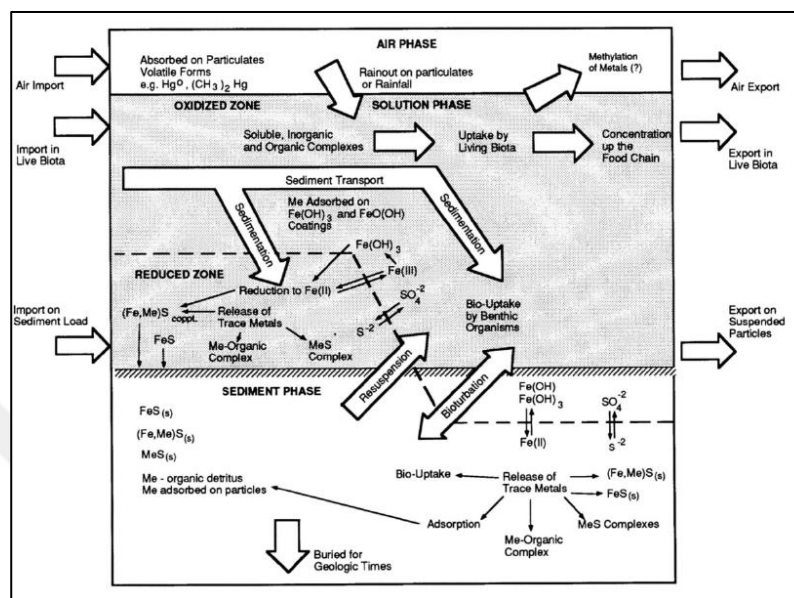
Figure 1.7. The metal biogeochemical cycles with important reactions and processes (after Nelson et al.,1977 retrieved from Shulz and Zabel,2016)

 coast and water depth decreases even though total iron oxides and concentration increases (Haese et al., 2000).

Extended roles of iron oxides as in Figure 1.7 stems from surface properties of iron oxides due to having high affinity for adsorption of cations, anions, organic compounds and phosphate, trace metals. Hydroxylation of mineral surface by these compounds, in other words adsorption onto the minerals causes the removal from environment and precipitation through the seafloor. Further, redox processes in seafloor induces the changes in particulate iron minerals forms, hence, adsorbed element concentration in the environment. As an example, reduction of Fe oxides in reducing conditions such as the presence of H_2S results in release of adsorbed material through upper zones and formation of pyrite (FeS_2).

Phosphate is a crucial micronutrient especially for P limited, oligotrophic marine environments such as Eastern Mediterranean. Particulate phosphorus is well studied in

such regions due to direct impact on organic matter production (Krom, 1980, Yılmaz and Tuğrul, 1998, Doğan-Sağlamtimur, 2007, Sert, 2010). The extraction techniques of P species to reveal P speciation in marine sediments is varied, however, the extraction schemes such as SEDEX (Ruttenberg, 1992) (in N_2 atmosphere) is common technique helps to fractionate exchangeable P, Fe-bound P, authenic Ca-P, organic and detrial Ca-P with extraction steps of different chemicals. The Fe-bound P gains importance from the final accumulation P species due to high adsorption capacity of iron oxides, therefore, Fe-bound P pool is reffered as a measure of total Fe-oxides in the sediments and to asses the role of amorphous Fe-oxides in oxic conditions for binding P in sediment (Slomp, 2013). Solid–phase Fe-bound P pool in sediment is increased through sulfate reduction front in sediment and this pool is assumed to be made up 33-45% of total P in the surface sediments and act as major burial sink for P (Slomp 2013). Adsorption and burial in seafloor is not

POC Degradation pathway	Reaction	ΔG° (kJ mol^{-1})
Oxygen reduction	$CH_2O + O_2 \rightarrow CO_2 + H_2O$	-479
Denitrification	$5CH_2O + 4NO_3^- \rightarrow 2N_2 + 4HCO_3^- + CO_2 + 3H_2O$	-453
Manganese reduction	$CH_2O + 3CO_2 + H_2O + 2MnO_2 \rightarrow 2Mn^{2+} + 4HCO_3^-$	-349
Iron reduction	$CH_2O + 7CO_2 + 4Fe(OH)_3 \rightarrow 4Fe^{2+} + 8HCO_3^- + 3H_2O$	-114
Sulfate reduction	$2CH_2O + SO_4^{-2} \rightarrow H_2S + 2HCO_3^-$	-77
Methanogenesis	$CH_3COO^- + H^+ \rightarrow CH_4 + CO_2$	-28

Figure 1.8. Organic matter degradation pathways (Yücel, 2015)

only process of Fe-P but also formation of Fe(II)-P phases in redox zones (such as sulfate methane transition zones) gains importance as its link to recent changes in environmental dynamics, possible upward shift of the redox zone. Therefore, it is studied in lake, eustuarine, near shore coastal; suboxic sediments (Slomp et al., 2013, Ruttenberg, 2003, Sivan et al., 2011).

One of the potential source of reactive Fe and Mn is continental shelf sediments due to river input from terrestrial environments (Johnson et al.,1992, Poulton and Raiswell, 2000, Elrod et al., 2004; Moore et al., 2004, Roy et al.,2013). The studies show that river-derived sediments are rich in reactive Fe (Poulton and Raiswell, 2005). Reactive Fe and Mn are contained in amorphous and poorly crystalline (and presumably Mn) metal hydroxides and oxides (Canfield, 1989; Poulton and Raiswell, 2002, Poulton and Canfield, 2005, Roy et al., 2013). River-derived sedimentary reactive Fe and Mn are accepted as micronutrient supply to the coastal ocean (e.g., Poulton and Raiswell, 2002; Severmann et al., 2010, Yucel, 2010) and also potential supply to the open ocean via transportation and mobilization.

The reactive iron in seafloor is claimed to be strongly interlinked with organic carbon with the findings of preservation of organic matter up to a global mass of $19\text{-}45\text{x}10^{15}$ grams of organic carbon (Lalonde et al., 2012). This relationship is studied so far to estimate the accurate budgets of carbon cycle since the global warming has reached up to drastic levels. Thus, the reactive iron in diverse seafloor environments such as oxic, coastal to open marine ecosystems, oxygen minimum zones and euxinic environments (Scholz, 2014, Roy et al, 2013, Shields et al., 2016, Lalonde et al., 2012). One of the major findings of OC-Fe association is that organic carbon and reactive Fe have significant correlation (Shields et al., 2016). These authors examined the role of reactive iron (Fe_R) in preserving organic carbon (OC) across Wax Lake Delta, a prograding delta within the Mississippi River Delta complex. They have found that ~15.0% of the OC was bound to Fe_R with the estimation of ~8% of the OC initially deposited in deltaic systems is bound to Fe_R (equivalent to 6×10^{12} gC yr^{-1}). This percentage increases post-depositionally, as coprecipitation of Fe_R and OC allows for an even greater amount of OC to be bound to Fe_R. Another study in coastal to open basin showed that reactive Fe enrichment (terrestrial Fe input to seafloor) decreases with depth in oxic waters and start to increase in oxygen minimum zones (OMZ). Below the OMZ, high lithogenic Fe enrichments are observed. Futher, grain size is also found to have significant correlation with reactive iron and organic carbon (Roy et al., 2013) in Oregon–California (USA) continental margin near the mouths of six small mountainous rivers. This work revealed that sediments are also enriched in Fe_R and Mn_R

with comparisons among grain size, Fe_R and Mn_R suggesting mud size suspended sediments be a carrier of the riverine reactive metals to the seabed. The deposition and mobilization of $OC:Fe_R$ suggests that these two components have a common source or a common processes that provides the mutual preservation. On the other hand, Mn_R is found to be least partially decoupled from $OC:Fe_R$ and grain size, that brings questions of diagenetic water column and sediment processes preferentially mobilizing the reactive Mn over Fe.

2. BIOGEOCHEMICAL DISTRUBUTION OF IRON IN CILICIAN BASIN

2.1 Cilician Basin

The Mediterranean Sea is a mid-latitude semi-enclosed basin and a nearly isolated oceanic system. It is connected to the Atlantic Ocean, the Red Sea and to the Black Sea via Turkish Straits. The Atlantic Ocean is the milestone of the general water mass circulation, also called global thermohaline circulation that includes the Atlantic, Indian, Pacific Oceans. The connection with the Atlantic Ocean makes Mediterranean Sea important to affect this
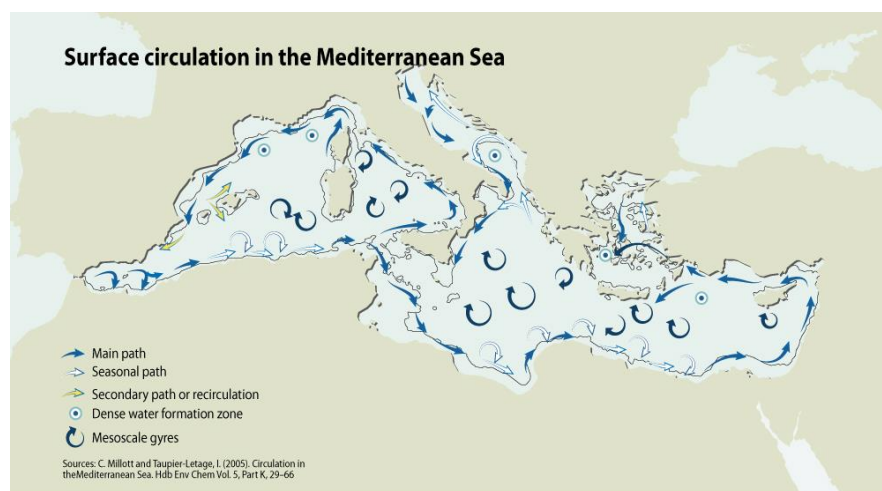
Figure 2.1. Surface Circulation of in the Mediterranean Sea(Millott, 2005)

circulation within its characteristic seawater properties.

The Mediterranean Sea has complex, integrated spatial scales; i) basin scale (or thermohaline) circulation, ii) the sub-basin scale circulation, and iii) the mesoscales (Pinardi et al., 2005 and references therein). These scales are driven from differences in topography, coastal influences, internal processes. Among the large scale circulation, dynamic sub-basin scale cyclonic and anticyclonic gyres and energetic mesoscale eddies influences the seawater of the whole basin. As the Figure 2.1 shows that coastal sites interact with the main path of the circulation so coastal environments could affect the whole Mediterranean Sea and even the Atlantic Ocean.

The main path of the water circulation is driven by less dense Atlantic water entering through Gibraltar and formation of intermediate and deep water formations. These water masses are Modified Atlantic with increase in salinity to the east, Levantine intermediate water (LIW) and Mediterranean Deep Water. Further, the Sicily Strait is a natural boundary which prevents mixing of western and eastern Mediterranean seawaters. The western and eastern seawaters differ in various properties such as temperature, salinity as well as the biology.
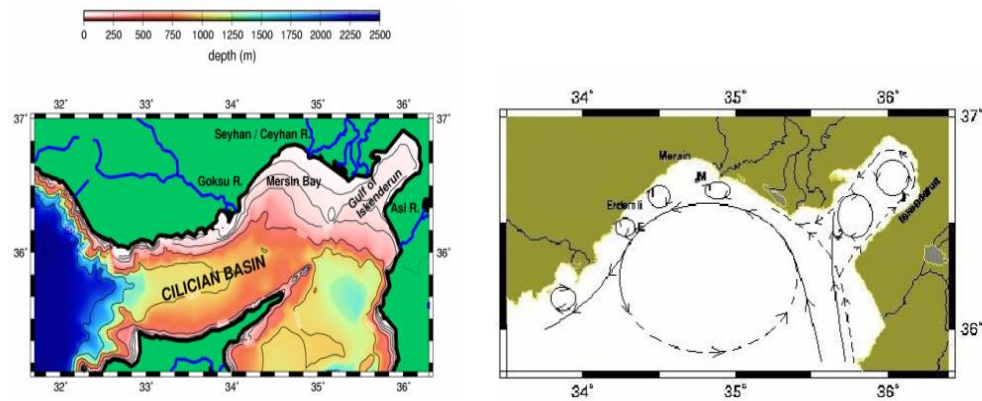
Figure 2.3. Cilician Basin depth profile and water circulation(Özsoy and Sözer, 2006, Collins and Banner, 1979)

Unlike the Western, the Eastern Mediterranean Sea is one of the utmost oligotrophic seas in the world (Figure 2.2). Nutrient rich Atlantic surface water losses its nutrients and becomes nutrient deficient to the east by phytoplankton growth in the surface of the
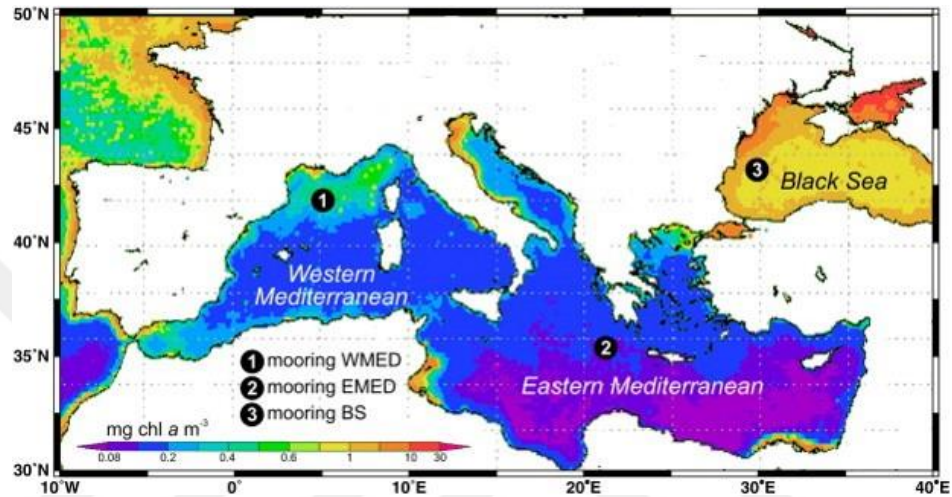
Figure 2.4. Chl-a concentration (mg m^{-3}) in surface waters Mediterranean Sea covering a complete annual cycle (from September 2007 to September 2008) and visualization has been produced with the Giovanni online data system, developed and maintained by the NASA GES DISC from Gogou et al., 2013.

Atlantic flow and complete its cycle and reaches to Atlantic again after hundred years (Krom et al., 199). Moreover, limited number of rivers, low precipitation, high temperature and evaporation makes other sources extremely valuable such as seafloor, too. For that reason, the surface sediment which is a sinks of major and limiting nutrients (Fe, N, P, trace metals) especially in shallow waters could lead the new production via release of these compounds.

In Cilician Basin, the mean currents show relatively simple pattern, the actual time-dependent currents in this region is complicated specifically in the coastal regions. The Cilician Basin is located in the Eastern Levantine with a depth range of approximately 0-1250 m. The shallower coastline mainly affected from Seyhan, Ceyhan, Göksu Rivers in

which local eddies observed with diverse seafloor types. The seafloor topography changes from east to west part with an increase in submarine canyons (Talas et al., 2015). The coastal lines affected from fresh water that carries organic matters, nutrients to the seawater so as to seafloor. Despite the river inputs, the open sea is still oligotrophic water framing seafloor deficient in organic matter for microbial communities as opposed to coastal area.

The chemical properties of Cilician Basin show similar vertical pattern in dissolved oxygen and salinity. Dissolved oxygen concentrations vary between 250 and 300 µM levels, for oxic waters with almost 100% saturation in the first 100 m depth. Deeper than 100m depth and below the euphotic zone dissolved oxygen tends to decrease until constant deep water concentrations of 180-200 µM. The cyclonic region has the 75-85m euphotic layer, up to 110-120 m in anticyclonic regions. According to depth and location, dissolved oxygen concentrations similar to density profiles show variations in deep water which imply the rapid horizontal movement of deep water without creating any significant regional characteristics (Yılmaz and Tuğrul, 1998; Ediger et al., 2007).

2.2 Iron in marine sediments of Cilician Basin

The reactive iron in river dominated to open shelf sediments has been studied in various marine environments (Yucel, 2010, Roy et al., 2013, Scholz et al., 2014, Shields et al., 2015, Salvado et al., 2015). The behavior of reactive Fe and Mn from river sediments is found to have different trends and correlations. To illustrate, Fe_R from suspended Umpqua river sediments is about 2 wt% whereas Fe_R from the depocenter is just a little higher than that value. The decrease in Mn_R from suspended sediments to depocenter is more than an order of magnitude. Based on these findings, authors claimed a depletion in terrestrially derived reactive Mn may be larger than for Fe. The reason for the higher depletion of Mn_R compared to Fe_R may resulted from the higher mobility of manganese compared to iron during remobilization from Fe–Mn-oxyhydroxides, which is a well-documented process in marine and riverine settings (Bruland, 2005, Shulz and Zabel,2016).

The reactive iron record in Cilician Basin will be the first record of the region. However, the abundance and distribution of Fe, Mn and other trace metals and heavy metals has been reported in the literature. The weight percent of Fe in shore sediments of Mersin Bay is 2.7% (Bodur, 1988), 3.79 in Mersin Harbour and 4.27 in shore sediments of Lamas, Mersin Bay (Ramelov et al., 1978), 3.61 in Cilician Basin (Shaw and Bush,1978).

The Cilician Basin coastal seafloor are composed of diverse sediment textures ranging from mud to gravelly mud. The grain size distribution pattern of the surface sediments is mainly shaped by the irregular bottom topography of the region and terrigeneous inputs carried by perennial rivers. The complex wave and current system as with local eddies and coastal filaments are also the factors controlling the grain size composition of the sediments. The surface sediments are predominantly characterized by their relatively high mud contents with varying silt and clay fractions. The total proportion of coarse-grained fractions(sand and gravel) accounts for less than 10% in most sediment. The wind-generated coastal filaments plays an important role in the general $CaCO_3$ distribution pattern of the Mersin Bay sediments with significant correlation of grain size fraction (Tunç and Yemenicioğlu, 2013). However, there is limited knowledge on geochemistry of open Cilician seafloor.

2.3 Aims of this study

Cilician Basin has specific ecological properties owing to relatively high productive coastal seafloor and very oligotrophic open seafloor. The mobilization and transportation of the particles generated in the coastal sites could therefore affect the open seawater. The reactive Fe and Mn transportation to open seafloor, therefore, is an important mechanism that needs to be investigated in the region. Key questions can be listed as:

a- Can the sedimentary reactive iron species reach environmentally significant concentrations?

b- Could we find fingerprints of Fe-derived microbial respiration in the seafloor of Cilician Basin seafloor?

c- Is there any evidence for cross-shelf transport of Fe and Mn?

There are three main objectives of this study:

(i) To determine the concentrations of sedimentary reactive iron species along four transects covering the entire Cilician Basin.

(ii) Through generating an extensive geochemical data set covering overlying water column and sedimentary parameters, to explore the geochemical factors that control reactive iron cycling.

(iii) Based on a synthesis of findings, to establish a first conceptual model of iron cycle in the Cilician Basin seafloor.

3. MATERIAL METHODS

3.1 Sampling Site

The sampling site is located in the Cilician Basin in the Eastern Mediterranean, distributed along four transects between Seyhan River to Göksu River Delta. A total of 25 stations in these transects were sampled during three cruises in the winter of late 2015 to early 2016. Seyhan transect samples were collected in October 2015, and the Göksu and Aydıncık transect samples were collected in November 2015. The sampling of Erdemli Time Series (ETS) sediments followed on: the stations 8-11 were visited in January 2016, and the samples 12 and 13 collected in March 2016. Coastal surface sediments were sampled from 10-100m depth whereas deep seafloor samples were taken between 100-500m depth. The
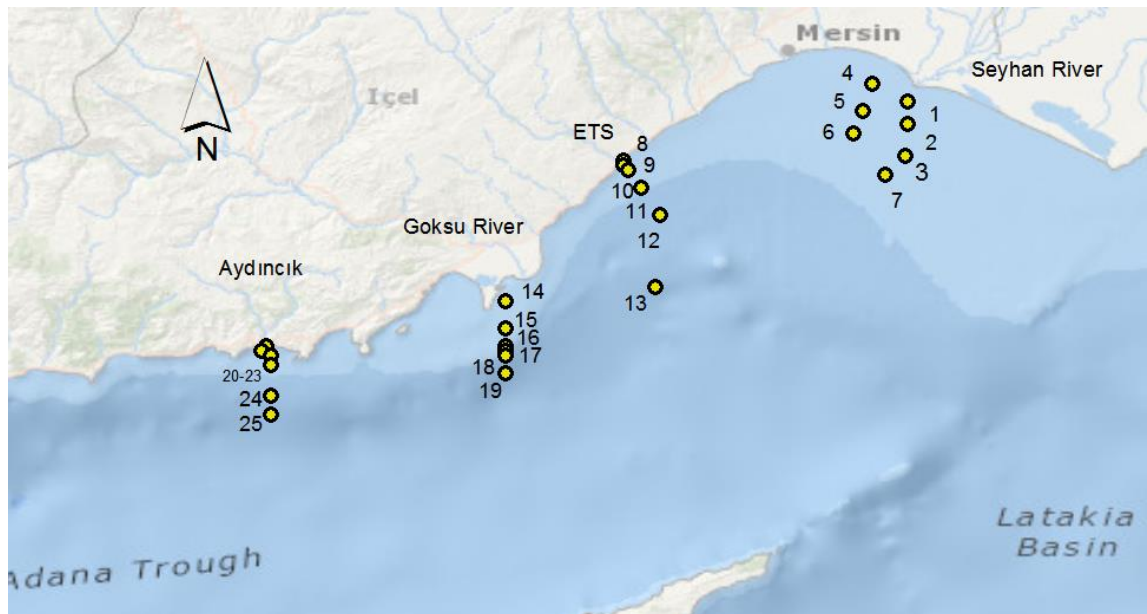
Figure 3.1. Locations of the sampling stations between Seyhan river to Aydıncık in Cilician Basin (Eastern Mediterranean).

river effect on seafloor biogeochemistry in coastal seafloor sediments was investigated in Seyhan, and Göksu transects. Further, open seafloor samples from oligotrophic Cilician Basin is studied in ETS, Göksu transects. Table 3.1 gives the collected samples transect, station name, latitude, longitude, bottom water depth in this study.

Table 3.1. The collected samples transect, station name, latitude, longitude, bottom water depth in this study.

Transect	Station	Latitude (North) (degrees:minute)	Longitude (East) (degrees:minute)	Water Depth (m)
Seyhan	1	36 41.3322	34 53.4667	15
	2	36 38.5128	34 53.2777	35
	3	36 34.3012	34 52.9920	53
Seyhan	4	36 43.9848	34 48.8900	11
	5	36 40.1305	34 47.6186	40
	6	36 37.3350	34 45.9650	56
	7	36 31.8159	34 50.2792	77
ETS	8	36 33.4523	34 15.6063	20
	9	36 32.8978	34 15.8745	50
	10	36 32.1065	34 16.4436	75
	11	36 29.9112	34 18.1119	100
	12	36 26.2417	34 20.6981	200
	13	36 17.0056	34 19.7347	400
Göksu	14	36 14 9669	33 59 9059	22
	15	36 11.5848	34 00.1412	48
	16	36 09.2119	33 59.8947	75
	17	36 08.5606	33 59.9116	97
	18	36 07.8363	33 59.7481	180
	19	36 05.1350	33 59.8549	450

Table 3.1. The collected samples transect, station name, latitude, longitude, bottom water depth in this study (continued).

Transect	Station	Latitude (North) (degrees:minute)	Longitude (East) (degrees:minute)	Water Depth (m)
Aydıncık	20	36 08.9364	33 28.3013	21
	21	36 08.6783	33 27.6789	40
	22	36 07.7701	33 28.6966	76
	23	36 06.8098	33 28.9397	100
	24	36 02.5571	33 28 9200	220
	25	35 59.9011	33 28.9314	500

3.2 Sampling and analysis of seawater biogeochemical parameters

The sampling site seawater properties were determined by main physical and biogeochemical parameters. Seawater was sampled via a General Oceanics rosette sampler having 12 bottles of 8 liter volume coupled with a Sea-Bird Model 9 conductivity-depth-temperature (CTD) sensor. The CTD and the rosette sampler were operated using a Lebus hydrographic winch with a 2000m-long cable. The CTD profiling system provided the physical characteristics of seawater such as temperature, salinity and density during the downcast of rosette sampler whereas the water was sampled (i.e. bottles closed) during the up cast. Then, the following biogeochemical analyses were performed on the water samples.

3.2.1. Sampling and Analysis of Dissolved Oxygen (DO):

Seawater was immediately subsampled from Rosette system bottles into the 100 ml Pyrex bottles with careful handling. The water transferred into Pyrex bottles with the help of silicon tube as filling twice of its volume without any air bubbles to prevent atmospheric oxygen contribution contamination followed by immediate addition of manganese(II) chloride and alkaline potassium iodide reagents. After addition of reagents the samples were shaken vigorously and put in dark for at least 30 minutes for complete reaction of entire oxygen with the reagents (Strickland and Parsons, 1972, Furuya and Harada, 1995).

Dissolved oxygen levels of water column at each station were determined via Winkler titration using an on-board automated titrator (Grasshoff et al., 1983). This method is based on measurement of dissolved oxygen level from iodometric titration by using Manganous Chloride, Potassium iodide as redox reagents. First, dissolved oxygen is precipitated as $Mn(OH)_2$ then followed by acidification of medium to achieve iodide ion to form iodine which is titrated by sodium thiosulfate. The automated Winkler titration instrument measures and calculates the dissolved oxygen level in the samples using the amount of thiosulfate consumed during titration. Analysis of samples were performed on board with Metrohm model automated Winkler titration instrument and redox electrode prior to addition of diluted sulfuric acid before titration with thiosulfate solution.

3.2.2. Sampling and analysis of Nutrients and Total Phosphorus(TP)

The sampling for nutrients (Nitrate, nitrite, ammonium, silicate and phosphate) and total phosphorus was performed separately after oxygen subsampling into the high density polyethylene bottles. All bottles were pre-cleaned with 10% hydrochloric acid, and later on rinsed three times with MilliQ water. The seawater was subsampled into bottles after three flushes before final volume and put into freezer until analysis for nutrients and TP.

The nutrients of seawater were analyzed by a Bran-Luebbe model four-channel auto-analyzer. The main principle for this analysis is to convert each nutrient into a color-forming molecular complex by a series of reactions with specific reagents to measure concentration in the samples with certain wavelengths (Grasshoff, 1983, Sağlamtimur and Tugrul, 2003)

    a. *Nitrate and nitrite analysis:*

Firstly, nitrate is reduced to nitrite via cadmium column. Nitrite in the medium reacts with sulfonamide and coupled with N-(1-naphthyl)-ethylenediamine dihyrochloride to form a red-purple dye. The concentration of the dye is measured at 520 nm wavelength.

    b. *Ammonium Analysis:*

Ammonium is determined via addition of Berthelot reagent in basic medium to form a colored compound measured at 660 nm wavelength. During colorimetric determination of

ammonium, high concentration citrate buffer was used to prevent precipitation of seawater calcium and manganese ions.

c. *Silicate Analysis*

Silicate analysis includes the acidification of solution by ascorbic acid, then reduced to silicomolybdous acid (a blue compound) following the addition of oxalic acid to eliminate positive interference of phosphate. The sample is passed through flowcell and measured at 660nm.

d. *Phosphate Analysis:*

Ortho-Phosphate is analyzed as addition of acidified ammonium molybdate to seawater sample to produce phosphomolybdic acid. Then, addition of dihydrazine sulfate reduces phosphomolybdic acid to phosphomolybdous acid (a blue compound. The absorbance measured at 820nm .

e. *Total Phosphorus:*

Total phosphorus is measured as initial digestion of phosphorus species into the phosphate form, then followed by addition of certain reagents for colorimetric determination of phosphate-compounds. For this analysis, seawater samples were place into Teflon capped bottles with addition of potassium persulphate, and then Teflon bottles were put into autoclave system for oxidation under 2 atm pressure and 120 °C about 60 minutes. After cooling, each samples pH were adjusted 7-8 by diluted NaOH solution, then diluted with deionized water to final 50 ml volume. By ascorbic acid and colorimetric reagent addition, the measurements at 880 nm were done. The concentration of samples were calculates from calibration standards.

f. *Chlorophyll a:*

Seawater subsampled into amber 1L amber Nalgene bottles and immediately filtered through GF/F filter with 47 mm pore size. After filtration, filters were placed into aluminum covers and frozen until analysis.

Analysis of chlorophyll-a is a spectrophotometric determination(florescence) via extraction of chlorophyll-a into acetone medium. To do this, filters were placed into centrifuge tubes and 8 ml 90% acetone solution was added. This solution was centrifuged at 6000 rpm for 5 minutes, then measured by HITACHI model F-2500 Florescence Spectrophometer. The concentration of chl-a was decided with measurements at the 420 nm excitation and 669 nm emission wavelengths (Wasmund et al. 2006).

3.3 Determination of sediment properties

Surface seafloor sediments were sampled by 5 L volume Van Veen Grab sampler. This sampler collects the upper few centimeters of surface sediments. The upper surface sediment about one cm length were swept by clean spatula to get rid of the metal-touched surface of the sediment. In order to perform a consistent sampling, sediments were deliberately subsampled with average of 10 cm length from the light-brown areas that are thought to represent the oxidized, surface sediment. Subsamples were taken first for iron and trace metal analysis, followed by total organic carbon and grain size analyses.

For each of the solid-phase parameters the results will be reported as micromoles of element per gram dry weight of sediment. In order to convert the wet weight of sediments to dry weight, subsamples of about 0.5 g were dried at 60°C for 24 hours and then re-weighed. Using the weight loss upon drying porosity was assessed, which was then used to calculate dry sediment weights.

3.3.1. Extraction of reactive iron by buffered dithionite solution

The sediments were subsampled into pre-cleaned (10 % HCl acid, Analytical Grade, then MilliQ water) 50 ml centrifuge tubes with pre-cleaned plastic spatulas (trace metal free). The leftover space in the 50-mL tubes were then saturated by nitrogen gas to prevent oxidation of samples that were kept in -20°C until analysis.

In this study, reactive iron is defined as the Fe-(oxyhydr) oxides that have a potential of going through relatively fast (days to months) geochemical interactions with organic carbon, phosphorus, trace metals as defined by Kostka and Luther (1994). This extraction method is sufficient to dissolve the major iron oxide phases (ferrihydrite, goethite, trace amount of magnetite) with partially extracting some hematite and minor amounts of iron

from chlorite and silicates (Canfield, 1989; Kostka and Luther, 1994). Mass of triplicate of each sample was approximately 0.5 g wet sediments in vials. 10 ml of dithionite solution was added to vials. The freshly prepared dithionite solution includes 0.3 M dithonite, 0.35M Na-acetate /0.2 M Na-citrate (pH 4.8) per L. The vials were shaken for 48 h. Followed by 0.45µm filtration and filtrate stored in dark environment at +4 °C until analysis. In order to prevent matrix effects due to concentrated dithionite matrix, the filtrates were diluted 50 fold and analyzed by ICP-MS NexIon 350X.

Inductively Coupled Plasma Mass Spectroscopy (ICP-MS) instrument basically detects the ions via ions mass to charge ratio, in other words molecular mass. To achieve this, sample is needed to be in aqueous phase for sample introduction system consisting auto sampler, pumps, nebulizer, inductively coupled plasma, plasma interface, cones, quadrupole mass filters and detector. The samples are introduced to system from spray chamber forming micrometer diameters droplets to the system. Then, the nebulized particles are carried to plasma with the help of a carrier gas (an inert gas), to ionize the elements. The desired nebulized element passes through the sample interface which consist of three nested Ni cones and quadrupole ion deflector providing the eliminate undesired elements before affecting detector. Then the mass filters separate the ions as their mass to charge ratio, and detector gives the signal. This instrument has three modes of operation improves to interference removal for specific elements and applications.

The detection limits for all elements and blank contributions was far less than the concentration in the seafloor samples. However, some stations were observed to have Pb concentrations less than ppb levels and indicated as 'b.d' in the table. Further, the calibration curves for the all elements has the coefficient, R^2, greater than 0.99.

3.3.2 Determination of other trace metal concentrations

The trace metal concentrations were determined in the same samples that were analyzed by reactive iron.

Total acid digestion method was applied for determination of total iron, and other trace metals concentration. This method includes microwave-assisted digestion of dry sediments with nitric acid (HNO_3) and hydrofluoric acid (HF). The dried triplicate samples

weighed about 0.1 g put in Teflon Microwave digestion containers with addition of 5 ml concentrated HNO_3. The containers were placed in microwave digestion system at 1000 Watt and 120°C for 15 minutes. After cooling, 2 ml concentrated hydrofluoric acid were added and the samples were re-digested with the same procedure. Digested aqueous samples were added 0.6 g boric acid then placed into 50 ml centrifuge tubes, containers were three times rinsed with MilliQ water for minimize sample loss and diluted to 50 ml with distilled MilliQ water. The analysis of digested samples was measured as 10 fold and with 100 fold dilution and analyzed by ICP-MS NexIon 350X instrument. The calibration standards were prepared by using Perkin Elmer multi-element calibration standard solution of metals (including Fe, Al, As, Mn, Mg, K, V, Cr, Co, Ni, Ca, Mg, Se, Sr, Ga, Ba, Be,Pb, Cs) in 5% HNO_3 with concentration of 10 µg/ml each element. Internal Yttrium standard was added in each sample before analysis to correct the intensity deviations during measurement with ICP-MS. The net intensity data were automatically corrected by using Yttrium internal standard intensity. The molar concentrations of each element were calculated by standard calibration curve of each element with multiplication of volume, dilution and division of molar mass.

The METU-IMS laboratory metal digestion and measurement technique has been evaluated for MEDPOL Proficiency Test in 2015 by International Atomic Energy Agency (IAEA) Marine Environmental Studies Laboratory. According to intercalibration results, the results of metals analysis (Al, Co, Cr, Cu, Fe, Mn, Ni, Pb, V, Zn, Ag, Hg) have been satisfactory except for the Ag and Hg elements. For Hg the applied digestion methods are expected not to be efficient, so the result is not surprising. For Ag, despite the low confidence in the intercalibration effort, we had good internal and external calibration curves.

3.3.3 Organic carbon Analysis

Sediments were subsampled during the cruises in glass bottles kept in 4°C. The concentration of total organic carbon in sediments was determined by weighing about 30 mg of dry sediment samples in silver capsules. The removal of inorganic carbon is treated by 20% HCl acid addition to the samples in silver capsules since carbonates were transformed into CO_2 gas. After removal of carbonates, samples were dried at 70°C for 24

hours. The dried samples then measured by Vario El Cube Elementar CHN analyzer. Total carbon and total nitrogen analysis were done with the same procure except HCl addition (Yucel 2011, Nieuwenhuize et al., 1994).

3.3.4 Grain Size Analysis

For laboratory determinations of grain size, subsamples were placed into nylon bags and kept in -20 C until analysis. For grain size analysis, coarse samples were thawed, then sieved by 2 mm, 1 mm, 0.5 mm, 0.25mm meshes. The total amount of each size separated fraction was weighted, and each fraction in total percent is calculated. The sediments grain size less than 0.25 mm was analyzed by laser diffraction Mastersizer Model instrument. The percent weight of each size is calculated together with sieving and Mastersizer instrument.

CHAPTER III

4. RESULTS

In this chapter the major parameters seawater data is presented by transects, followed by sedimentary solid phase data collected from seafloor of Cilician basin. The seawater data in this study has been used to present the difference in biogeochemistry of the overlying water. Therefore, each station and transect in this study is likely to help to geochemical factors that controls reactive iron species.

4.1 Major properties of Seawater in sampling site

Seyhan Transect: Physical and biogeochemical data of oxic seawater column of Seyhan stations is represented in Table 3. Depth of six stations was in the range of 11-56 m. Station 7 (100m depth) had no seawater data in this transect. Seyhan stations could be divided into two sub-transects; the stations 1-3 are closer to the mouth of Seyhan River and the stations 4-6 were located in shelf area of Seyhan transect. Seawater temperature is around 26 °C and increases from shallower to deeper stations by around +0.4°C. Salinity values with 38-39 psu. The surface seawater salinity slightly increases through deep stations as similar increase in density showing the river effect on shallower stations. Essential nutrients for new production such as phosphate, nitrate and nitrite and silicate were ranging from, 0.03-0.10 μM for phosphate, 0.05-2.68 μM for nitrate and nitrite, and 1.01-7.04 μM for silicate. Chlorophyll-a levels, which is a proxy for the production in sea, were between 0.11-2.98 μg/L.

Data for station 4 was observed to have the lowest temperature, salinity and density with more than 2 times high nutrient values indicating that this station contained waters affected by the low-salinity and high-nutrient containing river waters. Bottom water of Station 6 was found to have maximum chlorophyll-a value of 2.98 μg/L that could stem from sufficient seawater penetration to the bottom water and optimum conditions for production of specific organisms.

Table 4.1. Station name, depth (m), temperature (°C), salinity (psu), density (kg.m^{-3}), dissolved oxygen(μM/L) , phosphate (μM), nitrate and nitrite (μM), silicate (μM) and chlorophyll-a (µg/L) data in the Seyhan transect.

Station name	Depth	Temp.	Salinity	Density	Dissolved Oxygen	Phosphate	Nitrate+ Nitrite	Silicate	Chlorophyll-a
	(m)	(°C)	(psu)	kg.m^{-3}	(μM/L)	(μM)	(μM)	(μM)	(µg/L)
1-Seyhan	0	26.35	38.84	25.82	203.45	0.06	0.64	4.21	1.02
	15	27.13	39.31	25.93	171.45	0.09	0.70	4.05	1.05
2-Seyhan	0	26.57	39.10	25.95	207.64	0.06	0.12	2.86	0.32
	10	26.58	39.10	25.95	203.02	0.04	0.10	2.67	0.42
	35	26.90	39.35	26.03	202.96	0.04	0.06	2.27	0.30
3-Seyhan	0	27.07	39.36	25.98	200.15	0.02	0.05	1.96	2.58
	10	27.08	39.36	25.98	200.24	0.02	0.06	1.27	0.13
	45	26.92	39.41	26.07	207.50	0.02	0.07	1.66	0.19
	53	22.18	38.88	27.12	208.69	0.02	0.14	2.32	0.25
4-Seyhan	0	25.85	38.13	25.45	210.80	0.10	2.68	7.04	2.30
	11	26.20	38.83	25.86	205.50	0.10	1.75	6.08	1.09
5-Seyhan	0	26.91	39.37	26.04	199.39	0.03	0.07	1.60	0.16
	10	26.93	39.37	26.03	200.24	0.03	0.06	1.43	0.16
	40	26.77	39.41	26.12	199.85	0.03	0.09	1.05	0.11
6-Seyhan	0	26.77	39.40	26.11	199.07	0.03	0.12	1.14	0.14
	10	26.78	39.41	26.11	202.35	0.05	0.14	1.04	0.11
	40	24.94	39.11	26.47	218.42	0.05	0.15	1.01	0.25
	56	20.77	38.91	27.54	217.76	0.06	0.17	1.44	2.98
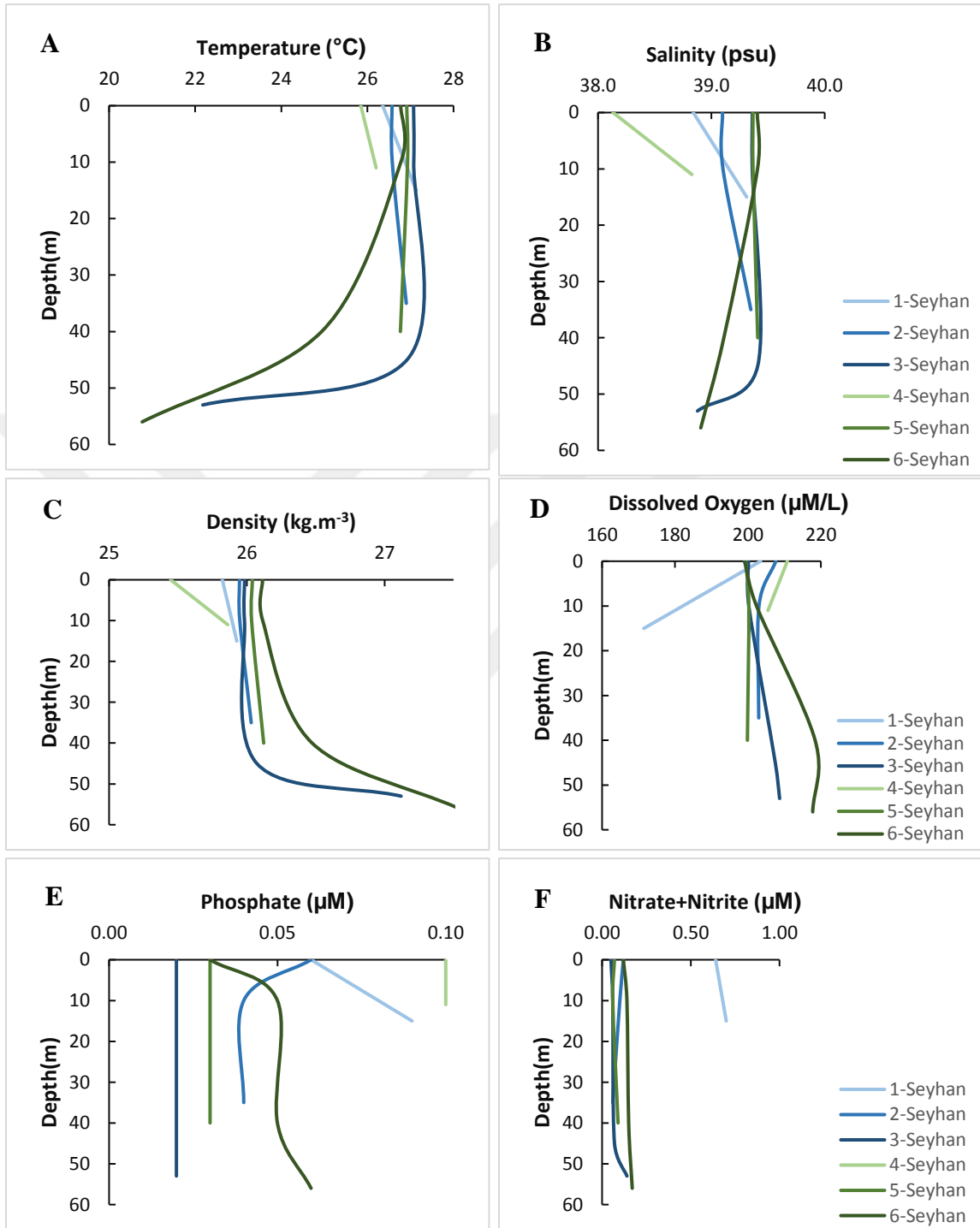
Figure 4.1. Seawater parameter profiles of Stations 1-3(blue lines) and Stations 4-6(green lines) in Seyhan Transect. **A.** Temperature (°C) **B.** Salinity (psu) **C.** Density (kg.m^{-3}) **D.** Dissolved Oxygen (µM/L), **E.** Phosphate (µM) **F.** Nitrate+Nitrite (µM), **G.** Silicate (µM) **H.** Chlorophyll-a (µg/L).
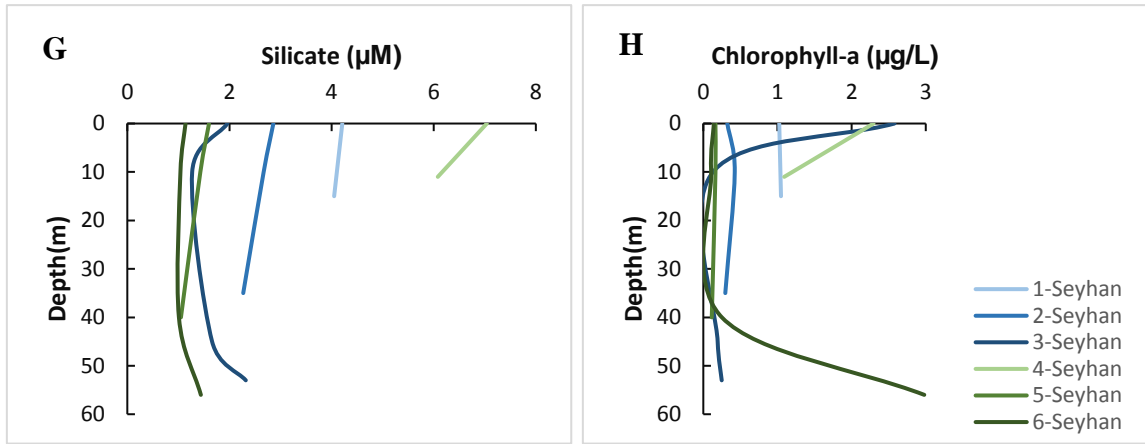
Figure 6.1. Seawater parameter profiles of Stations 1-3(blue lines) and Stations 4-6(green lines) in Seyhan Transect. **A.** Temperature (°C) **B.** Salinity (psu) **C.** Density (kg.m^{-3}) **D.** Dissolved Oxygen (µM/L) **E.**Phosphate (µM) **F.**Nitrate+Nitrite (µM) **G.**Silicate (µM) **H.** Chlorophyll-a (µg/L) (continued).

ETS transect: Stations along ETS transect reflected oligotrophic and oxic nature of the typical Eastern Mediterranean waters in Table 4. Seawater temperature decreased through water column with depth. In coastal stations, water temperature and salinity values represented strong mixing in winter season through oxic water column. Nutrient data ranged between as in the following; 0.03-0.16 (µM) for phosphate, 0.08-4.66 (µM) for nitrate and nitrite, 0.65-4.33 (µM) for silicate. Chlorophyll-a concentrations changed between 0.01-0.07 (µg/L).

In the coastal station, phosphate, nitrate and nitrite, silicate levels were approximately similar from surface to bottom water due to strong mixing. On the other hand, there was slight increase in nutrient data with depth. For instance, phosphate increased to 0.11 µM resulting from detrital accumulation of organic matter and subsequent remineralization processes. Remineralization result in the breakdown of organic matter into inorganic nutrients. As the water column of the Eastern Mediterranean is oxygenated, we can presume that oxic remineralization pathway is responsible with the accumulation of nutrients with depth, releasing nitrate and phosphate which were previously bounded to organic matter. As a result, the bottom waters of deeper stations become progressively enriched in nitrate and phosphate in all transects (Figure 4.2 to 4.4).

Table 4.2. Station name, depth (m), temperature (°C), salinity (psu), density (kg.m^{-3}), dissolved oxygen(µM/L) , phosphate (µM), nitrate and nitrite (µM), silicate (µM) and chlorophyll-a (µg/L) data in the ETS transect.

Station Name	Depth	Temp	Salinity	Dissolved Oxygen	Total Phos.	Phosphate	Nitrate+ nitrite	Silicate	Chlorophyll-a
	(m)	(°C)	(psu)	(µM/L)	(µM)	(µM)	(µM)	(µM)	(µg/L)
8-ETS	0	18.35	39.21	233.42	0.24	0.08	0.40	1.52	0.04
	10	18.36	39.21	230.90	0.21	0.05	0.38	1.06	0.03
	20	18.28	39.20	232.22	0.21	0.05	0.42	1.02	0.03
9-ETS	0	18.35	39.21	216.18	0.17	0.03	0.23	0.75	0.07
	10	18.35	39.21	231.11	0.15	0.03	0.27	0.84	0.03
	25	18.31	39.21	233.81	0.18	0.05	0.21	0.82	0.06
	46	18.29	39.21	228.42	0.19	0.05	0.33	0.83	0.06
10-ETS	0	18.27	39.21	232.10	0.15	0.04	0.14	0.79	0.07
	10	18.27	39.21	234.53	0.15	0.04	0.16	0.75	0.06
	25	18.28	39.21	230.21	0.16	0.04	0.20	0.73	0.05
	50	18.27	39.21	229.06	0.16	0.04	0.20	0.77	0.07
	73	18.10	39.20	234.75	0.19	0.05	0.21	0.74	0.05
11-ETS	0	18.22	39.17	235.39	0.13	0.04	0.32	0.74	0.04
	10	18.23	39.17	235.05	0.16	0.05	0.13	0.94	0.03
	25	18.23	39.17	234.45	0.10	0.06	0.30	0.87	0.06
	50	18.17	39.19	236.46	0.11	0.05	0.40	0.90	0.06
	75	17.66	39.22	235.77	0.14	0.03	0.44	0.90	0.13
	95	17.53	39.23	235.77	0.18	0.05	0.56	0.79	0.18
12-ETS	0	18.19	39.02	234.59	0.18	0.06	0.10	0.65	0.03
	10	18.10	39.02	235.97	0.16	0.06	0.08	0.75	0.01
	25	18.03	39.02	236.29	0.16	0.06	0.10	0.71	0.01
	50	18.03	39.04	229.83	0.17	0.08	0.10	0.70	0.01
	75	18.00	39.08	228.46	0.17	0.08	0.28	0.88	0.02
	100	17.86	39.08	225.87	0.18	0.07	0.37	0.91	0.01
	150	17.53	39.09	226.84	0.18	0.09	0.39	1.39	0.02
	195	16.78	39.09	213.52	0.19	0.09	1.15	1.20	0.01
13-ETS	0	17.94	39.03	233.74	0.15	0.05	0.08	0.81	0.03
	10	17.94	39.03	234.75	0.15	0.07	0.08	0.67	0.00
	25	17.92	39.03	232.72	0.16	0.05	0.08	0.76	0.02
	50	17.91	39.03	232.80	0.16	0.06	0.09	0.77	0.01
	75	17.76	39.11	229.48	0.17	0.06	0.36	0.89	0.01
	100	17.69	39.11	228.74	0.17	0.05	0.44	0.97	0.01
	150	17.14	39.09	223.79	0.18	0.06	0.55	0.97	0.02
	200	16.83	39.10	200.56	0.18	0.08	1.13	1.24	0.01
	300	15.35	39.03	197.00	0.20	0.14	4.66	4.33	
	400	14.48	38.91	186.41	0.20	0.13	2.96	3.52	
	500	13.92	38.80	183.49	0.21	0.16	2.96	4.28	

Figure 4.2. Seawater parameter profiles of Stations 8-11 in ETS Transect. **A.** Temperature (°C) **B.** Salinity (psu) **C.** Density (kg.m^{-3}) **D.** Dissolved Oxygen (µM/L) **E.**Phosphate (µM) **F.**Nitrate+Nitrite (µM) **G.**Silicate (µM) **H.** Chlorophyll-a (µg/L).
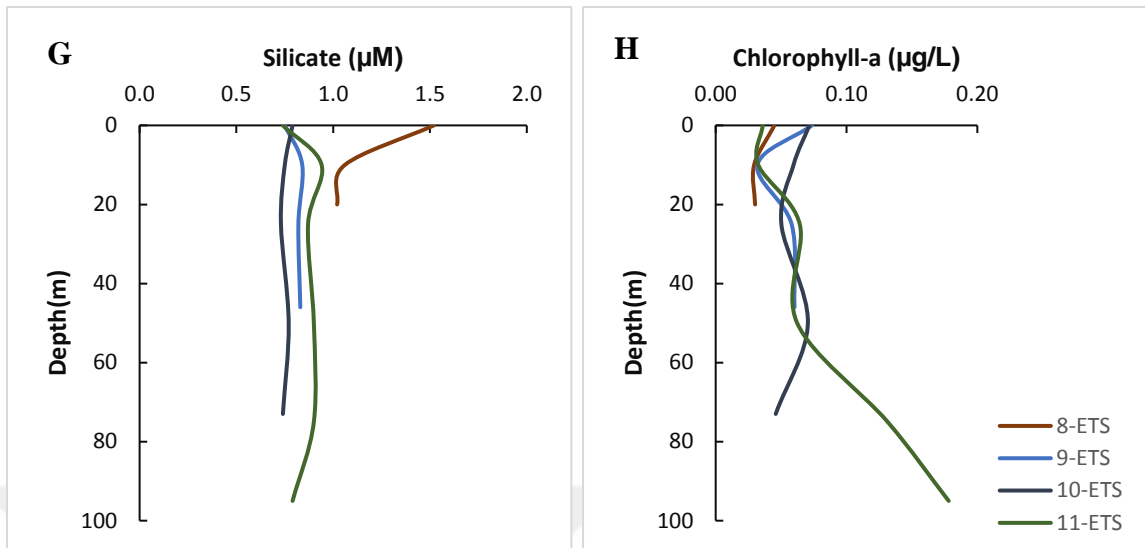
Figure 4.2. Seawater parameter profiles of Stations 8-11 in ETS Transect. **A.** Temperature (°C) **B.** Salinity (psu) **C.** Density (kg.m^{-3}) **D.** Dissolved Oxygen (μM/L) **E.**Phosphate (μM) **F.**Nitrate+Nitrite (μM) **G.**Silicate (μM) **H.** Chlorophyll-a (μg/L) (continued).

Figure 4.3. Seawater parameter profiles of Stations 12-13 in ETS Transect. **A.** Temperature (°C) **B.** Salinity (psu) **C.** Density (kg.m^{-3}) **D.** Dissolved Oxygen (µM/L) **E.** Phosphate (µM) **F.** Nitrate+Nitrite (µM) **G.** Silicate (µM) **H.** Chlorophyll-a (µg/L).

The open seafloor differed from coastal stations with lower productivity and lower nutrient values. The nitrate, silicate decreased more than 2 times, with the increase in these nutrients in depth. The bottom water oxygen of open seawater decreased up to 180 µM, coupled to an increase in nitrate, silicate and phosphate The typical open seawater profile was found here, as demonstrated by the increase of nutrient values in deeper water layers resulting from remineralization processes.

Göksu and Aydıncık transects: Stations of Göksu and Aydıncık transects were located in the western part of the Cilician Basin. Seawater temperature decreased through water column with depth as typical behavior of seawater profile in Table 5. Surface seawater temperature was around 22.6°C ±1°C. Upper layer of the water column was uniform, pointing to mixing. Nutrient data ranged between 0.02-0.24 μM for phosphate, 0.06-6.28 μM for nitrate and nitrite, and 0.70-8.05 μM for silicate. Chlorophyll-a ranged between 0.01-0.19 μg/L.

Coastal area was found to be 1-2 times more productive than open seawater in euphotic zone. Nitrate concentration in coastal stations was low, whereas open stations displayed an increase with depth due to remineralization processes. A decrease in oxygen concentration in bottom water of open station was observed, with a corresponding increase in nutrient levels. Table 4.3 gives the seawater data in Göksu and Aydıncık transects.

Table 4.3. Station name, depth (m), temperature (°C), salinity (psu), density (kg.m^{-3}), dissolved oxygen(μM/L), phosphate (μM), nitrate and nitrite (μM), silicate (μM) and chlorophyll-a (μg/L) data in Göksu and Aydıncık transects.

Station Name	Depth (m)	Temp. (°C)	Salinity (psu)	Density kg.m^{-3}	Dissolved Oxygen (μM/L)	Phosphate (μM)	Nitrate+ nitrite (μM)	Silicate (μM)	Chl-a (μg/L)
14-Göksu	22	22.45	39.38	27.42	221.83	0.03	0.08	0.83	
15-Göksu	48	23.30	39.34	27.15	216.89	0.04	0.31	0.76	
16-Göksu	0	23.39	39.36	27.13	214.06	0.10	0.81	0.76	0.12
	10	23.39	39.36	27.13	214.45	0.05	0.36	0.74	0.12
	25	23.40	39.36	27.13	215.20	0.02	0.12	0.72	0.12
	50	23.26	39.35	27.17	222.92	0.05	0.10	0.84	0.16
	75	20.47	38.85	27.58	233.18	0.05	0.33	0.83	0.19
17-Göksu	100	18.57	38.89	28.11	240.03	0.06	0.15	0.98	0.11
18-Göksu	160	17.36	39.06	28.56	213.93	0.08	0.65	1.12	0.05
19-Göksu	450	14.16	38.87	29.16	180.13	0.24	6.28	8.05	0.01
20-Aydıncık	21	22.62	39.37	27.36	217.83	0.03	0.26	1.04	0.15
21-Aydıncık	40	22.67	39.36	27.34	216.05	0.02	0.06	0.77	0.19

Table 4.3. Station name, depth (m), temperature (°C), salinity (psu), density (kg.m^{-3}), dissolved oxygen(µM/L), phosphate (µM), nitrate and nitrite (µM), silicate (µM) and chlorophyll-a (µg/L) data in the Göksu and Aydıncık transects (continued).

Station Name	Depth (m)	Temp. (°C)	Salinity (psu)	Density kg.m^{-3}	Dissolved Oxygen (µM/L)	Phosphate (µM)	Nitrate+ nitrite (µM)	Silicate (µM)	Chl-a (µg/L)
22-Aydıncık	76	22.56	39.38	27.39	214.60	0.03	0.27	1.18	0.18
23-Aydıncık	0	22.82	39.35	27.29	216.20	0.02	0.06	0.88	0.19
	10	22.83	39.35	27.29	216.01	0.03	0.06	0.62	0.14
	25	22.83	39.36	27.29	213.17	0.03	0.13	0.68	0.16
	50	22.60	39.36	27.36	219.19	0.06	0.10	0.58	0.11
	75	22.54	39.38	27.40	223.56	0.05	0.25	1.18	0.15
	100	17.92	39.03	28.39	228.93	0.06	0.46	1.06	0.12
24-Aydıncık	220	16.35	39.11	28.84	203.54	0.10	2.09	2.05	0.02
25-Aydıncık	0	21.42	39.26	27.62	222.68	0.03	0.20	0.76	0.09
	10	21.43	39.26	27.62	223.03	0.03	0.23	0.70	0.12
	25	21.44	39.26	27.62	222.38	0.02	0.34	0.72	0.07
	50	21.40	39.25	27.62	224.15	0.02	0.25	0.78	0.12
	75	17.99	39.01	28.35	238.32	0.03	0.48	0.78	0.23
	100	17.34	39.09	28.58	227.56	0.05	0.50	1.00	0.17
	150	16.50	39.12	28.81	207.07	0.07	2.03	1.33	0.05
	200	15.59	39.07	28.99	190.42	0.12	3.77	3.25	0.01
	300	14.40	38.91	29.14	180.74	0.21	5.47	6.06	
	500	13.87	38.81	29.18	178.39	0.23	6.16	8.04	

Figure 4.4 gives only the bottom seawater data in the transects. In these graphs depth only gives the total depth of the station represented as the blue in Aydıncık and red in Göksu transect. In other words, the coastal stations are close to zero-meter depth. The Göksu transect starts from station 14-Göksu and ends in station 19-Göksu.
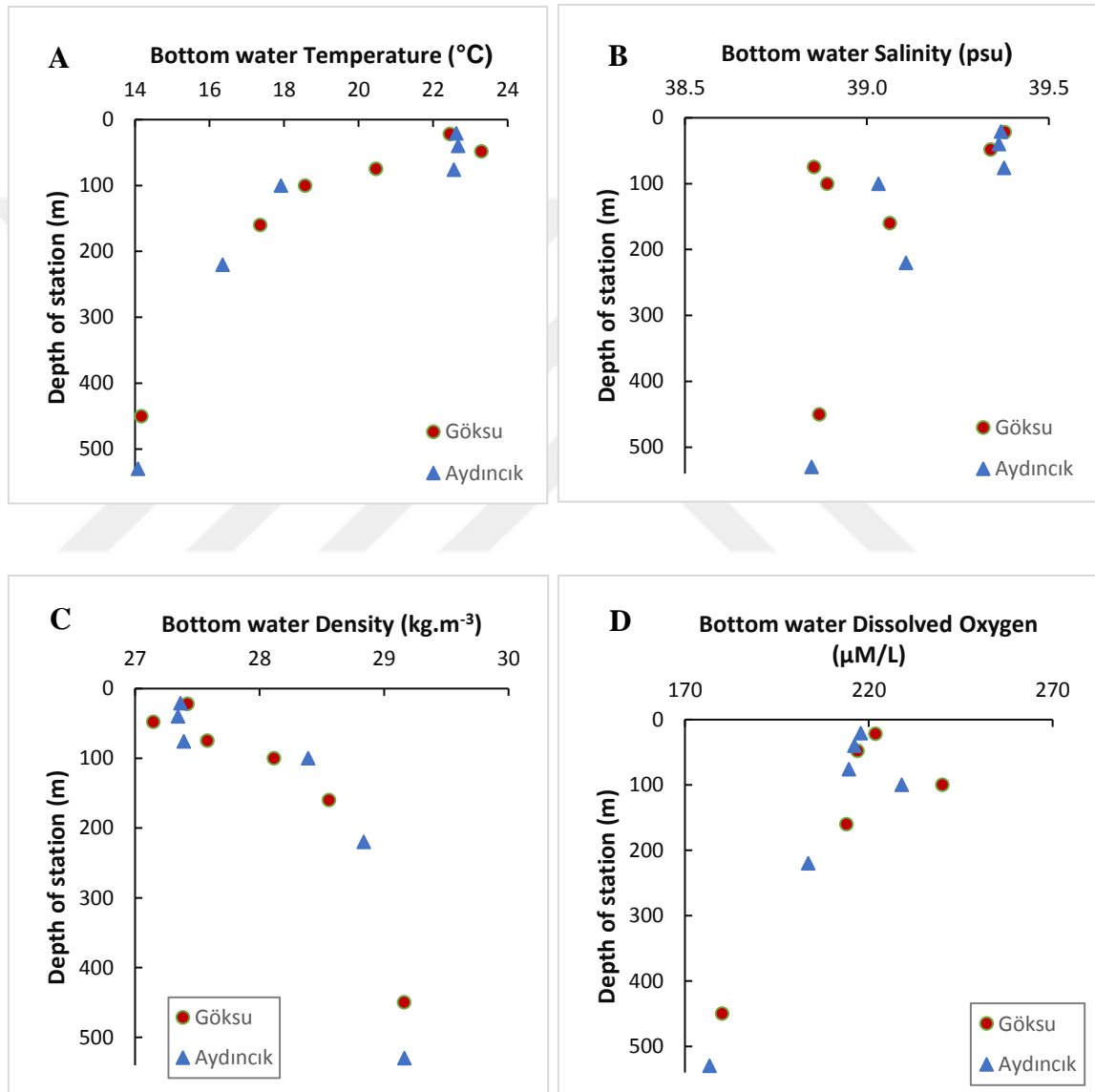
Figure 4.4. Bottom seawater parameter data of Stations 14-19 in Göksu and 20-25 in Aydıncık Transects. **A.** Temperature (°C) **B.** Salinity (psu) **C.** Density (kg.m^{-3}) **D.** Dissolved Oxygen (µM/L), **E.** Phosphate (µM) **F.** Nitrate+Nitrite (µM) **G.** Silicate (µM) **H.** Chlorophyll-a (µg/L). Each dot is a station from shallow to deep sea. Red dots represent Göksu stations, blue triangles represent Aydıncık stations.
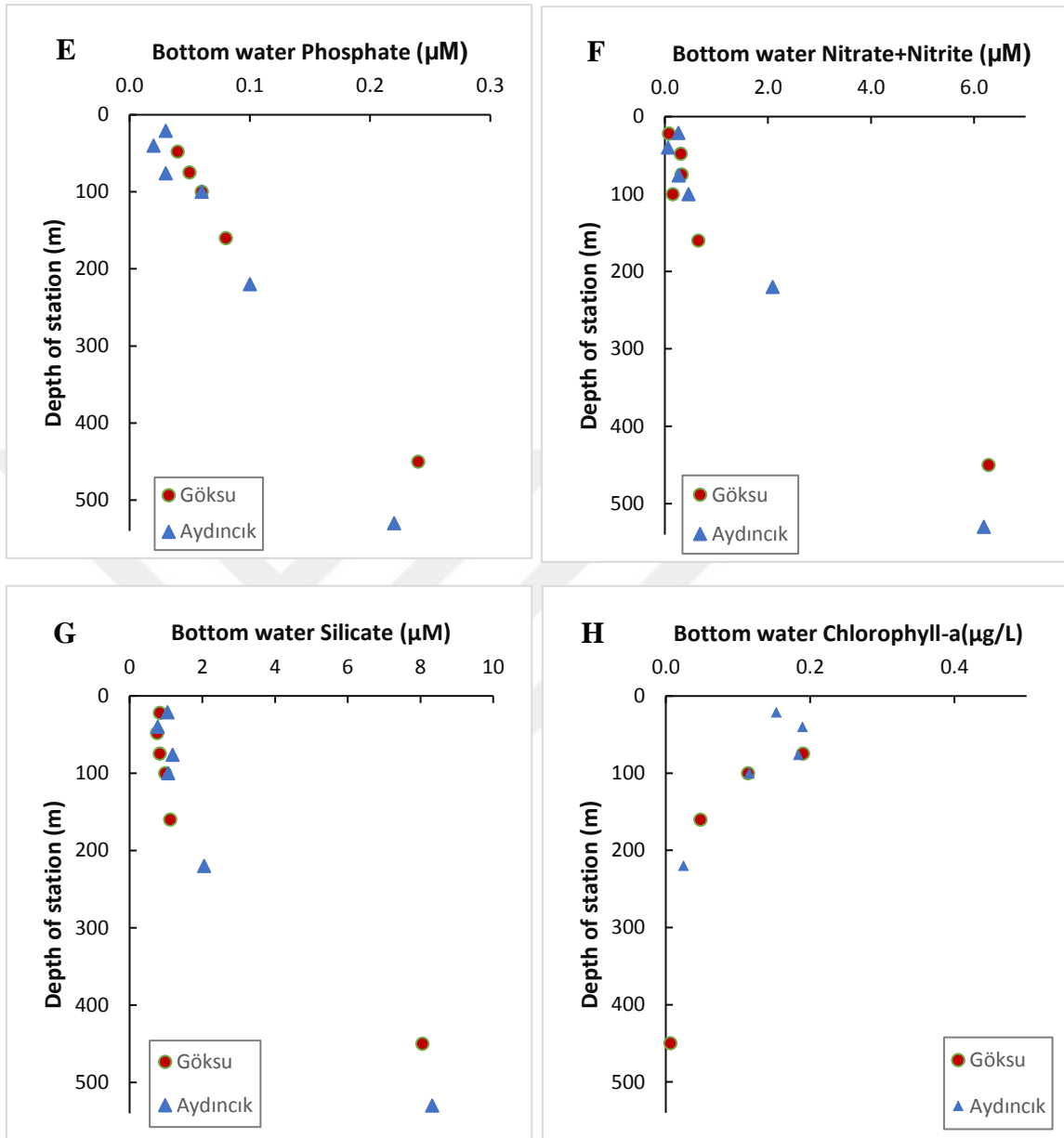
Figure 4.4. Bottom seawater parameter data of Stations 14-19 in Göksu and 20-25 in Aydıncık Transects. **A.** Temperature (°C) **B.** Salinity (psu) **C.** Density (kg.m^{-3}) **D.** Dissolved Oxygen (µM/L) **E.**Phosphate (µM) **F.**Nitrate+Nitrite (µM) **G.**Silicate (µM) **H.** Chlorophyll-a (µg/L). Each dot is a station from shallow to deep sea. Red dots represent Göksu stations, blue triangles represent Aydıncık stations (continued).

Bottom Water Properties of all transects:

The biogeochemistry of seawater is an effective key to reveal seafloor ecosystem in terms of microbial life, available energy sources, and to estimate the possible survival pathways for organisms. Therefore, the composition of the bottom water that overlays the upper surface sediment (the penetration depends on biogeochemistry of seafloor) is important for understanding how reactive iron is associated with organic carbon, nitrogen, other trace metals and how it is transported from coastal system to open oligotrophic marine ecosystem. For that reason, some of the important bottom water biogeochemical data is given in Table 4.4 and Figure 4.5.

Table 4.4. Station name, depth (m), temperature (°C), salinity (psu), density (kg.m^{-3}), dissolved oxygen(µM/L), phosphate (µM), nitrate and nitrite (µM), silicate (µM) and chlorophyll-a (µg/L) bottom water data in the all transects.

Station Name	Depth (m)	Temp. (°C)	Salinity (psu)	Density kg.m^{-3}	Dissolved Oxygen (µM/L)	Phosphate (µM)	Nitrate+ nitrite (µM)	Silicate (µM)	Chl-a (µg/L)
1-Seyhan	15	27.13	39.31	25.93	171.45	0.09	0.70	4.05	1.05
2-Seyhan	35	26.90	39.35	26.03	202.96	0.04	0.06	2.27	0.30
3-Seyhan	53	22.18	38.88	27.12	208.69	0.02	0.14	2.32	0.25
4-Seyhan	11	26.20	38.83	25.86	205.50	0.10	1.75	6.08	1.09
5-Seyhan	40	26.77	39.41	26.12	199.85	0.03	0.09	1.05	0.11
6-Seyhan	56	20.77	38.91	27.54	217.76	0.06	0.17	1.44	2.98
8-ETS	20	18.28	39.20	28.43	232.22	0.05	0.42	1.02	0.03
9-ETS	46	18.29	39.21	28.42	228.42	0.05	0.33	0.83	0.06
10-ETS	73	18.10	39.20	28.47	234.75	0.05	0.21	0.74	0.05
11-ETS	95	17.53	39.23	28.64	235.77	0.05	0.56	0.79	0.18
12-ETS	195	16.78	39.09	28.71	213.52	0.09	1.15	1.20	0.01
13-ETS	400	14.48	38.91	29.16	186.41	0.13	2.96	3.52	

Table 4.4. Station name, depth (m), temperature (°C), salinity (psu), density (kg.m^{-3}), dissolved oxygen(µM/L), phosphate (µM), nitrate and nitrite (µM), silicate (µM) and chlorophyll-a (µg/L) bottom water data in the all transects (continued).

Station Name	Depth (m)	Temp. (°C)	Salinity (psu)	Density kg.m^{-3}	Dissolved Oxygen (µM/L)	Phosphate (µM)	Nitrate+ nitrite (µM)	Silicate (µM)	Chl-a (µg/L)
14-Göksu	22	22.45	39.38	27.42	221.83	0.03	0.08	0.83	
15-Göksu	48	23.30	39.34	27.15	216.89	0.04	0.31	0.76	
16-Göksu	75	20.47	38.85	27.58	233.18	0.05	0.33	0.83	0.19
17-Göksu	100	18.57	38.89	28.11	240.03	0.06	0.15	0.98	0.11
18-Göksu	160	17.36	39.06	28.56	213.93	0.08	0.65	1.12	0.05
19-Göksu	450	14.16	38.87	29.16	180.13	0.24	6.28	8.05	0.01
20-Aydıncık	21	22.62	39.37	27.36	217.83	0.03	0.26	1.04	0.15
21-Aydıncık	40	22.67	39.36	27.34	216.05	0.02	0.06	0.77	0.19
22-Aydıncık	76	22.56	39.38	27.39	214.60	0.03	0.27	1.18	0.18
23-Aydıncık	100	17.92	39.03	28.39	228.93	0.06	0.46	1.06	0.12
24-Aydıncık	220	16.35	39.11	28.84	203.54	0.10	2.09	2.05	0.02
25-Aydıncık	500	14.07	38.85	29.16	176.69	0.22	6.19	8.32	0.08(0m)
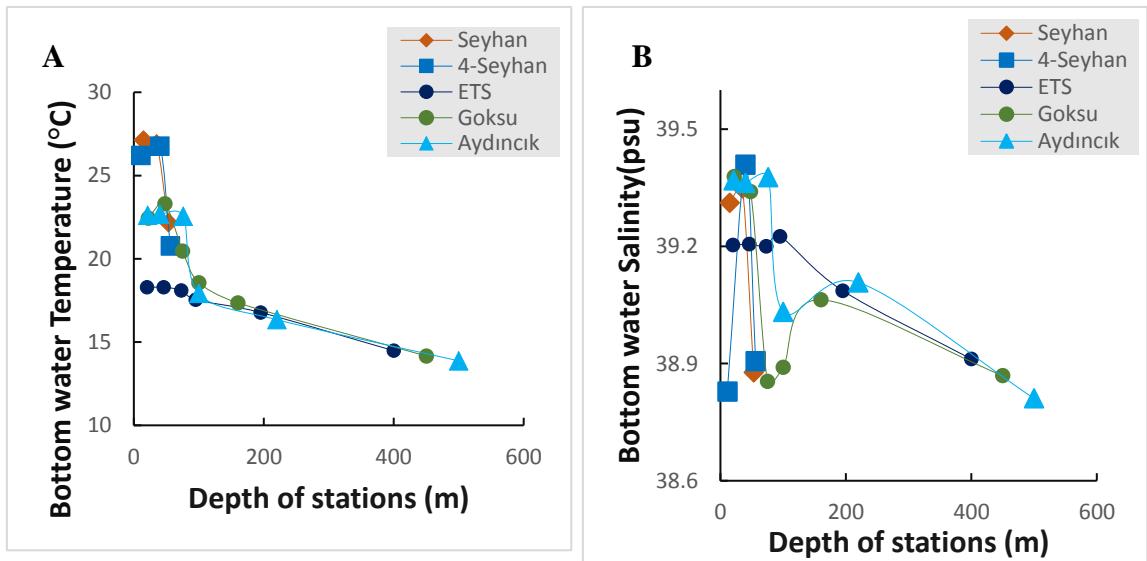
Figure 4.5. Bottom seawater parameter data of Stations in 4 transects. **A.** Temperature (°C) **B.** Salinity (psu) **C.** Density (kg.m^{-3}) **D.** Phosphate (µM) **E.** Nitrate+Nitrite (µM) **F.** Chlorophyll-a (µg/L). Each dot is a station from shallow to deep sea and represented as by different color.
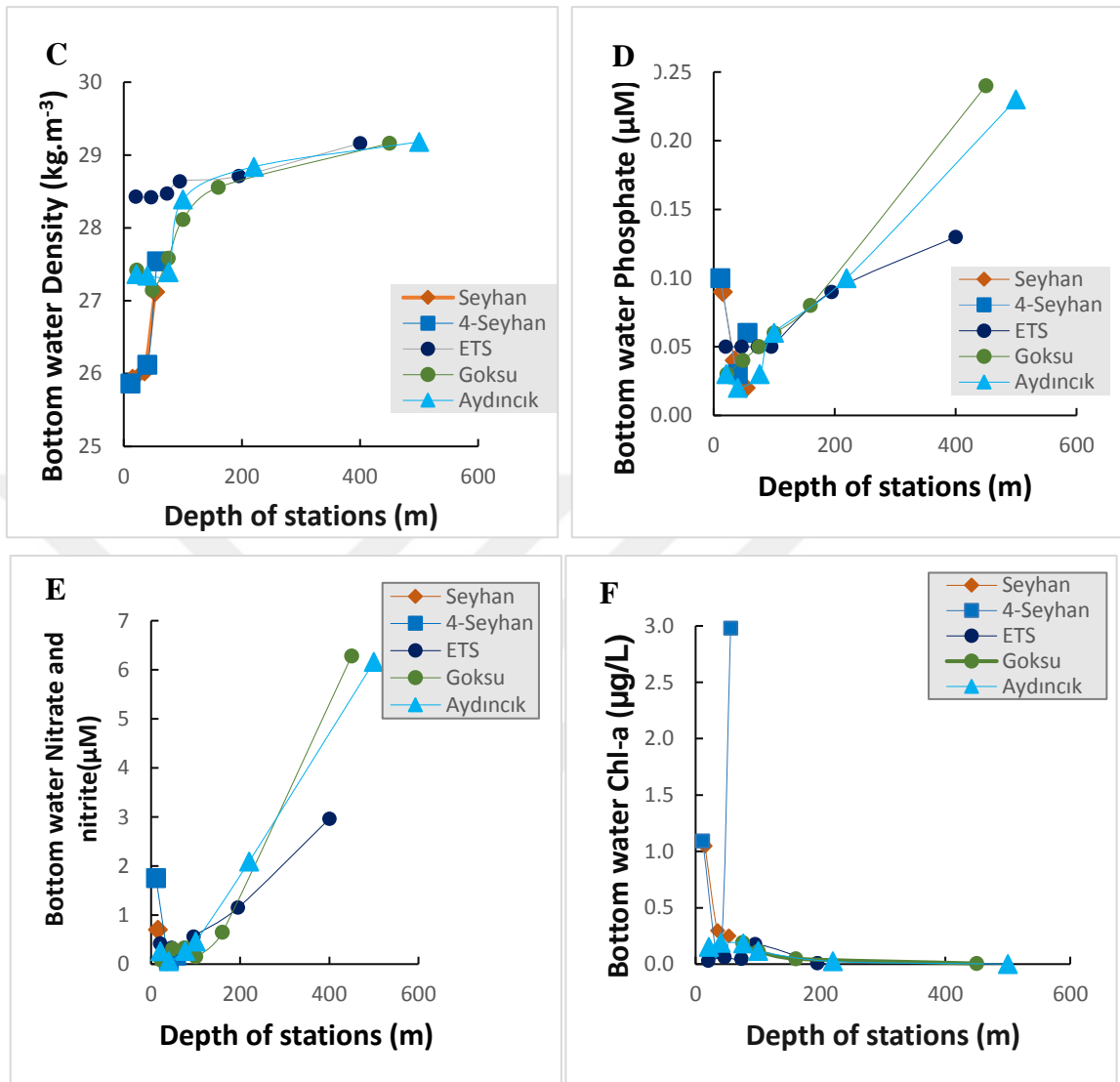
Figure 4.5. Bottom seawater parameter data of Stations in 4 transects. **A.** Temperature (°C) **B.** Salinity (psu) **C.** Density (kg.m^{-3}) **D.** Phosphate (µM) **E.** Nitrate+Nitrite (µM) **F.** Chlorophyll-a (µg/L). Each dot is a station from shallow to deep sea and represented as by different color (continued).

45

4.2 Grain size distribution

 Sediment samples comprised of diverse particle size distribution in Cilician Basin. Grain size is classified via particle diameter (Fig.4.6) giving hint to formation of the particle, settling velocity of the particle in the marine environment, biogeochemical processes in the sediment. The particles having diameter more than 2 mm are classified as gravel, 2-0.063 mm diameter particles as sand, less than 0.063 mm silt and clay (mud fraction) (Fig.4.6). The size of particle gains importance from its content, its interaction with biology and geochemistry. The particle size in sediment is also substantial since the micro-size particles being able to interact with microbes and adsorbed metals. In Seyhan transect, the sediments mostly consisted of mud in the range of 79-92% except the 63% station 7. ETS transect included non-uniform distribution with depth; coastal station was 63% gravel and sand. The grain size constantly decreased with depth in Göksu (20-89%) transect whereas Aydıncık transect showed large variation of particle sizes (28-94%) with water depth.

Millimeters (mm)	Micrometers (μm)	Phi (φ)	Wentworth size class	
4096		-12.0	Boulder	Gravel
256		-8.0	Cobble	
64		-6.0	Pebble	
4		-2.0	Granule	
2.00		-1.0		
1.00		0.0	Very coarse sand	Sand
1/2 0.50	500	1.0	Coarse sand	
1/4 0.25	250	2.0	Medium sand	
1/8 0.125	125	3.0	Fine sand	
1/16 0.0625	63	4.0	Very fine sand	
1/32 0.031	31	5.0	Coarse silt	Silt
1/64 0.0156	15.6	6.0	Medium silt	
1/128 0.0078	7.8	7.0	Fine silt	
1/256 0.0039	3.9	8.0	Very fine silt	
0.00006	0.06	14.0	Clay	Mud

Figure 4.6. :Udden-Wentworth grain-size classification of terrigeneous sediments (from Wentworth, 1922).

In Seyhan transect, sediments were classified mainly mud. The ETS transect samples were classified as mostly fine sand in the coastline and mud in the offshore whereas Goksu samples were dominated by coarse sand in the coast and mud in the offshore. The very

fine sand was predominant in the coastal Aydıncık samples, which became mud in the offshore sediment samples (Fig. 4.7).
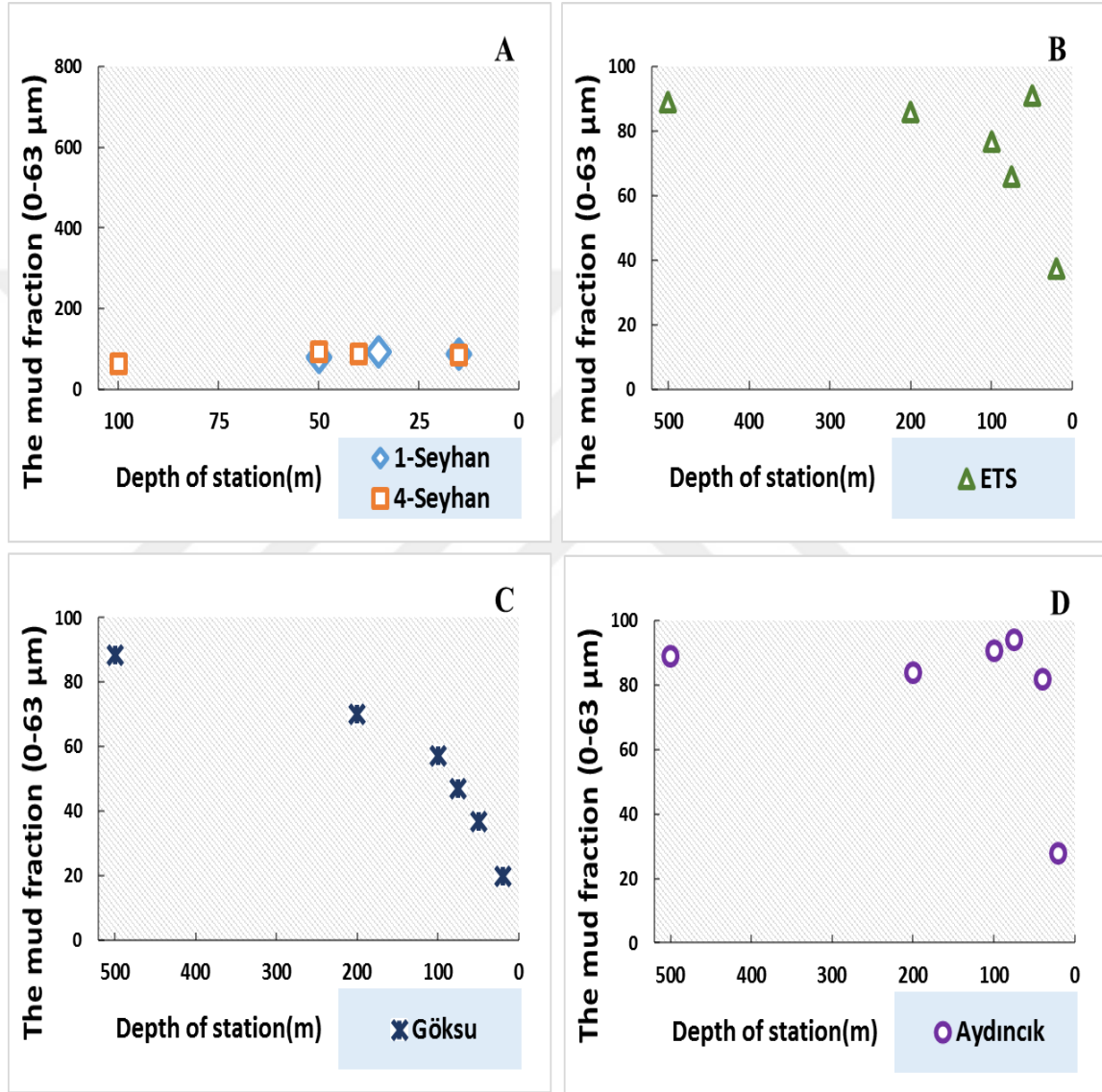
Figure 4.7. The distribution of mud fraction in Seyhan, ETS, Göksu and Aydıncık Transects sediment samples with depth of stations(m). **A.** Seyhan Transect Stations 1-7(0-63µm grain size), **B.** ETS Transect Stations 8-13 (0-63µm grain size), **C.** Göksu Transect Stations 14-19 (0-63µm grain size), **D.** Aydıncık Transect Stations 20-25 (0-63µm grain size).

Table 4.5. Station number, transect name and the grain size of sediments in this study.

Station number-Transect name/ Grain size	>2 mm	1 mm	500 μm	250 μm	125 μm	63 μm	32 μm	16 μm	8 μm	4 μm
1-Seyhan	0.01	0.02	0.24	2.91	8.49	18.55	19.22	15.71	12.86	21.86
2- Seyhan	0.02	0.02	0.04	2.31	5.80	11.0	16.93	18.88	17.02	27.82
3- Seyhan	1.51	1.42	1.80	6.28	9.77	13.94	15.62	15.15	13.31	21.07
4- Seyhan	0.07	0.20	0.52	3.45	10.78	23.12	20.94	13.77	10.22	16.84
5- Seyhan	0.09	0.08	0.32	4.94	6.21	8.67	14.91	18.34	17.43	28.86
6- Seyhan	0.57	0.29	0.34	1.43	4.72	9.31	14.72	18.45	18.66	31.32
7- Seyhan	3.11	3.33	4.98	13.89	11.75	11.57	12.13	11.99	10.59	16.55
8-ETS	0.70	0.45	8.17	31.65	21.64	12.38	7.15	5.03	4.44	8.31
9-ETS	0.05	0.02	0.03	1.36	7.31	16.61	17.33	15.41	14.20	27.56
10-ETS	1.99	3.27	5.06	16.24	7.45	8.18	9.90	12.10	12.92	22.71
11-ETS	1.95	2.03	3.08	8.35	7.70	9.62	12.54	14.62	14.62	25.31
12-ETS	n.a	n.a	n.a	n.a	n.a	n.a	n.a	n.a	n.a	n.a
13-ETS	n.a	n.a	n.a	n.a	n.a	n.a	n.a	n.a	n.a	n.a
14-Göksu	10.36	13.81	19.50	30.58	5.79	3.73	3.78	3.98	3.24	5.19
15-Göksu	18.19	9.51	11.32	20.89	3.13	3.27	5.80	7.79	7.82	12.11
16-Göksu	0.63	4.15	15.34	29.69	3.07	3.71	7.03	9.67	10.12	16.43
17-Göksu	7.29	5.88	8.39	15.62	5.33	7.29	10.00	11.57	11.12	17.35
18-Göksu	6.25	7.87	7.20	5.30	3.24	6.06	9.14	12.26	13.74	28.76
19-Göksu	0.00	0.00	0.07	4.27	6.87	9.46	14.20	16.83	16.96	31.11

Table 4.5. Station number, transect name and the grain size of sediments in this study(continued).

Station number-Transect name/ Grain size	>2 mm	1 mm	500 μm	250 μm	125 μm	63 μm	32 μm	16 μm	8 μm	4 μm
20-Aydıncık	0.00	0.03	0.18	25.95	45.92	16.13	2.88	2.76	2.15	3.99
21-Aydıncık	0.07	0.05	0.56	5.13	12.16	20.97	17.30	13.40	11.11	19.12
22-Aydıncık	0.09	0.06	0.21	1.47	4.04	12.20	18.76	19.63	16.45	26.96
23-Aydıncık	0.40	0.29	0.51	1.85	6.03	11.41	15.61	18.03	16.77	28.91
24-Aydıncık	0.00	0.00	0.42	5.46	10.17	12.92	13.78	14.61	14.61	27.86
25-Aydıncık	0.00	0.00	0.15	3.79	6.79	9.49	14.34	17.43	17.09	30.73

Table 4.6. Station number, transect name and the total % grain size of samples in this study.

Station number-Transect name/ Total % Grain size of samples	Mud Fraction 0-63 μm	>63 μm
1-Seyhan	88.20	11.68
2- Seyhan	91.66	8.18
3- Seyhan	79.09	20.78
4- Seyhan	84.89	15.03
5- Seyhan	88.21	11.63
6- Seyhan	92.46	7.35
7- Seyhan	62.82	37.06
8-ETS	37.32	62.60
9-ETS	91.10	8.77
10-ETS	65.80	34.01
11-ETS	76.71	23.11
12-ETS	n.a	n.a
13-ETS	n.a	n.a

Table 4.6. Station number, transect name and the total % grain size of samples in this study (continued).

Station number-Transect name/ Total % Grain size of samples	Mud Fraction 0-63 µm	>63 µm
14-Göksu	19.91	80.04
15-Göksu	36.78	63.04
16-Göksu	46.96	52.88
17-Göksu	57.34	42.52
18-Göksu	69.96	29.86
19-Göksu	88.56	11.22
20-Aydıncık	27.92	72.08
21-Aydıncık	81.89	17.98
22-Aydıncık	94.01	5.87
23-Aydıncık	90.73	9.08
24-Aydıncık	83.77	16.06
25-Aydıncık	89.07	10.73

4.3 Reactive iron, total iron and organic carbon content in seafloor samples.

Seyhan Transect:

Dithionite extracted iron and manganese in sediments were determined as in the following concentrations (all per g dry weight); reactive Fe (Fe_R) in Seyhan transect varied between 54-81 µmol/dry g and reactive Mn (Mn_R) between 1.9-2.7 µmol/dry g (Fig. 4.8). Total iron(Fe_T) ranged from 464-663 µmol/dry g and total Mn (Mn_T) was between 9.9-10.7 µmol/dry g. Al ranged within 1541-2251 µmol/dry g. The organic carbon in the transect varied between 0.38 and 0.54 mmol/dry g, in station 4. Maximum value was observed in station 4, whereas the minimum value was found in stations 3 and 7. Total nitrogen content of sediment samples varied within 0.03-0.05 mmol/dry g, the sub-transect stations 1-3 had its maximum in 35 m depth but the stations 4-6 had the same nitrogen for each depth (Fig.4.8).
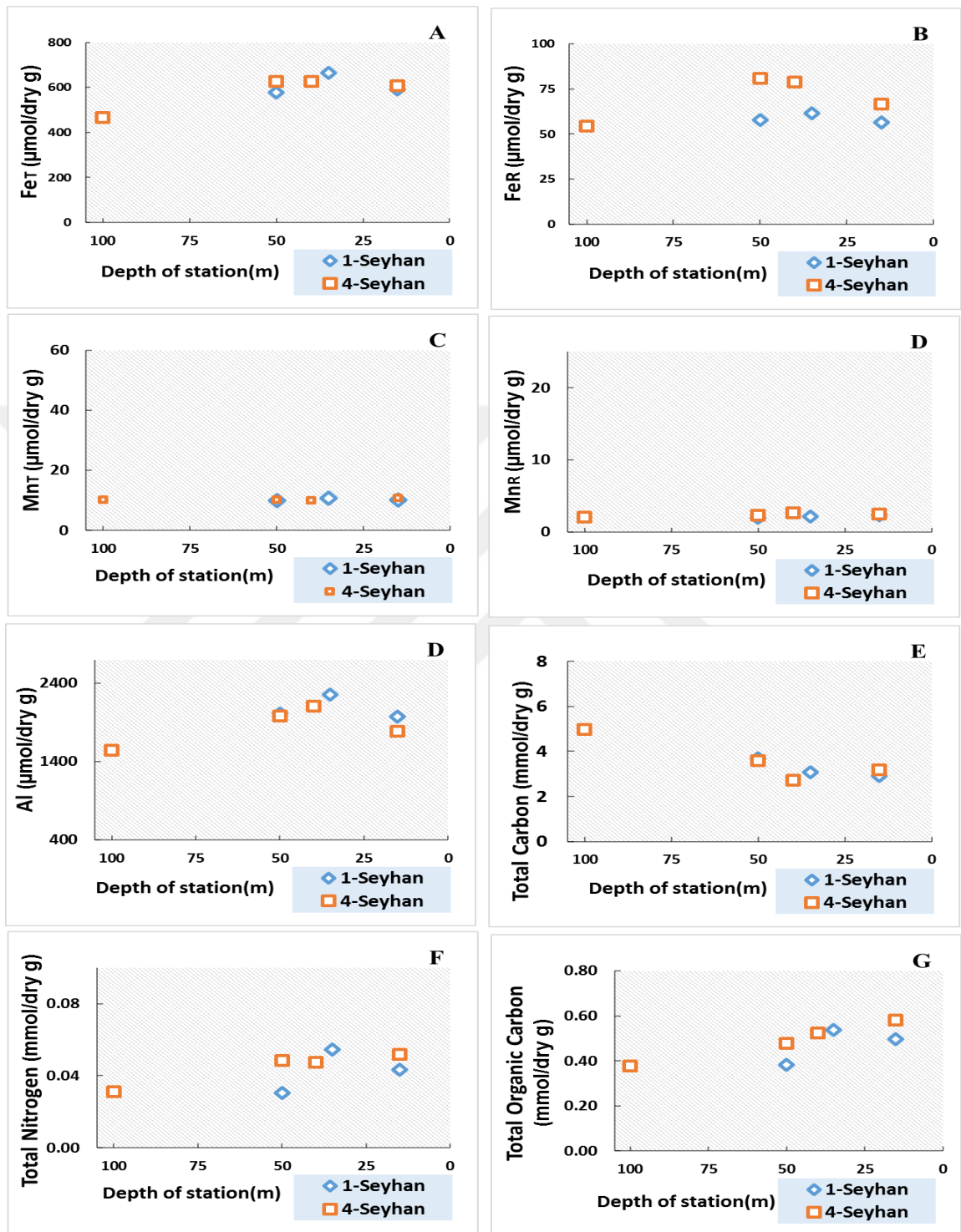
Figure 4.8. The distribution of **A.** Total Fe (Fe$_T$) (µmol/dry g), **B.** Reactive Fe (Fe$_R$) (µmol/dry g), **C.** Total Mn (Mn$_T$) (µmol/dry g), **D.** Reactive Mn (Mn$_R$) (µmol/dry g),, **E.**Total Aluminum(Al) (µmol/dry g), **F.** Total Carbon (mmol/dry g), G. Total Nitrogen (mmol/dry g), **H**. Total Organic Carbon (mmol/dry g) in the Seyhan sediments with depth of stations 1-7 in the transect.

In this transect, bottom water nitrate and nitrite ranged in 0.06-1.75 µM where the station 2 had the minimum value. No trend was observed within the transect except that stations at 40m depth had the minimum values in the transect.

The Fe_R/ Fe_T molar ratio/dry g ratio for each station was calculated to assess reactive iron and manganese enrichment in seafloor. The ratio for iron was averaged 0.10±0.017. For entire transect the range was 0.09-0.13. The Mn_R/ Mn_T molar ratio/dry g varied between 0.20±0.03. Station 5 and 6 (40m, 50m) had the highest value of the Fe_R/Fe_T ratio . The Mn_R/Mn_T ratio in stations 1, 4 (15m) and 7(100 m) was the highest. An alternative approach to determine Fe enrichment in sediment was total Fe to aluminum ratios (Lyons et al., 2003; Lyons and Severmann, 2006) since this ratio is independent of specific reactive phases, and preserved over lithogenic background (Scholz et al., 2014, Lyons and Severmann, 2006). The Fe_T/Al molar ratio/dry g was 0.34 in stations 4-6 and 0.32 in station 1-3 and 7. The increase in the reactive iron enrichment (Fe_R/Fe_T) in the station 4-6 was observed in the Fe_T/Al molar ratio/dry g in the stations 1-3 sub-transect.

ETS transect:

Fe_R in the coastal station was 40.5 µmol/dry g, there was a dramatic decrease in station 11 (100m depth) to 29.2 µmol/dry g, then reached to its maximum 56.6 µmol/dry g in the open station (500m) with a total average of 42.5 µmol/dry g (Fig.4.9). Total iron in the ETS transect was between 599-722 µmol/dry g. The average Mn_R concentration in station 8-12 (from 25 to 200 m depth) was 0.89 µmol/dry g but there was an interesting jump in the station 13 (500m) to 21.6 µmol/dry g. This jump correlated well with Mn_T data, which was approximately 4 times higher than average Mn_T through the transect. The average of Mn_T was 11.1 µmol/ dry g in station 8-12, the station 13 has 53.9 µmol /dry g. Fe_R/Fe_T in the transect in 25 m depth sediment was 0.07 molar ratio/dry g and decreased to its minimum in 100m depth station 11, 0.04 molar ratio/dry g. The Fe enrichment in station 13 was the maximum with 0.08 molar ratio/dry g. The Fe_T/Al ratio decreased through the transect from 0.47 to 0.33 molar ratio/dry g away from the coast. Likewise, Mn_R/Mn_T ratio increased through offshore from 0.06 to 0.12 molar ratio/dry g (200m) and finally to 0.40 the outlier data in the deepest station of this transect.
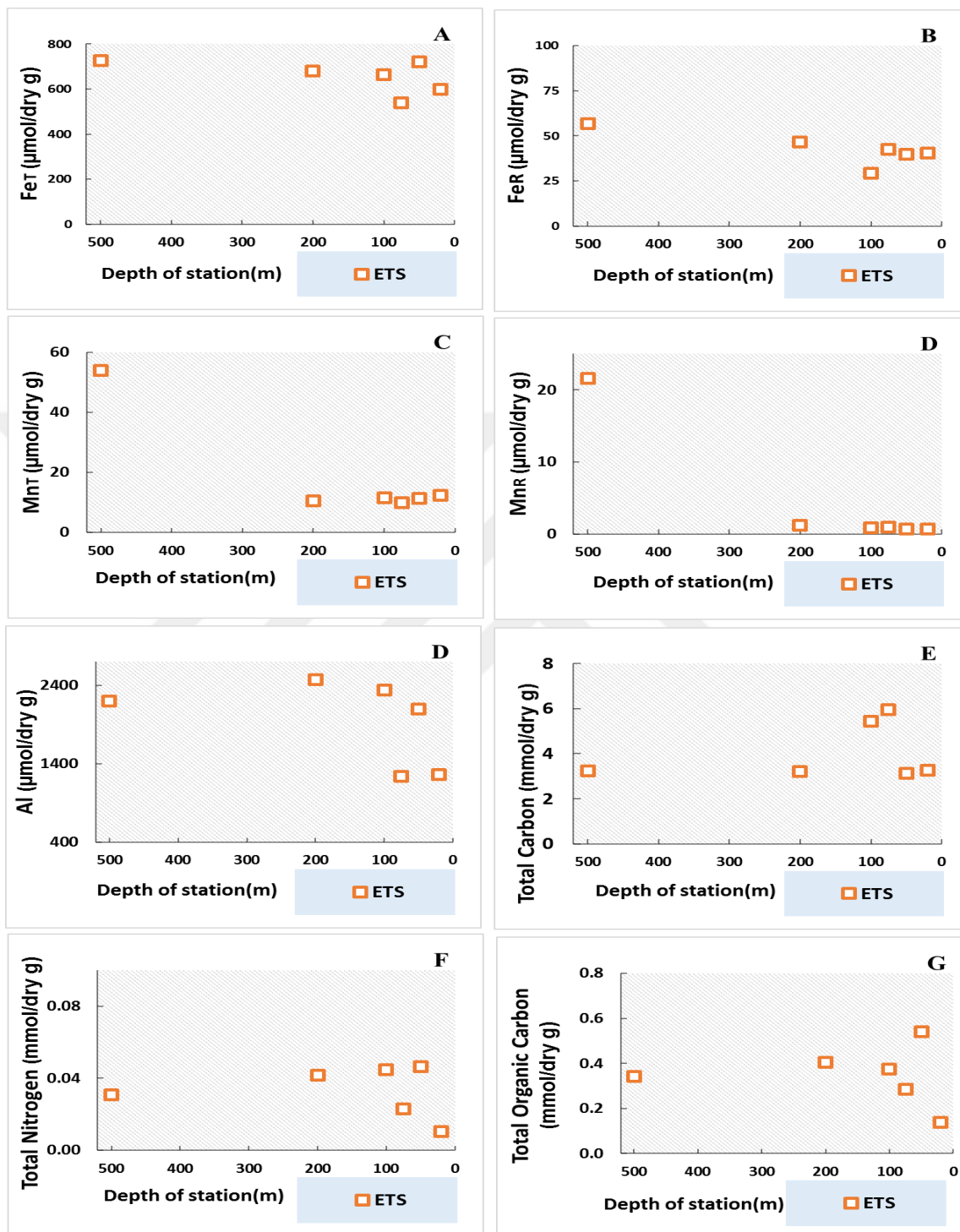
Figure 4.9. The distribution of **A.** Total Fe (Fe$_T$) (µmol/dry g), **B.** Reactive Fe (Fe$_R$) (µmol/dry g), **C.** Total Mn (Mn$_T$) (µmol/dry g), **D.** Reactive Mn (Mn$_R$) (µmol/dry g), **E.**Total Aluminum(Al) (µmol/dry g), **F.** Total Carbon (mmol/dry g), G. Total Nitrogen (mmol/dry g), **H**. Total Organic Carbon (mmol/dry g) in the ETS sediments with depth of stations 8-13 in the transect.

The total organic carbon concentration in the transect did not have trend, the data were only slightly different in the stations (between 0.14-0.54 mmol/dry g, maximum in 50m). Besides, the total organic carbon over total nitrogen slightly decreased with 200m depth (from 13.3 to 9.7 molar ratio/dry g), followed by increase in the 500 m station (11.1 ratio). The organic carbon over total carbon (TOC/TC) molar ratio/dry g changed in the range of 4-17 without a clear trend in transect.

Göksu Transect:

In Göksu transect, reactive iron varied between 34-56 µmol /dry g, slightly increasing from the coast to the open sea with an average of 43.9 µmol /dry g (Fig.4.10). In contrast to the reactive iron trend, Mn_R increased from 0.50 to 2.8 µmol /dry g towards to open sea with average of 1.30 µmol /dry g (Fig. 4.10). The total iron concentration displayed a continuous increase towards the offshore from 238 to 632 µmol /dry g whereas total Mn varied in the range of 7-13 µmol /dry g. In Göksu transect, both Fe_R and Fe_T increase with water depth but Fe_T increase is more than Fe_R increase. Therefore, the seafloor sediment was getting poor in relative % of reactive iron content as the Fe_R/Fe_T ratio showed a continuous decrease towards the offshore. The coastal station had 0.16 µmol /dry g Fe_R/Fe_T ratio which reached a minimum of 0.09 molar ratio /dry g in the 500m depth station. Similarly, the coastal Fe_T/Al molar ratio/dry g, 0.48, decreased to 0.28 as the open seafloor sediment. Contrary to the decrease in Fe enrichment, Mn_R/Mn_T ratio increased with water depth from 0.06 to 0.21 molar ratio /dry g in these seafloor sediments.

The open station 19 was found to contain the highest value with 0.54 mmol/dry g total organic carbon(TOC) with TOC content decreasing towards the coastal stations (Fig. 4.10). The total carbon(TC) decreases from coastal to open sea stations. TOC/TC molar ratio/dry g increases from coastal to open sea stations. However, there was a slight decrease in station 17 and 18 (200m) and massive increase up to 16.2 molar ratio/dry g in the station 19. Likewise, TOC/TN molar ratio/dry g rose up to11.8 from 10.27 towards in the open surface sediment 200m but then, a sharp decline to 10.07 was observed in 500 m depth.
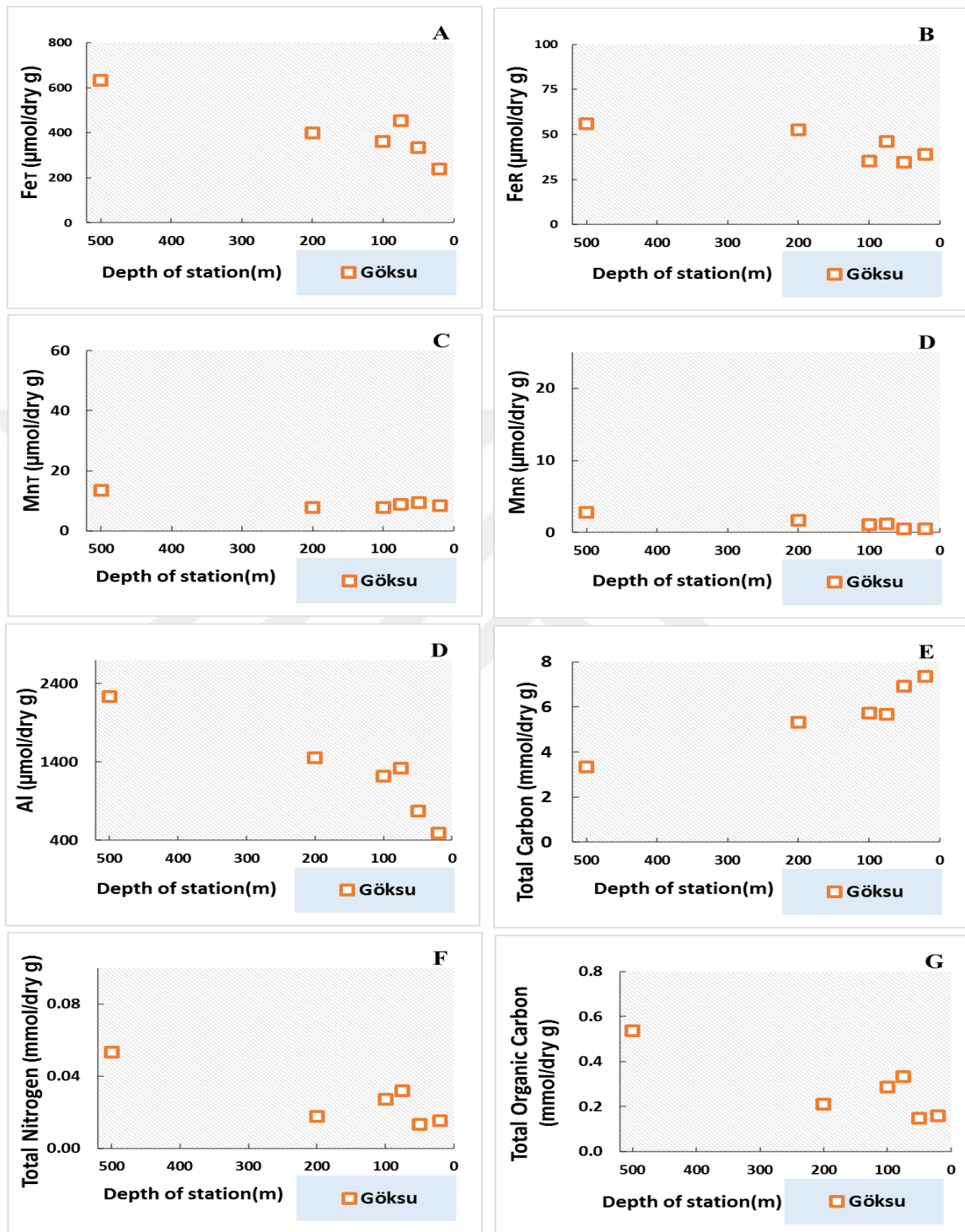
Figure 4.10. The distribution of **A.** Total Fe (Fe$_T$) (μmol/dry g), **B.** Reactive Fe (Fe$_R$) (μmol/dry g), **C.** Total Mn (Mn$_T$) (μmol/dry g), **D.** Reactive Mn (Mn$_R$) (μmol/dry g), **E.**Total Aluminum(Al) (μmol/dry g), **F.** Total Carbon (mmol/dry g), G. Total Nitrogen (mmol/dry g), **H**. Total Organic Carbon (mmol/dry g) in the Göksu sediments with depth of stations 14-19 in the transect.

Aydıncık Transect:

The reactive iron in Aydıncık transect varied between 53-97 µmol /dry g, Mn_R 0.64-1.68 µmol /dry g. The maximum concentrations were observed in station 22 (75m) and station 25 (500m). Total iron amount increased up to 644 µmol /dry g from 208 µmol /dry g with a similar increase of up to 3 fold in Mn_T towards the offshore. Total Mn_T amount increased up to 13.7 µmol /dry g from 4.1 µmol /dry g (Fig. 4.11). In this manner, the ratio of reactive iron to total iron content was in the range of 0.11-0.26 molar ratio/dry g being lower in the open stations. On contrary, the Mn_R/Mn_T molar ratio/dry g increased with depth (from 0.15 to 0.27). Fe_T/Al decreased with depth however the Fe enrichment in the transect did not have the same trend as Fe_T/Al molar ratio/dry g.

The total organic carbon in Aydıncık increased with depth from 0.21 to 0.77 mmol/ dry g, with a sharp rise in station 22 (Fig. 4.11). The total organic carbon to total carbon(TOC/TC) molar ratio/dry g was more than 3 times higher in the open station.
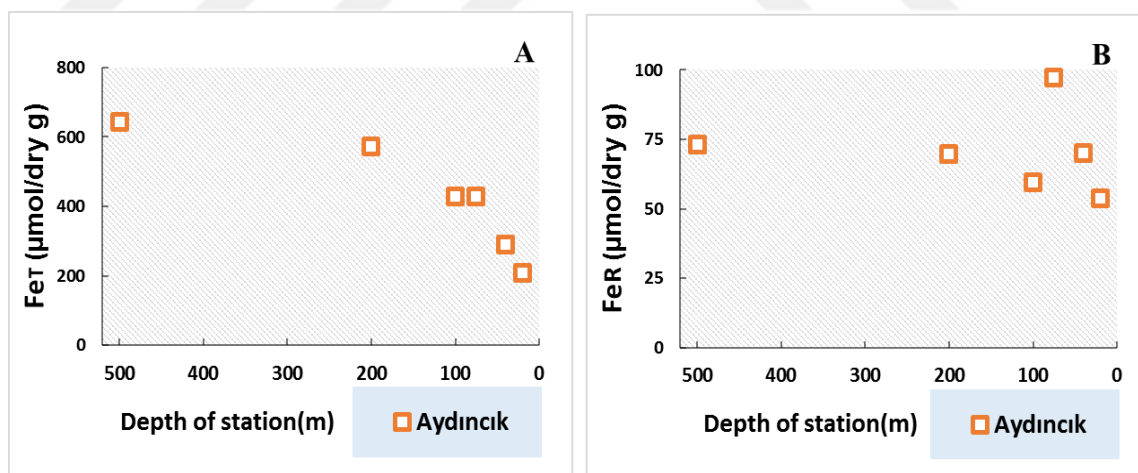
Figure 4.11. The distribution of **A.** Total Fe (Fe_T) (µmol/dry g), **B.** Reactive Fe (Fe_R) (µmol/dry g), **C.** Total Mn (Mn_T) (µmol/dry g), **D.** Reactive Mn (Mn_R) (µmol/dry g), **E.**Total Aluminum(Al) (µmol/dry g), **F.** Total Carbon (mmol/dry g), G. Total Nitrogen (mmol/dry g), **H**. Total Organic Carbon (mmol/dry g) in the Aydıncık sediments with depth of stations 20-25 in the transect.

The total organic carbon to total nitrogen(TOC/TN) molar ratio/dry g ranged within 8-14 with highest ratio in station 22. This station also had maximum mud fraction which was 94%.
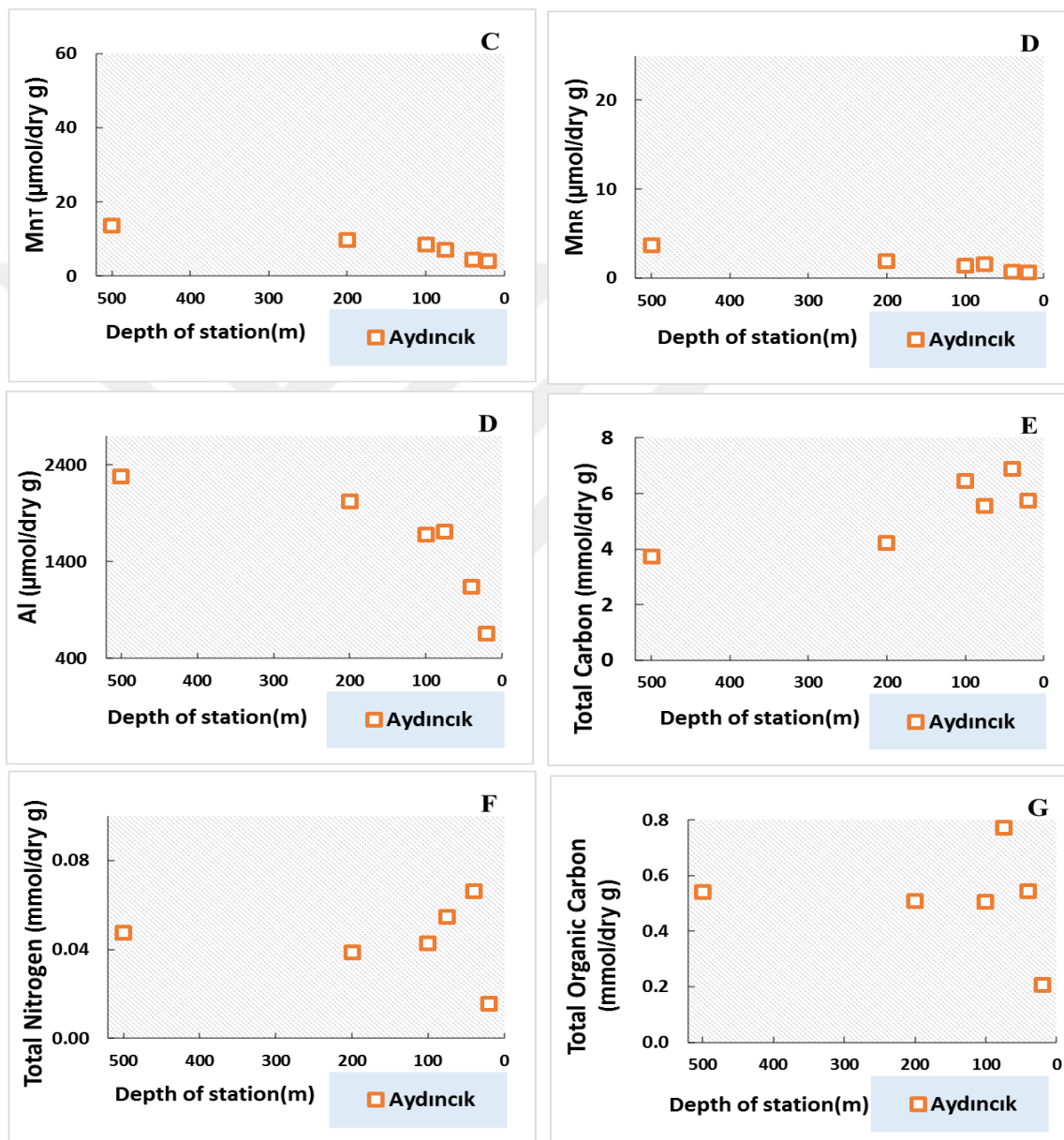
Figure 4.11. The distribution of **A.** Total Fe (Fe$_T$) (µmol/dry g), **B.** Reactive Fe (Fe$_R$) (µmol/dry g), **C.** Total Mn (Mn$_T$) (µmol/dry g), **D.** Reactive Mn (Mn$_R$) (µmol/dry g), **E.**Total Aluminum(Al) (µmol/dry g), **F.** Total Carbon (mmol/dry g), G. Total Nitrogen (mmol/dry g), **H**. Total Organic Carbon (mmol/dry g) in the Aydıncık sediments with depth of stations 120-25 in the transect(continued).

4.4 The distribution of other major elements and trace metals

Trace metals in marine environment have significant roles not only being essential micronutrient, but also having reduction-oxidation reaction capacity essential for microbial life in seafloor ecosystem. In this thesis, vanadium, zinc, nickel, cobalt, chromium, rubidium, strontium, magnesium and potassium concentrations of sediment samples were studied for 25 stations.

Total Mg, Ca and K major elements concentrations in Cilician seafloor sediments are presented in Table 4.7. Magnesium concentration varied in the range of 1116-2041 µmol/ dry g with the maximum in coastal ETS station 8, the minimum in Seyhan station 5. The concentration of potassium was in the range of 714-1058 µmol/dry g whereas the range of calcium concentration was 1312-2765 µmol/dry g. The geology of the region in other words the types of rocks in the drainage basin has great influence on the distribution of these elements.

The total content of trace metals is given in Table 4.8. The concentration of redox sensitive element vanadium in the transects was in the range of 0.15-0.20 µmol/dry g. There was a variation in Seyhan and ETS samples, but there were almost twice increase towards the open sea in Göksu and Aydıncık transects. The concentration of other trace metals is given in table with average values, minimum and maximum values.

Table 4.7. Station name, depth of station (m), Magnesium (µmol/dry g), Potassium (µmol/dry g), Calcium (µmol/dry g) in Cilician sediments.

Station Name	Depth (m)	Mg µmol/dry g	K µmol/dry g	Ca µmol/dry g
1-Seyhan	15	2026	768	1312
2-Seyhan	35	1312	876	1447
3-Seyhan	50	1184	743	1813
4-Seyhan	15	1542	930	1531
5-Seyhan	40	1116	776	1315
6-Seyhan	50	1288	822	1668

Table 4.7. Station name, depth of station (m), Magnesium (µmol/dry g), Potassium (µmol/dry g), Calcium (µmol/dry g) in Cilician sediments (continued).

Station Name	Depth (m)	Mg µmol/dry g	K µmol/dry g	Ca µmol/dry g
7-Seyhan	100	1511	871	2276
	minimum:	1116	743	1312
	maximum:	2026	930	2276
	Average:	1426	826	1623
	Standard Deviation:	308	69	340
8-ETS	20	2041	714	1898
9-ETS	50	1891	918	1753
10-ETS	75	1644	838	2451
11-ETS	100	1726	1058	2765
12-ETS	200	1541	1012	1577
13-ETS	500	1836	886	1836
	minimum:	1541	714	1577
	maximum:	2041	1058	2765
	Average:	1780	904	2047
	Standard Deviation:	180	124	459
14-Göksu	20	1369	743	2984
15-Göksu	50	1524	781	3620
16-Göksu	75	1625	902	3141
17-Göksu	100	1509	853	2785
18-Göksu	200	1465	853	2375
19-Göksu	500	1384	883	1573
	minimum:	1369	743	1573
	maximum:	1625	902	3620
	Average:	1479	836	2746
	Standard Deviation:	96	61	706
20-Aydıncık	20	1275	803	3100

Table 4.7. Station name, depth of station (m), Magnesium (µmol/dry g), Potassium (µmol/dry g), Calcium (µmol/dry g) in Cilician sediments (continued).

Station Name	Depth (m)	Mg µmol/dry g	K µmol/dry g	Ca µmol/dry g
21-Aydıncık	40	1343	893	2387
22-Aydıncık	75	1362	946	2695
23-Aydıncık	100	1402	902	2824
24-Aydıncık	200	1547	969	2202
25-Aydıncık	500	1452	936	1836
	minimum:	1275	803	1836
	maximum:	1547	969	3100
	Average:	1397	908	2507
	Standard Deviation:	94	59	457

Table 4.8. Station name, depth of station (m), Vanadium (µmol/dry g), Chromium (µmol/dry g), Cobalt (µmol/dry g), Nickel (µmol/dry g), Cupper (µmol/dry g), Zinc (µmol/dry g), Gallium (µmol/dry g) in Cilician sediments. The minimum (min), maximum (max), average (ave) and standard deviation (sd) of each transect is given.

Station Name	Depth (m)	V	Cr	Co	Ni	Cu	Zn	Ga
1-Seyhan	15	0.16	0.27	0.04	0.32	0.052	0.13	0.026
2-Seyhan	35	0.18	0.28	0.04	0.32	0.054	0.15	0.027
3-Seyhan	50	0.18	0.25	0.04	0.29	0.044	0.13	0.023
4-Seyhan	15	0.17	0.31	0.05	0.37	0.060	0.17	0.031
5-Seyhan	40	0.17	0.25	0.04	0.29	0.049	0.13	0.024
6-Seyhan	50	0.18	0.25	0.04	0.30	0.049	0.14	0.025
7-Seyhan	100	0.18	0.21	0.04	0.29	0.051	0.16	0.023
	min:	0.16	0.21	0.04	0.29	0.044	0.13	0.023
	max:	0.18	0.31	0.05	0.37	0.060	0.17	0.031
	Ave:	0.17	0.26	0.04	0.31	0.051	0.14	0.026
	sd:	0.01	0.03	0.00	0.03	0.005	0.02	0.003

Table 4.8. Station name, depth of station (m), Vanadium (µmol/dry g), Chromium (µmol/dry g), Cobalt (µmol/dry g), Nickel (µmol/dry g), Cupper (µmol/dry g), Zinc (µmol/dry g), Gallium (µmol/dry g) in Cilician sediments. The minimum (min), maximum (max), average (ave) and standard deviation (sd) of each transect is given (continued).

Station Name	Depth (m)	V	Cr	Co	Ni	Cu	Zn	Ga
8-ETS	20	0.20	0.51	0.07	0.79	0.050	0.15	0.017
9-ETS	50	0.18	0.35	0.05	0.57	0.053	0.16	0.022
10-ETS	75	0.22	0.31	0.06	0.47	0.049	0.17	0.018
11-ETS	100	0.22	0.30	0.05	0.39	0.060	0.19	0.025
12-ETS	200	0.20	0.26	0.04	0.33	0.059	0.16	0.026
13-ETS	500	0.19	0.33	0.05	0.49	0.060	0.16	0.023
	min:	0.18	0.26	0.04	0.33	0.049	0.15	0.017
	max:	0.22	0.51	0.07	0.79	0.060	0.19	0.026
	Ave:	0.20	0.34	0.05	0.51	0.055	0.17	0.022
	sd:	0.02	0.09	0.01	0.16	0.005	0.01	0.004
14-Göksu	20	0.09	0.08	0.03	0.14	0.034	0.12	0.012
15-Göksu	50	0.13	0.14	0.04	0.18	0.037	0.13	0.015
16-Göksu	75	0.16	0.16	0.04	0.27	0.045	0.14	0.019
17-Göksu	100	0.15	0.16	0.04	0.26	0.046	0.14	0.018
18-Göksu	200	0.17	0.18	0.04	0.29	0.049	0.14	0.019
19-Göksu	500	0.19	0.26	0.04	0.34	0.056	0.15	0.024
	min:	0.09	0.08	0.03	0.14	0.034	0.12	0.012
	max:	0.19	0.26	0.04	0.34	0.056	0.15	0.024
	Ave:	0.15	0.16	0.04	0.25	0.045	0.14	0.018
	sd:	0.03	0.06	0.00	0.07	0.008	0.01	0.004
20-Aydıncık	20	0.08	0.08	0.03	0.13	0.033	0.11	0.019
21-Aydıncık	40	0.15	0.13	0.03	0.19	0.056	0.16	0.023
22-Aydıncık	75	0.17	0.15	0.03	0.20	0.050	0.15	0.025
23-Aydıncık	100	0.16	0.15	0.03	0.23	0.051	0.15	0.022

Table 4.8. Station name, depth of station (m), Vanadium (µmol/dry g), Chromium (µmol/dry g), Cobalt (µmol/dry g), Nickel (µmol/dry g), Cupper (µmol/dry g), Zinc (µmol/dry g), Gallium (µmol/dry g) in Cilician sediments. The minimum (min), maximum (max), average (ave) and standard deviation (sd) of each transect is given(continued).

Station Name	Depth (m)	V	Cr	Co	Ni	Cu	Zn	Ga
24-Aydıncık	200	0.19	0.24	0.04	0.33	0.059	0.17	0.026
25-Aydıncık	500	0.19	0.24	0.04	0.33	0.060	0.15	0.026
	min:	0.08	0.08	0.03	0.13	0.033	0.11	0.019
	max:	0.19	0.24	0.04	0.33	0.060	0.17	0.026
	Ave:	0.16	0.16	0.04	0.24	0.052	0.15	0.024
	sd:	0.04	0.06	0.01	0.08	0.010	0.02	0.003

Table 4.9. Station name, depth of station (m), Arsenic (µmol/dry g), Selenium (µmol/dry g), Rubidium (µmol/dry g), Strontium (µmol/dry g), Caesium (µmol/dry g), Barium (µmol/dry g), Lead (µmol/dry g) in Cilician sediments. The minimum (min), maximum (max), average (ave) and standard deviation (Sd) of each transect is given.

Station Name	Depth (m)	As	Se	Rb	Sr	Cs	Ba	Pb
1-Seyhan	15	0.025	0.0040	0.051	0.19	0.0029	0.14	0.0037
2-Seyhan	35	0.029	0.0047	0.055	0.19	0.0034	0.12	0.0040
3-Seyhan	50	0.026	0.0024	0.047	0.50	0.0029	0.10	0.0034
4-Seyhan	15	0.030	0.0066	0.055	0.25	0.0031	0.16	0.0031
5-Seyhan	40	0.025	0.0039	0.053	0.17	0.0033	0.10	0.0042
6-Seyhan	50	0.031	0.0046	0.050	0.45	0.0030	0.10	0.0032
7-Seyhan	100	0.036	0.0024	0.044	1.01	0.0025	0.09	0.0025
	min:	0.025	0.0024	0.044	0.17	0.0025	0.09	0.0025
	max:	0.036	0.0066	0.055	1.01	0.0034	0.16	0.0042
	Ave:	0.029	0.0041	0.051	0.40	0.0030	0.11	0.0034

Table 4.9. Station name, depth of station (m), Arsenic (µmol/dry g), Selenium (µmol/dry g), Rubidium (µmol/dry g), Strontium (µmol/dry g), Caesium (µmol/dry g), Barium (µmol/dry g), Lead (µmol/dry g) in Cilician sediments. The minimum (min), maximum (max), average (ave) and standard deviation (Sd) of each transect is given(continued).

Station Name	Depth (m)	As	Se	Rb	Sr	Cs	Ba	Pb
	sd:	0.004	0.0015	0.004	0.30	0.0003	0.03	0.0006
8-ETS	20	0.030	0.0018	0.024	0.23	0.0010	0.04	b.d
9-ETS	50	0.029	0.0047	0.045	0.22	0.0025	0.08	0.0009
10-ETS	75	0.054	0.0017	0.039	1.03	0.0024	0.05	0.0045
11-ETS	100	0.032	0.0020	0.057	0.83	0.0037	0.10	0.0046
12-ETS	200	0.042	0.0057	0.054	0.28	0.0033	0.10	0.0030
13-ETS	500	0.034	0.0047	0.040	0.34	0.0022	0.08	0.0017
	min:	0.029	0.0017	0.024	0.22	0.0010	0.04	b.d
	max:	0.054	0.0057	0.057	1.03	0.0037	0.10	0.0046
	Ave:	0.037	0.0034	0.043	0.49	0.0025	0.07	0.0021
	sd:	0.009	0.0018	0.012	0.35	0.0009	0.02	0.0026
14-Göksu	20	0.048	0.0012	0.026	1.96	0.0012	0.03	b.d
15-Göksu	50	0.050	0.0009	0.029	1.50	0.0016	0.05	b.d
16-Göksu	75	0.039	0.0012	0.040	1.19	0.0024	0.08	0.0006
17-Göksu	100	0.030	0.0014	0.043	1.36	0.0026	0.07	0.0001
18-Göksu	200	0.027	0.0026	0.047	0.83	0.0032	0.07	b.d
19-Göksu	500	0.033	0.0044	0.049	0.27	0.0031	0.09	0.0055
	min:	0.027	0.0009	0.026	0.27	0.0012	0.03	b.d
	max:	0.050	0.0044	0.049	1.96	0.0032	0.09	0.0055
	Ave:	0.038	0.0019	0.039	1.19	0.0024	0.06	0.0001
	sd:	0.010	0.0013	0.010	0.58	0.0008	0.02	0.0029

Table 4.9. Station name, depth of station (m), Arsenic (µmol/dry g), Selenium (µmol/dry g), Rubidium (µmol/dry g), Strontium (µmol/dry g), Caesium (µmol/dry g), Barium (µmol/dry g), Lead (µmol/dry g) in Cilician sediments. The minimum (min), maximum (max), average (ave) and standard deviation (Sd) of each transect is given(continued).

Station Name	Depth (m)	As	Se	Rb	Sr	Cs	Ba	Pb
20-Aydıncık	20	0.030	0.0002	0.030	0.77	0.0011	0.12	b.d
21-Aydıncık	40	0.032	0.0020	0.051	0.86	0.0029	0.11	0.0025
22-Aydıncık	75	0.033	0.0031	0.055	0.60	0.0035	0.12	0.0026
23-Aydıncık	100	0.029	0.0024	0.050	0.77	0.0033	0.10	0.0020
24-Aydıncık	200	0.036	0.0042	0.058	0.48	0.0038	0.11	0.0052
25-Aydıncık	500	0.034	0.0046	0.054	0.33	0.0035	0.10	0.0053
	min:	0.029	0.0002	0.030	0.33	0.0011	0.10	b.d
	max:	0.036	0.0046	0.058	0.86	0.0038	0.12	0.0053
	Ave:	0.032	0.0028	0.050	0.64	0.0030	0.11	0.0025
	sd:	0.003	0.0016	0.010	0.20	0.0010	0.01	0.0027

CHAPTER IV

5. DISCUSSION

5.1 The comparison of results of 3 main transects in Cilician Basin

The reactive iron enrichment, in other words reactive iron to iron molar ratio/dry g (Fe_R/Fe_T) in Seyhan and ETS transects displays varied distribution with water depth but the Göksu and Aydındık transects it clearly shows a decrease in enrichment with water depth. There is little increase in Fe_R/Fe_T with water depth. ETS transect shows no significant change in Fe_R/Fe_T. Göksu transect decreases in reactive Fe with water depth. There is a distinct decrease in reactive Fe fraction with water depth. The reactive Fe fraction with water depth has the minimum average 0.07 in ETS and the maximum average 0.18 in Aydıncık transect (Table 5.1).

The Fe_T/Al molar ratio/dry g in the transects has the minimum average 0.27 molar ratio/dry g in Aydıncık and maximum average 0.36 in ETS. The decrease in Fe_T/Al ratio with water depth in the transect indicates that the Fe content decreases with increasing clay fraction due to finer grain size fraction is related to high Al content in sediment. Thus, Fe_T/Al is a normalization method used in sediment geochemistry that gives hints about the enrichment of Fe in the clay fraction (Çağatay, 2004). The reactive iron enrichment in Aydıncık from coastal to open seafloor imply a non-lithogenic enrichment of reactive iron in the surface sediments which is supported by the minimum Fe_T/Al ratio within all transects. This indicates that Fe_T is enriched in coarser fraction.In Seyhan transect Fe_T/Al molar ratio/dry g decreases with water depth whereas Fe_R/Al inreases with water depth. ETS transect decreases in Fe_T/Al ratio and shows no significant change in Fe_R/Al. Both Fe_T/Al and Fe_R/Al molar ratios decrese in Aydıncık and Göksu transects. Average Fe_R/Fe_T ratio of all transects is comparable with Oregon and California Margins surface sediments (Roy et al., 2013) and Black Sea sediments (Scholz et al., 2014b). Thus, Cilican Basin has high amount of reactive Fe species. Although, Fe_R/Fe_T ratio decreases towards the open sea, there are still sufficient and relatively high amount Fe for microbial reduction in open sea.

Further, organic matter decomposition in microbial reduction also is affected by the origin of organic matter. The marine organic matter is more prone to use by marine bacteria and promotes the high rates of biogeochemical reactions (Çağatay et al., 2001). The low TOC/TN ratio indicates the organic matter of marine origin. In all transects, TOC/TN ratio indicates the organic matter of terrestrial origin in the coastal surface sediments. This ratio decreases and gets close to <10 indicating the organic matter of marine origin. A striking finding in distribution of TOC/TN ratio in all transects is that the distinct decrease in this ratio (<10) up to 100 m water depth. Therefore, the organic matter of marine origin presents up to 100 m driving the biogeochemical reactions in the surface sediments.

The reactive Mn enrichment in the all transects shows increase in reactive Mn towards the open seafloor. Seyhan transect has no significant change in Mn_R/Mn_T molar ratio/dry g. ETS transect enriches 7 times in Mn_R/Mn_T molar ratio/dry g towards the open sea. Göksu and Aydıncık transects increase twice times in Mn_R/Mn_T ratio towards the open surface sediments. The highest Mn enrichment belongs to Seyhan 0.22, the lowest ratio 0.13 is in the ETS transect. The highest reactive manganese to organic carbon ratio in ETS transect resulted in an outlier (extremely high content of Mn compared to other stations). Previous works stated that in river dominated margins sediments Mn tends to mobilize towards the open seafloor, and reactive Mn dominates the coastal surface sediments than Fe (Roy et al., 2013).This trend in reactive Mn mobilization is seen in Cilican Basin seafloor. The enrichment of Mn towards the open seafloor infers the both upward vertical mobilization of Mn species formed by microbial reduction in downcore sediment and lateral transportation of Mn species towards to open seafloor in ETS, Göksu and Aydıncık transects. Table 5.2 shows the iron, manganese and related ratios in the transect with minimum, maximum, average and standard deviation for each transect.

Table 5.1. Station name, depth of station (m), Fe_R / Fe_T molar ratio/dry g, Fe_T/ Al molar ratio/dry g, Fe_R/Al molar ratio/dry g, TOC/TN molar ratio/dry g, TOC/TC molar ratio /dry g, TC/TN molar ratio/dry g in Seyhan, ETS, Göksu and Aydıncık Transects. Minimum(min), maximum (max), average (ave) and standard deviation (sd) of each transect is given.

Station Name	Depth (m)	Fe_R / Fe_T	Fe_T/ Al	Fe_R/Al	TOC/TN	TOC/TC	TC/TN
1-Seyhan	15.00	0.10	0.30	0.03	11.48	17.02	67.44
2-Seyhan	35.00	0.09	0.29	0.03	9.86	17.58	56.09
3-Seyhan	50.00	0.10	0.29	0.03	12.53	10.35	121.02
4-Seyhan	15.00	0.11	0.34	0.04	11.19	18.23	61.37
5-Seyhan	40.00	0.13	0.30	0.04	11.02	19.24	57.30
6-Seyhan	50.00	0.13	0.32	0.04	9.83	13.33	73.73
7-Seyhan	100.00	0.12	0.30	0.04	12.22	7.61	160.63
	min:	0.09	0.29	0.03	9.83	7.61	56.09
	max:	0.13	0.34	0.04	12.53	19.24	160.63
	ave:	0.11	0.31	0.03	11.16	14.76	85.37
	sd:	0.01	0.02	0.01	1.05	4.43	40.03
8-ETS	20.00	0.07	0.47	0.03	13.33	4.21	316.25
9-ETS	50.00	0.05	0.34	0.02	11.61	17.22	67.46
10-ETS	75.00	0.08	0.43	0.03	12.31	4.78	257.40
11-ETS	100.00	0.04	0.28	0.01	8.40	6.91	121.62
12-ETS	200.00	0.07	0.27	0.02	9.74	12.68	76.82
13-ETS	500.00	0.08	0.33	0.03	11.11	10.60	104.78
	min:	0.04	0.27	0.01	8.40	4.21	67.46
	max:	0.08	0.47	0.03	13.33	17.22	316.25
	ave:	0.07	0.36	0.02	11.08	9.40	157.39
	sd:	0.01	0.08	0.01	1.78	5.05	103.79

Table 5.1. Station name, depth of station (m), Fe_R / Fe_T molar ratio/dry g, Fe_T/ Al molar ratio/dry g, Fe_R/Al molar ratio/dry g, TOC/TN molar ratio/dry g, TOC/TC molar ratio /dry g, TC/TN molar ratio/dry g in Seyhan, ETS, Göksu and Aydıncık Transects. Minimum(min), maximum (max), average (ave) and standard deviation (sd) of each transect is given (continued).

Station Name	Depth (m)	Fe_R / Fe_T	Fe_T/ Al	Fe_R/Al	TOC/TN	TOC/TC	TC/TN
14-Göksu	20.00	0.16	0.48	0.08	10.27	2.15	477.81
15-Göksu	50.00	0.10	0.43	0.04	11.02	2.12	519.50
16-Göksu	75.00	0.10	0.34	0.03	10.40	5.87	177.31
17-Göksu	100.00	0.10	0.30	0.03	10.60	5.01	211.44
18-Göksu	200.00	0.13	0.28	0.04	11.79	3.94	299.21
19-Göksu	500.00	0.09	0.28	0.03	10.07	16.16	62.32
	min:	0.09	0.28	0.03	10.07	2.12	62.32
	max:	0.16	0.48	0.08	11.79	16.16	519.50
	ave:	0.11	0.35	0.04	10.69	5.88	291.27
	sd:	0.03	0.09	0.02	0.63	5.26	178.17
20-Aydıncık	20.00	0.26	0.32	0.08	13.14	3.60	365.28
21-Aydıncık	40.00	0.24	0.25	0.06	8.23	7.92	103.92
22-Aydıncık	75.00	0.23	0.25	0.06	14.16	13.92	101.75
23-Aydıncık	100.00	0.14	0.25	0.04	11.83	7.86	150.52
24-Aydıncık	200.00	0.12	0.28	0.03	13.20	12.05	109.52
25-Aydıncık	500.00	0.11	0.28	0.03	11.36	14.48	78.42
	min:	0.11	0.25	0.03	8.23	3.60	78.42
	max:	0.26	0.32	0.08	14.16	14.48	365.28
	ave:	0.18	0.27	0.05	11.99	9.97	151.57
	sd:	0.07	0.03	0.02	2.10	4.23	107.28

Table 5.2. Station name, depth of station (m), Mn_R / Mn_T molar ratio/dry g, Mn_T/ Al molar ratio/dry g, Mn_R/Al molar ratio/dry g, Mn_R/TOC molar ratio/dry g, Fe_R/TOC molar ratio /dry g in Seyhan, ETS, Göksu and Aydıncık Transects. Minimum(min), maximum (max), average (ave) and standard deviation (sd) of each transect is given.

Station Name	Depth(m)	Mn_R/Mn_T	Mn_T/ Al	Mn_R/ Al	Mn_R/TOC	Fe_R/TOC
1-Seyhan	15.00	0.23	0.0051	0.0012	0.0047	0.11
2-Seyhan	35.00	0.20	0.0048	0.0010	0.0040	0.11
3-Seyhan	50.00	0.20	0.0050	0.0010	0.0052	0.15
4-Seyhan	15.00	0.23	0.0060	0.0014	0.0042	0.11
5-Seyhan	40.00	0.27	0.0047	0.0013	0.0051	0.15
6-Seyhan	50.00	0.23	0.0051	0.0012	0.0049	0.17
7-Seyhan	100.00	0.21	0.0066	0.0014	0.0055	0.14
	min:	0.20	0.0047	0.0010	0.0040	0.11
	max:	0.27	0.0066	0.0014	0.0055	0.17
	Ave:	0.22	0.0053	0.0012	0.0048	0.14
	sd:	0.02	0.0007	0.0002	0.0005	0.02
8-ETS	20.00	0.06	0.0097	0.0006	0.0051	0.29
9-ETS	50.00	0.07	0.0054	0.0004	0.0014	0.07
10-ETS	75.00	0.09	0.0081	0.0008	0.0033	0.15
11-ETS	100.00	0.07	0.0049	0.0004	0.0023	0.08
12-ETS	200.00	0.12	0.0043	0.0005	0.0031	0.12
13-ETS	500.00	0.40	0.0245	0.0098	0.0631	0.17
	min:	0.06	0.0043	0.0004	0.0014	0.07
	max:	0.40	0.0245	0.0098	0.0631	0.29
	Ave:	0.13	0.0095	0.0021	0.0130	0.15
	sd:	0.13	0.0089	0.0038	0.0246	0.08

Table 5.2. Station name, depth of station (m), Mn_R / Mn_T molar ratio/dry g, Mn_T/ Al molar ratio/dry g, Mn_R/Al molar ratio/dry g, Mn_R/TOC molar ratio/dry g, Fe_R/TOC molar ratio /dry g in Seyhan, ETS, Göksu and Aydıncık Transects. Minimum(min), maximum (max), average (ave) and standard deviation (sd) of each transect is given (continued).

Station Name	Depth(m)	Mn_R/Mn_T	Mn_T/ Al	Mn_R/ Al	Mn_R/TOC	Fe_R/TOC
14-Göksu	20.00	0.06	0.0167	0.0010	0.0032	0.25
15-Göksu	50.00	0.06	0.0120	0.0007	0.0036	0.24
16-Göksu	75.00	0.13	0.0066	0.0009	0.0035	0.14
17-Göksu	100.00	0.14	0.0064	0.0009	0.0038	0.12
18-Göksu	200.00	0.22	0.0054	0.0012	0.0082	0.25
19-Göksu	500.00	0.21	0.0060	0.0013	0.0052	0.10
	min:	0.06	0.0054	0.0007	0.0032	0.10
	max:	0.22	0.0167	0.0013	0.0082	0.25
	Ave:	0.14	0.0088	0.0010	0.0046	0.18
	sd:	0.07	0.0045	0.0002	0.0019	0.07
20-Aydıncık	20.00	0.15	0.0062	0.0010	0.0031	0.26
21-Aydıncık	40.00	0.15	0.0039	0.0006	0.0013	0.13
22-Aydıncık	75.00	0.22	0.0042	0.0009	0.0021	0.13
23-Aydıncık	100.00	0.17	0.0051	0.0008	0.0028	0.12
24-Aydıncık	200.00	0.19	0.0048	0.0009	0.0037	0.14
25-Aydıncık	500.00	0.27	0.0060	0.0016	0.0068	0.14
	min:	0.15	0.0039	0.0006	0.0013	0.12
	max:	0.27	0.0062	0.0016	0.0068	0.26
	Ave:	0.19	0.0050	0.0010	0.0033	0.15
	sd:	0.05	0.0009	0.0003	0.0019	0.05

The major trace metal concentrations in the surface sediments in the surface seafloor of Mediterranean, Black Sea and Aegean and crustal averages are given Table 5.3. Our finding is in concordance with literature values. Fe and Mn levels in Cilician Basin are high in surface sediments, and other trace metals concentrations are in the within the range reported in literature. High Ni concentration relative to the crustal averages are remarkable. High Ni and Cr values are resulted from the mafic and ultramafic rocks in the drainage area, namely the Taurus Mountains.

Table 5.3: The findings of major trace metal concentrations in the surface sediments within the Cilician Basin and Marmara and Black Sea comparison with crustal average rocks.

	Fe (%)	Mn (ppm)	Cu (ppm)	Ni (ppm)	Cr (ppm)	Zn (ppm)	Co (ppm)
Crustal Average[1]	3.5	600	25	20	35	71	10
Crustal Average[2]	3.09	527	14.3	18.6	35	52	11.6
Crustal Average[3]	5.0	950	55	75	100	70	25
Iskenderun Bay[4]	1.5-9.0	281-1130	9-39	179-808	70-694	30-117	6-99
Mersin Bay[5]	5.3	1103	42	326	5551	107	-
Eastern Aegean Shelf [6]	0.5-5.7	103-2625	3-77	11-406	9-312	19-162	2-41

[1]Taylor and McLennan(1985,1995), [2] Wedepohl (1995), [3] Mason and Moore(1982), [4] Ergin et al.(1996), [5] Shaw and Bush(1978), [6] Ergin et al.(1993), [7] Bodur and Ergin(1994), [8] Yücesoy(1991), [9] Çağatay et al.(1987), [10,11] Aslaner(1973), [12] Turekian and Wedepohl(1961), [13]Sevim(1991), [14] Tunç(2008).

Table 5.3: The findings of major trace metal concentrations in the surface sediments within the Cilician Basin and Marmara and Black Sea comparison with crustal average rocks (continued).

	Fe (%)	Mn (ppm)	Cu (ppm)	Ni (ppm)	Cr (ppm)	Zn (ppm)	Co (ppm)
Marmara Sea Shelf [7]	1.7-5.1	307-2059	14-104	42-173	89-186	50-169	13-33
Black Sea[8]	3.28	570	49	77	110	87	11
Black Sea[9]	-	722	36	51	93	-	22
Ultrabasic Rocks[10]	5.0-7.6	700-2600	46-62	1700-2900	500-700	-	75-101
Basic Rocks[11]	1.5-8.5	500-4900	39-87	200-3200	400-3000	-	25-112
Shales[12]	4.7	850	45	68	90	90	9
Ceyhan River[13]	3.2-5.9	285-2159	40-84	115-1066	124-683	121-318	25-95
Mersin Bay[14]	2.95	668	25	230	147	57	5
Iskenderun Bay[14]	2.91	684	28	333	170	71	3

[1]Taylor and McLennan(1985,995), [2] Wedepohl (1995), [3] Mason and Moore(1982), [4] Ergin et al.(1996), [5] Shaw and Bush(1978), [6] Ergin et al.(1993), [7] Bodur and Ergin(1994), [8] Yücesoy(1991), [9] Çağatay et al.(1987), [10,11] Aslaner(1973), [12] Turekian and Wedepohl(1961), [13]Sevim(1991), [14] Tunç(2008).

Table 5.3: The findings of major trace metal concentrations in the surface sediments within the Cilician Basin and Marmara and Black Sea comparison with crustal average rocks (continued).

	Fe (%)	Mn (ppm)	Cu (ppm)	Ni (ppm)	Cr (ppm)	Zn (ppm)	Co (ppm)
Seyhan Transect	3.32	563	32	311	135	95	24
ETS Transect	3.67	1004	35	218	179	109	32
Göksu Transect	2.26	508	28	107	85	90	23
Aydıncık Transect	2.40	438	32	101	85	98	21
Average This Study	2.93	626	32	190	122	98	25

[1]Taylor and McLennan(1985,995), [2] Wedepohl (1995), [3] Mason and Moore(1982), [4] Ergin et al.(1996), [5] Shaw and Bush(1978), [6] Ergin et al.(1993), [7] Bodur and Ergin(1994), [8] Yücesoy(1991), [9] Çağatay et al.(1987), [10,11] Aslaner(1973), [12] Turekian and Wedepohl(1961), [13]Sevim(1991), [14] Tunç(2008).

The comparison of reactive iron enrichment and its relation with organic carbon and with water depth in Seyhan, ETS, Göksu and Aydıncık transects could be seen more clearly in the Figure 5.1. Further, the trace metal and major element concentrations is given in Figure 5.1 to reveal the variation with depth and interrelation.
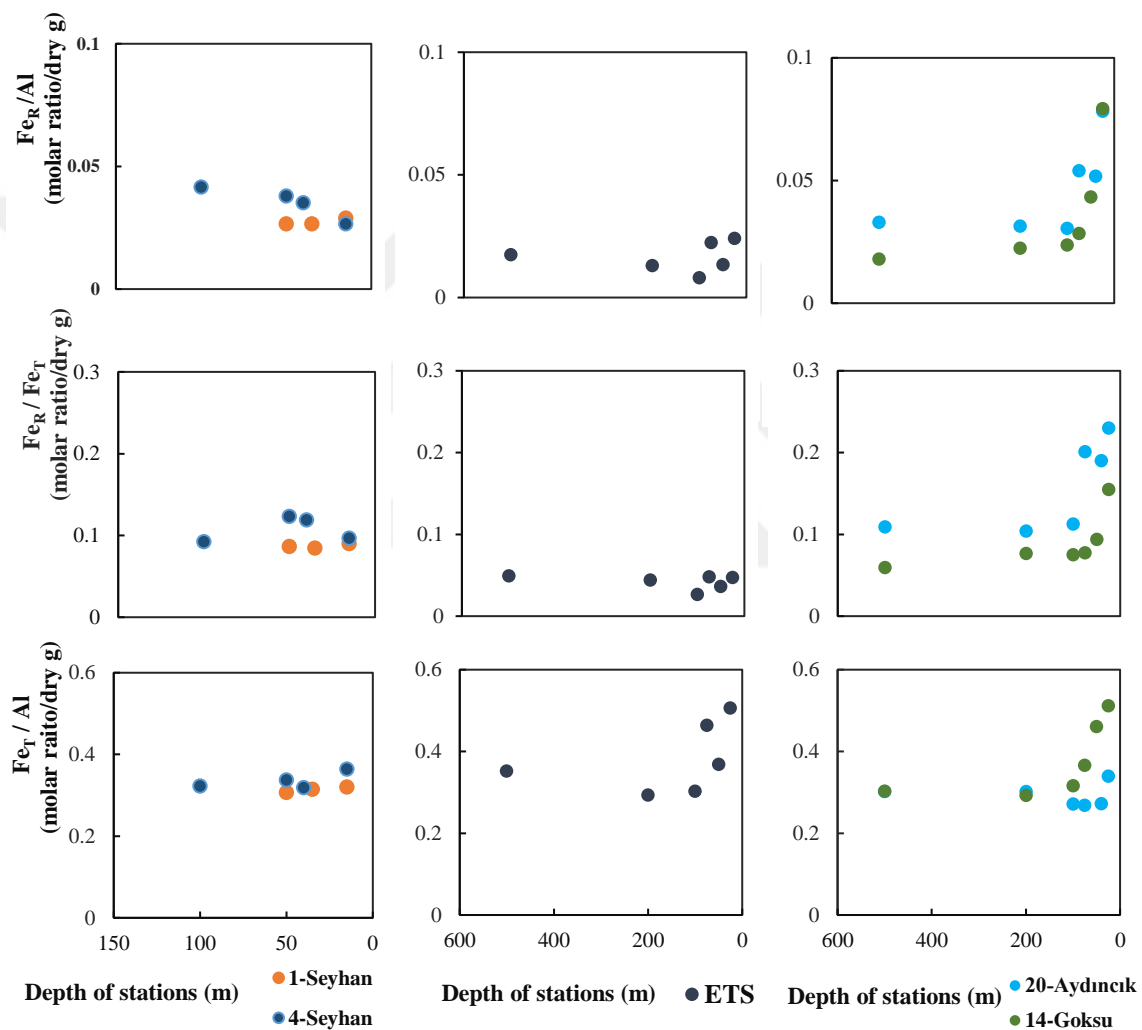
Figure 5.1: Fe_T/Al (molar ratio/dry g), Fe_R/Fe_T (molar ratio/dry g), Fe_R/Al (molar ratio/dry g) with the depth of stations in Seyhan (orange dot and blue dot), ETS (navy dot), Göksu (Green dot) and Aydıncık (turquoise dot) transects.
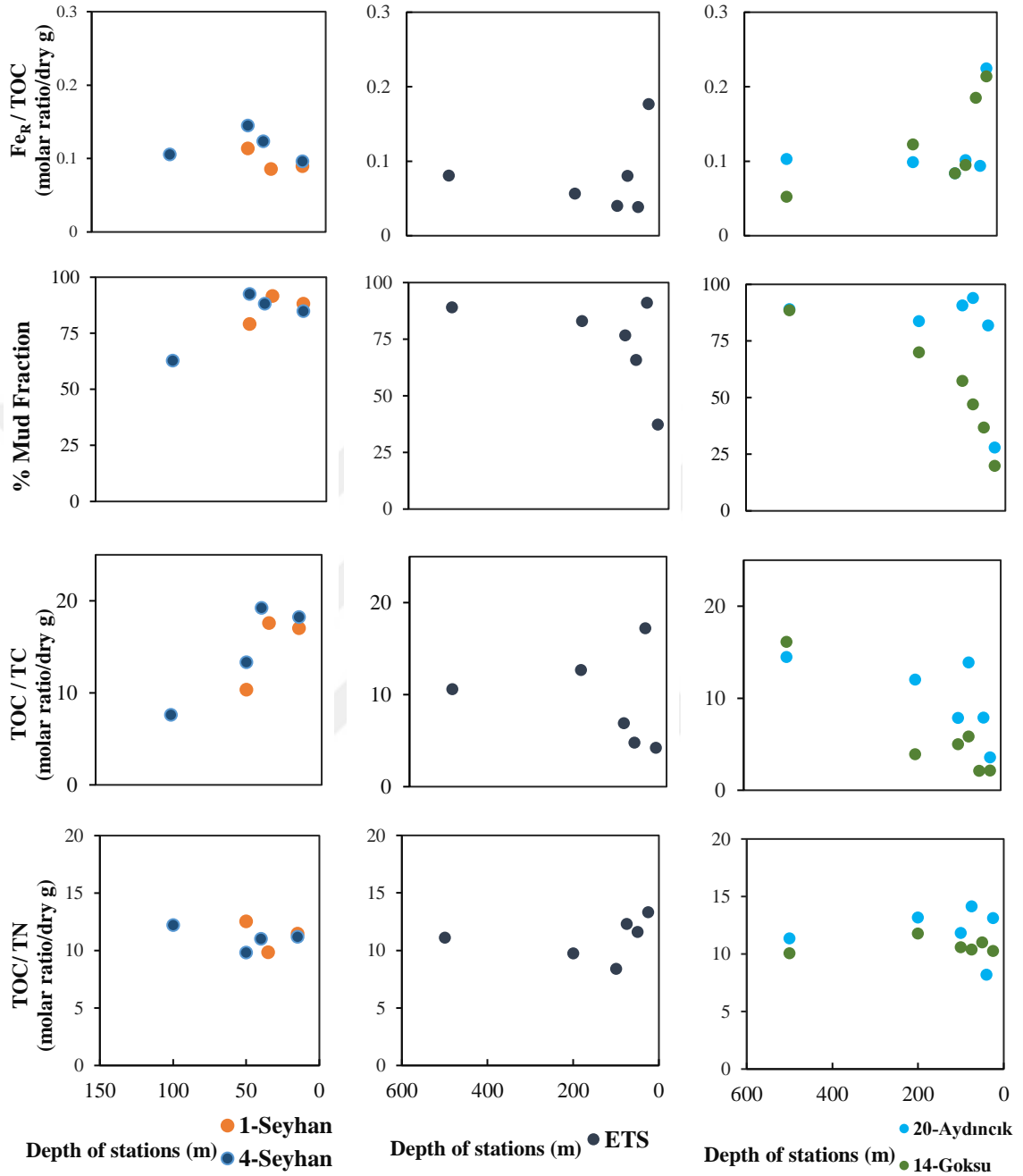
Figure 5.2 TOC/TN (molar ratio/dry g), TOC/TC (molar ratio/dry g), mud fraction, Fe$_R$/TOC (molar ratio/dry g) with the depth of stations in Seyhan (orange dot and blue dot), ETS (navy dot), Göksu (Green dot) and Aydıncık (turquoise dot) transects.

Trace Metals distributions in the Cilician Basin sediments

Vanadium has strong correlation with Cr, Co, Ni, Cu, Zn, Ga, Rb, Cs, Al, Fe, Mg and K ($R^2 > 0.7$) and these strong correlation is in concordance with literature (Çağatay, 2007). Cd, Zn, Cu, Ni is consumed in the euphotic zone by phytoplankton as micronutrient, and increase in concentration with depth via remineralization processes (Boyle et al., 1976, Bruland 1983, Çağatay, 2007). The accumulation of these elements in the oxic surface sediments occurs as a result of adsorption onto Fe- Mn- oxyhdroxides and organic matter that precipitate or accumulate in the seafloor (Boyle, 1977). Specifically Ni and Cu can concentrate in the oxic sediments with adsorption on the Fe-, Mn- oxyhydroxides and organic material . In this study, the high correlation of Ni and Cu with Fe_T ($R^2 > 0.78$) is in agreement with this conclusion. In Marmara Sea surface sediments Pb shows significant correlation with Cu, Zn, Sn but in this study Pb was found to correlate with Al, Cs and Se (>0.66). Sr is related to the biogenic carbonate fraction (Fig. 5.3) of the sediments and displayed negative correlation with Al and Fe. Sr and total inorganic carbon (carbonates) has significant correlation in all samples analyzed (Fig. 5.3).
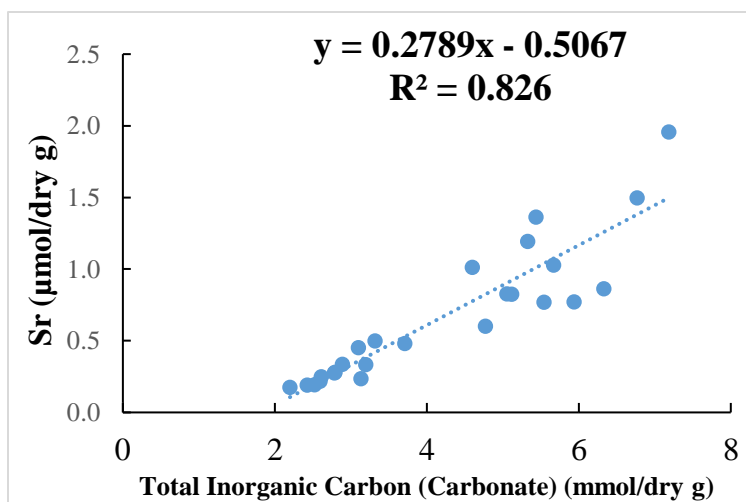
Figure 5.3 Sr and total inorganic carbon (carbonate) in the 25 surface sediments of Cilician Basin correlation plot.

Enrichment factors in the Cilician Basin surface sediments are calculated as below (Çağatay, 2007);

Enrichment Factor(EF) =(Element/Al) sample/(Element/Al) crustal

Birth (2003) classified the enrichment factor(EF) as follows:

i.   EF<1; no enrichment
ii. $1 \leq EF < 3$; minor enrichment
iii. $3 \leq EF < 5$; moderate enrichment
iv. $5 \leq EF < 10$; moderate severe enrichment
v. $10 \leq EF < 25$; severe enrichment
vi. $25 \leq EF < 50$; very severe enrichment
vii. $50 \leq EF$; extremely severe enrichment

The EF values and the enrichment factors in prior studies held on the Sudanese harbors along the Red Sea and Anaximander mud volcanoes in coast is given (İdris,2008, Talas et al., 2015). The crustal averages were retrieved from (Turekian and Wedepohl, 1961, Wedepohl, 1995 (for Rb and Cs)), and Al is reference element due to its immobile character and high abundance in the crust.

The enrichment factors in this study correlates with prior studies. To illustrate, Fe enrichment is found 1.13 which is very close to the EF value, 1.14, in Çağatay (2007) study. Se severe enrichment also in concordance with Talas et al. (2015) study. Talas et al. (2015) investigated the surface sediments collected from the Anaximander mud volcanoes in the Eastern Mediterranean Sea to reveal sedimentary and geochemical properties. The mud volcano environment differs in enrichment factors of trace metals than normal marine environment. Yet, the enrichment factors for sediments were compared to background levels of Earth's crust in a similar with this study.

The detailed geological characteristics is represented in the Figure 5.4. The magmatic rocks contain high concentration of Cr which influence the coastal surface sediments.

Figure 5.4 Geologic map of the surrounding region of study area retrieved from Yemenicioğlu and Tunc (2013).

Nickel enrichment in Seyhan takes attention with very severe enrichment, this high level could be sourced from mafic and ultramafic rocks drainage basin of Seyhan river. The overall average enrichment of Ni is moderate in the Cilican Basin. Arsenic shows a minor enrichment in the basin whereas Sr has moderate enrichment. Selenium enrichment in the basin sediments is also at a moderate level. However, Seyhan and ETS transects have relatively high enrichment factors. On the other hand, Göksu and Aydıncık transects shows very clear trend that reveals the terrestrial enrichments of Ga, As, Rb and Ba in coastal seafloor decrease towards the open marine seafloor. This may imply that these elements are enriched from drainage of terrestrial sources (local geology) in marine environment (Tunç 2013). Similarly, V, Cr, Co, Ni, Cu, Zn enrichments factors in Göksu and Aydıncık transects decreases towards the open seafloor. ETS and Seyhan transects do not possess such clear trends in enrichment factors. Both the Aydıncık and Göksu transects show trends in enrichment factors of trace elements in sediments.

Table 5.4 The transect, station number, and the enrichment factor of the Fe_R, Fe_T, Mn_R, Mn_T, V, Cr, Co, Ni, Cu, Zn in surface sediments.

Transect	Station	Fe_R	Fe_T	Mn_R	Mn_T	V	Cr	Co	Ni	Cu	Zn
Seyhan	1	0.10	1.05	0.23	0.98	0.95	2.29	1.89	30.46	1.10	1.35
	2	0.10	1.04	0.18	0.91	0.97	2.10	1.69	2.68	1.00	1.37
	3	0.10	1.01	0.19	0.95	1.03	2.15	1.79	2.73	0.91	1.28
Seyhan	4	0.13	1.19	0.26	1.15	1.14	2.99	2.42	3.87	1.39	1.99
	5	0.13	1.05	0.24	0.91	0.95	2.02	1.63	2.61	0.97	1.23
	6	0.14	1.11	0.23	0.98	1.05	2.16	1.79	2.84	1.03	1.45
	7	0.12	1.06	0.26	1.26	1.39	2.34	2.52	3.54	1.39	2.08
ETS	8	0.11	1.67	0.11	1.87	1.91	6.86	4.92	11.65	1.64	2.43
	9	0.07	1.21	0.07	1.03	1.02	2.88	2.32	5.13	1.04	1.54
	10	0.12	1.53	0.14	1.55	2.12	4.23	4.04	7.03	1.64	2.80
	11	0.04	1.00	0.07	0.94	1.10	2.16	1.94	3.15	1.06	1.67
	12	0.07	0.97	0.10	0.82	0.95	1.81	1.59	2.52	0.99	1.35
	13	0.09	1.16	1.89	4.71	1.04	2.56	2.27	4.20	1.14	1.46

Table 5.4 The transect, station number, and the enrichment factor of the Fe_R, Fe_T, Mn_R, Mn_T, V, Cr, Co, Ni, Cu, Zn in surface sediments (continued).

Transect	Station	Fe_R	Fe_T	Mn_R	Mn_T	V	Cr	Co	Ni	Cu	Zn
Göksu	14	0.28	1.69	0.20	3.21	2.21	2.89	6.38	5.43	2.83	4.78
	15	0.16	1.52	0.13	2.31	1.99	3.04	4.46	4.29	1.98	3.34
	16	0.12	1.21	0.17	1.27	1.39	2.07	2.84	3.89	1.42	2.18
	17	0.10	1.04	0.17	1.23	1.41	2.30	2.92	3.94	1.56	2.35
	18	0.13	0.97	0.23	1.03	1.34	2.08	2.54	3.79	1.42	1.97
	19	0.09	1.00	0.24	1.15	1.01	1.97	1.81	2.89	1.05	1.40
Aydıncık	20	0.29	1.11	0.19	1.20	1.50	2.05	3.46	3.83	2.11	3.46
	21	0.22	0.89	0.12	0.76	1.54	1.91	2.56	3.09	2.03	2.82
	22	0.20	0.88	0.18	0.81	1.16	1.48	1.76	2.22	1.23	1.78
	23	0.12	0.89	0.16	0.98	1.14	1.56	1.84	2.55	1.25	1.83
	24	0.12	0.99	0.18	0.93	1.12	2.01	2.02	3.08	1.22	1.75
	25	0.11	0.99	0.31	1.16	0.97	1.78	1.73	2.69	1.10	1.35
Ave.		0.13	1.13	0.25	1.36	1.30	2.47	2.60	4.96	1.38	2.04
±		0.06	0.23	0.35	0.88	0.39	1.08	1.20	5.66	0.46	0.85

Table 5.5 The transect, station number, and the enrichment factor of the Ga, As, Se, Rb, Sr, Cs, Ba, Pb in surface sediments.

Transect	Station	Ga	As	Se	Rb	Sr	Cs	Ba	Pb
Seyhan	1	1.41	2.24	8.20	0.58	0.83	0.99	0.48	0.49
	2	1.29	2.22	8.48	0.55	0.74	1.03	0.36	0.46
	3	1.21	2.26	4.90	0.53	2.13	0.98	0.34	0.44
Seyhan	4	1.85	2.94	15.05	0.69	1.19	1.18	0.63	0.44
	5	1.23	2.09	7.54	0.57	0.71	1.08	0.34	0.51
	6	1.34	2.76	9.33	0.57	1.95	1.04	0.35	0.41
	7	1.56	4.02	6.34	0.65	5.63	1.12	0.39	0.42

Table 5.5 The transect, station number, and the enrichment factor of the Ga, As, Se, Rb, Sr, Cs, Ba, Pb in surface sediments (continued).

Transect	Station	Ga	As	Se	Rb	Sr	Cs	Ba	Pb
ETS	8	1.43	4.17	5.65	0.43	1.59	0.52	0.23	b.d
	9	1.10	2.39	9.06	0.48	0.89	0.82	0.25	0.11
	10	1.52	7.54	5.58	0.71	7.10	1.33	0.28	0.94
	11	1.15	2.39	3.42	0.55	3.03	1.07	0.29	0.50
	12	1.12	2.91	9.27	0.49	0.97	0.89	0.28	0.32
	13	1.12	2.71	8.74	0.41	1.31	0.67	0.26	0.20
Göksu	14	2.64	16.77	9.49	1.16	33.72	1.67	0.49	b.d
	15	2.06	11.27	4.64	0.83	16.58	1.37	0.44	b.d
	16	1.57	5.17	3.77	0.68	7.75	1.24	0.40	0.12
	17	1.61	4.30	4.61	0.78	9.59	1.47	0.40	0.01
	18	1.41	3.26	7.28	0.72	4.87	1.50	0.32	b.d
	19	1.15	2.57	7.89	0.49	1.06	0.93	0.29	0.63
Aydıncık	20	3.09	7.86	1.21	1.03	10.01	1.16	1.31	b.d
	21	2.14	4.82	7.24	1.01	6.49	1.71	0.69	0.56
	22	1.56	3.37	7.30	0.72	3.02	1.39	0.50	0.39
	23	1.38	3.01	5.67	0.67	3.94	1.32	0.41	0.30
	24	1.38	3.07	8.48	0.65	2.04	1.29	0.36	0.65
	25	1.21	2.56	8.20	0.53	1.25	1.03	0.31	0.59
Ave.		1.54	4.35	7.09	0.66	5.14	1.15	0.42	0.43
±		0.49	3.37	2.71	0.19	7.10	0.29	0.22	0.21

	Al	FeT	FeR	MnR	MnT	Mg	K	Ca	V	Cr	Co	Ni	Cu	Zn	Ga	As	Se	Rb	Sr	Cs	Ba	Pb
Al	1.00																					
FeT	0.89	1.00																				
FeR	0.31	0.11	1.00																			
MnR	0.31	0.37	0.13	1.00																		
MnT	0.34	0.46	-0.02	0.97	1.00																	
Mg	0.08	0.34	-0.48	0.22	0.35	1.00																
K	0.52	0.33	0.09	0.07	0.08	0.07	1.00															
Ca	-0.73	-0.77	-0.37	-0.25	-0.25	-0.09	0.00	1.00														
V	0.72	0.81	0.04	0.21	0.31	0.36	0.43	-0.51	1.00													
Cr	0.51	0.80	-0.14	0.24	0.38	0.60	0.01	-0.63	0.76	1.00												
Co	0.31	0.65	-0.36	0.28	0.44	0.72	0.05	-0.36	0.73	0.92	1.00											
Ni	0.34	0.67	-0.26	0.24	0.39	0.70	-0.01	-0.45	0.69	0.95	0.95	1.00										
Cu	0.80	0.73	0.27	0.35	0.37	0.29	0.68	-0.60	0.77	0.53	0.46	0.44	1.00									
Zn	0.51	0.52	-0.05	0.10	0.19	0.36	0.77	-0.20	0.77	0.49	0.54	0.46	0.81	1.00								
Ga	0.80	0.62	0.57	0.18	0.11	-0.07	0.55	-0.67	0.46	0.28	0.02	0.07	0.77	0.49	1.00							
As	-0.42	-0.25	-0.37	-0.07	0.02	0.07	0.01	0.49	-0.04	-0.19	0.10	-0.11	-0.27	0.08	-0.51	1.00						
Se	0.79	0.76	0.44	0.33	0.33	0.07	0.40	-0.82	0.49	0.46	0.27	0.29	0.74	0.42	0.81	-0.30	1.00					
Rb	0.78	0.49	0.54	0.01	-0.06	-0.22	0.66	-0.50	0.48	0.07	-0.12	-0.11	0.74	0.53	0.88	-0.43	0.65	1.00				
Sr	-0.77	-0.77	-0.45	-0.26	-0.25	-0.15	-0.19	0.84	-0.54	-0.64	-0.34	-0.50	-0.65	-0.29	-0.75	0.61	-0.75	-0.54	1.00			
Cs	0.74	0.46	0.49	-0.03	-0.08	-0.25	0.65	-0.40	0.50	0.03	-0.11	-0.12	0.69	0.51	0.77	-0.35	0.57	0.97	-0.43	1.00		
Ba	0.45	0.21	0.60	0.03	-0.09	-0.22	0.36	-0.43	0.01	-0.06	-0.35	-0.25	0.42	0.17	0.86	-0.56	0.53	0.70	-0.57	0.55	1.00	
Pb	0.77	0.63	0.44	0.11	0.09	-0.14	0.48	-0.57	0.64	0.25	0.10	0.07	0.71	0.54	0.77	-0.17	0.59	0.83	-0.54	0.80	0.52	1.00

Figure 5.5 The correlation coefficients of Al, Fe_T, Fe_R, Mn_R, Mn_T, Mg, K, Ca, V, Cr, Co, Ni, Cu, Zn, Ga, As, Se, Rb, Sr, Cs, Ba, Pb in µmol/dry g in 25 surface sediments.

5.2 A deep look in interrelation of reactive Fe and Mn with organic carbon, mud fraction, nitrogen and phosphorus.

A deep look in interrelation of iron is needed to shed the light on its interaction with organic carbon, manganese, and trace metals. Thus, reactive iron correlation plots give the correlation coefficients of related parameters.

The reactive iron(Fe_R) for all stations do not have significant correlation with Fe_T ($R^2=0.011$, p=0.62), but the correlation coefficient for Göksu transect is significant ($R^2=0.59$). According to previous reports, Fe_R is expected to have a positive relationship with Fe_T (Anderson and Raiswell, 2004; Poulton and Raiswell, 2005, Roy et al., 2013). Roy et al. (2013) studied the reactive iron and manganese distributions along the continental shelf near the mouth of the Umpqua River, Oregon (USA). The sediments were defined as muddy (silt&clay) characterizing the Oregon margin. The correlation between Fe_R and Fe_T were found $R^2=0.74$ in river suspended, slope and inner sand seafloor sediments, excluding mid-shelf sand (Roy et al., 2013). This correlation was calculated for all data, six rivers in the region and in this time correlation decreases to $R^2=0.47$. The differences in correlation is explained as larger data sets includes diverse variations in geology and hydro-climatology of the river that influence sediment signature, grain size variation, sediment sorting and post-depositional processes (e.g., Canfield, 1997; Poulton and Raiswell, 2002). Likewise, in this study, as we found less coherence for all data set but significant correlation between Fe_R and Fe_T in Göksu sediment that could result from diverse variations in geology and hydro-climatology of the river that influences sediment. The Fe_T and % mud has strong correlation ($R^2=0.76$) and the moderate correlation between Fe_R and % mud ($R^2=0.57$) is remarkable, too. Further, in the Seyhan transect Fe_R has weak correlation with Fe_T whereas in the ETS and Aydıncık transects there is no correlation. The Seyhan transect Fe_T almost perfectly correlates with the mud fraction $R^2=0.92$ that could support the sediment grain size on this correlation likewise the findings of Göksu transect.

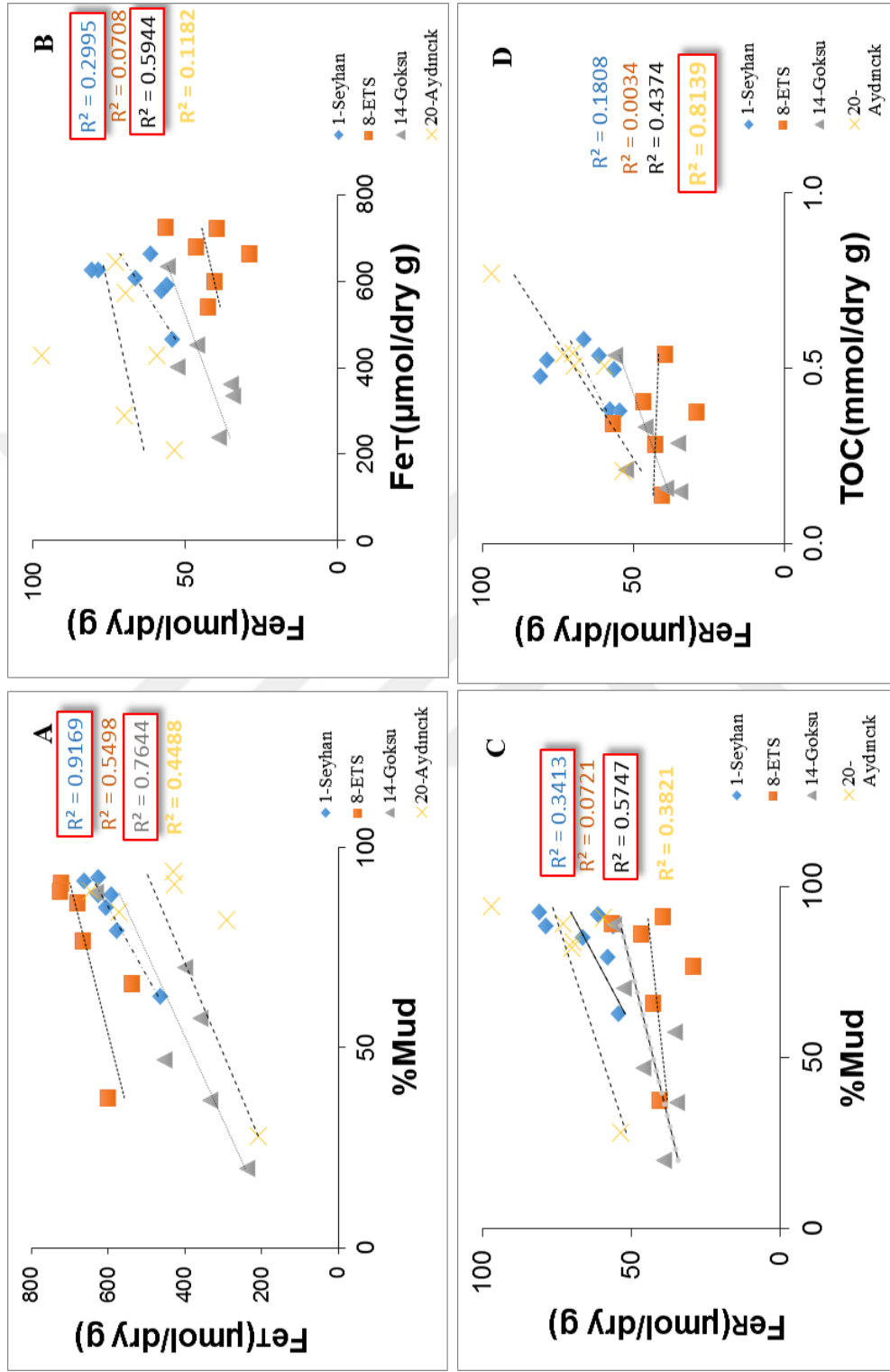**Figure 5.6** The correlation plots of **A.** Fe$_T$ (μmol/dry g) to %mud, **B.** Fe$_R$ (μmol/dry g) to Fe$_T$ (μmol/dry g), **C** Fe$_R$ (μmol/dry g) to %mud, **D.** Fe$_R$ (μmol/dry g) to TOC(mmol/dry g) in total 25 surface sediments.

The most striking findings we expected to see in this study is that remarkable correlation between reactive iron and organic carbon in the Aydıncık transect. Further, for all stations the reactive iron and organic carbon has a positive correlation (R^2=0.60) within the region as recognized in prior works that there are common mechanisms leading a coupling between Fe and OC within terrestrial biosphere, marine, aquatic settings (e.g., Kaiser et al., 1996; Jones and Edwards, 1998; Kaiser and Guggenberger, 2000; Wagai and Mayer, 2007, Poulton and Raiswell, 2005; Lalonde et al., 2012). Lalonde et al. 2012 found that the 23–27% of the total organic carbon remains bound to reactive iron oxide phases in marine sediments. Thus, they claimed that strong association between iron and organic carbon may inhibit microbial organic carbon degradation and enhance organic carbon preservation. Shileds et al. (2016) found that the average 8.1% of the OC in deltaic sediments in the in the Wax Lake Delta, Louisiana. is directly sorbed (OC:Fe<1) to Fe_R. Thus, the interaction has been shown to increase the residence time of carbon in the organic form, Fe_R must be an important component of long-term atmospheric carbon sequestration in these systems. Referring these studies and the findings of this study implies that reactive iron species could reach environmentally significant concentrations in Cilicin Basin.

Reactive manganese in the region is in a high correlation with Mn_T in ETS transect. Similarly Aydıncık transect has a high correlation ($R^2 = 0.93$).. Total Mn has strong correlation with Al in Aydıncık transect (Fig. 5.7 B). There is no significant correlation of total Mn with % mud in Seyhan, ETS, Göksu and Aydıncık transects. Mn_R has strong correlation with Al (Fig. 5.7 A) and % mud (Fig. 5.7 D) (R^2= 0.89) and organic carbon (R^2=0.76). Also, in this transect Mn_R shows a remarkable correlation with Fe_R(>0.70). Roy et al. (2013) found 0.59 correlation between Mn_R and OC in deltaic sediments of Louisiana shelf similar to our findings.
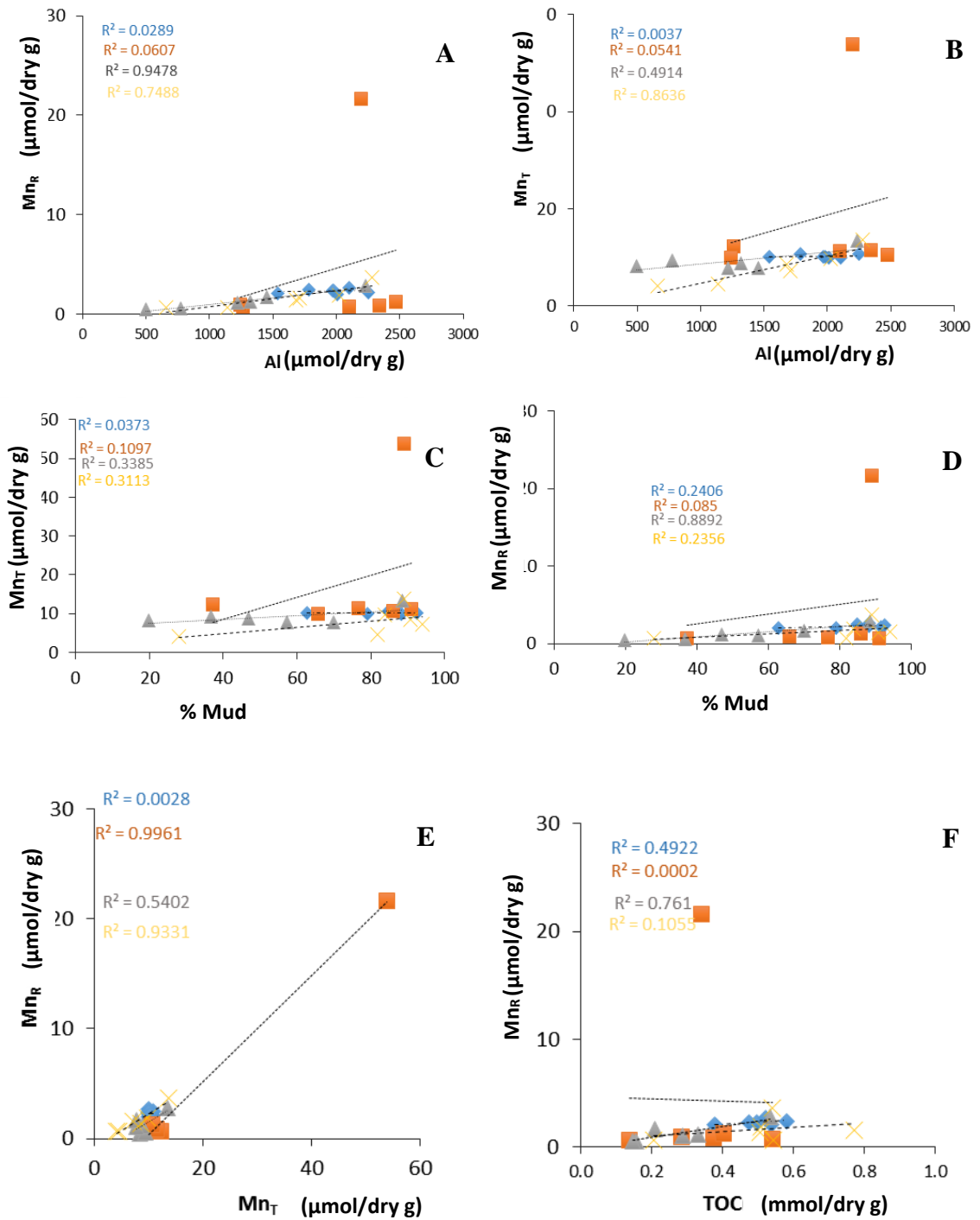
Figure 5.7 The correlation plots of **A.** Mn_R (µmol/dry g) to Al(µmol/dry g), **B.** Mn_T (µmol/dry g) to Al(µmol/dry g), **C** Mn_T (µmol/dry g) to % mud, **D.** Mn_R (µmol/dry g) to % mud, **E.** Mn_R (µmol/dry g) to Mn_T (µmol/dry g), **F.** Mn_R (µmol/dry g) to TOC(mmol/dry g) in total 25 surface sediments.

ETS transect shows only significant relation of reactive with total manganese results from the non-lithogenic upward vertical manganese accumulation in sediments and lateral transportation towards the open station. Roy et al. (2013) found that Mn_R is more prone to loss from sediment particles during transit to the seabed as compared to Fe_R. This is also seen in Cilician Basin surface sediments.

Table 5.6 summarizes the weight percent of sedimentary reactive iron species along four transect covering the entire Cilician Basin. The reactive iron (%) increases with depth in the Cilican Basin whereas reactive manganese and organic carbon increases towards offshore. Roy et al. (2013) found that the Fe_R (%) in the range of 0.35-0.85 with water depth that is similar to average 0.31 of this study. The minimum and maximum of the Fe_R (%) differs in this two study. This diffrence could be resulted from river, local geology, sedimentation rate and type of organic matter.

Mn_R (%) 0.001-0.003 whereas in this thesis this value is ten times higher 0.010 than Louisiano deltaic sediments. The differences between two studies may have resulted from the difference in depth of transects, former study had the data up to 200m. Thus, there is no information about the lateral transportation of Mn towards the open seafloor to compare with our findings. However, both two studies found that increase in Mn concentration towards the open seafloor. Mn_R is more prone to loss from sediment particles during transit to the seabed as compared to Fe_R.

The overlying water column and geochemical factors that controls the reactive iron in Cilician Basin seafloor sediments seems to be strongly coupled to the river inputs. Seyhan river seems to have greater impact on seafloor ecosystem; the shallow station which is rich in reactive iron, iron, reactive manganese and manganese in surface sediments is also rich in chlorophyl-a, nitrate, silicate, phosophate and total phosphorus. Also low oxygen levels in the coastal stations gives a hint about high production in the region due to high nutrient load from Seyhan. Therefore, the seafloor is drived from the overlying water as high organic carbon accumulation, reactive iron and manganese levels. Also, high percent of muddy sediments indicates the iron hydroxides enrichment in the mud grain size. The grain size, organic carbon and iron relationship is assumed to be enrichment in the surface of small grain sizes (clay layers) due to adsorption of iron oxyhydroxides and organic carbon on the surface of the clay particles. It is known that clay minerals contribute to a

Table 5.6 The transect, station number, the weight percent of Fe_R(Fe_R%), the weight percent of Mn_R(Mn_R%), the weight percent of Fe_T(Fe_T%), the weight percent of Mn_T(Mn_T%), the weight percent of organic carbon(OC%), the weight percent of N(N%), the weight percent of Fe_R/OC(molar ratio/dry g)

Transect	Station	Fe_R(%)	Mn_R(%)	Fe_T(%)	Mn_T(%)	OC(%)	N(%)	Fe_R/OC
Seyhan	1	0.32	0.013	3.31	0.06	0.60	0.06	0.11
	2	0.34	0.012	3.71	0.06	0.65	0.08	0.11
	3	0.32	0.011	3.23	0.05	0.46	0.04	0.15
Seyhan	4	0.37	0.014	3.40	0.06	0.70	0.07	0.11
	5	0.44	0.015	3.51	0.05	0.63	0.07	0.15
	6	0.45	0.013	3.50	0.06	0.57	0.07	0.17
	7	0.31	0.011	2.60	0.06	0.45	0.04	0.14
ETS	8	0.23	0.004	3.35	0.07	0.17	0.01	0.29
	9	0.22	0.004	4.05	0.06	0.65	0.07	0.07
	10	0.24	0.005	3.02	0.05	0.34	0.03	0.15
	11	0.16	0.005	3.72	0.06	0.45	0.06	0.08
	12	0.26	0.007	3.81	0.06	0.49	0.06	0.12
	13	0.32	0.119	4.06	0.30	0.41	0.04	0.17
Göksu	14	0.22	0.003	1.34	0.05	0.19	0.02	0.25
	15	0.19	0.003	1.87	0.05	0.18	0.02	0.24
	16	0.26	0.006	2.53	0.05	0.40	0.04	0.14
	17	0.20	0.006	2.02	0.04	0.34	0.04	0.12
	18	0.29	0.009	2.24	0.04	0.25	0.02	**0.25**
	19	0.31	0.015	3.54	0.07	0.64	0.07	0.10
Aydıncık	20	0.30	0.003	1.17	0.02	0.25	0.02	0.26
	21	0.39	0.004	1.62	0.02	0.65	0.09	0.13
	22	0.54	0.009	2.40	0.04	0.93	0.08	0.13
	23	0.33	0.008	2.39	0.05	0.61	0.06	0.12
	24	0.39	0.010	3.20	0.05	0.61	0.05	0.14
	25	0.41	0.020	3.61	0.08	0.65	0.07	0.14
ave		0.31	0.010	2.93	0.06	0.49	0.05	0.15
±		0.09	0.020	0.85	0.05	0.19	0.02	0.06

large proportion of the total surface area in fine-grained sediments, and fine-grained sediments are likely to be rich in Fe and heavy metals which are particularly reactive towards sulfide (Canfield et al., 1992; Poulton et al., 2004a, 2004b).

On the other hand, ETS transect having no high river load capacity is poor in nitrate, phosphate and chlorophyl-a do not show clear trends of biogeochemical controls on the seafloor. In this region, the coastal seafloor grain size is coarser and rich in iron and manganese in the seafloor with low chlorophyl-a (some stations has 10 times lower value), nitrate and phosphate values. In this region, seafloor of ETS 10 (75 m depth) station has interesting behaviour since the OC:N ratio shows the marine origin organic matter also seen in Aydıncık transect with similar depth station. The most intriguing data in this transect is the outlier $Mn_T(0.30\%)$ 5 times higher than average Mn in Cilician Basin and reactive Mn 0.119% approximately 10 times higher than the average value. This station is also very rich in iron and reactive iron but moderate organic carbon. The bottom water nitrate and phosphate reaches its maximum for the deep sea(>100m) stations in the all transect as expected behaviour of deep sea water column profile.

However, the total phosphorus in this transect contains 65% phosphate form, in other words, ion form which could be readily adsorbed onto iron oxyhyroxides and potential accumulation in the seafloor. The iron bound phosphorus pools is studied via specific extraction schemes to reveal P speciation in marine sediments. The extraction schemes such as SEDEX (Ruttenberg, 1992)(in N_2 atmosphere) is common technique helps to fractionate exchangeable P, Fe-bound P, authenic Ca-P, organic and detrital Ca-P with extraction steps of different chemicals. Reactive P is defined as the sum of exchangeable P, Fe-bound P, authegenic Ca-P and organic P. In this procedure, Fe-bound P pool is used as a measure of total Fe-oxides in the sediments and to asses the role of amorphous Fe-oxides in oxic conditions for binding P in sediment (Slomp, 2013). Fe-bound P pool is found to have significant negative correlation with porewater phosphate and to be made up 33-45% of total P in the surface sediments (Jensen et al., 1995) and act as major burial sink for P (Slomp 2013). The Fe-bound (both for amosphous and pyrite) P pool is not the only burial sink for P, but also the formation of Fe(II)-P phases in redox zones(such as sulfate methane transition zones) gains importance as its link to recent changes in environmental dynamics, possible upward shift of the redox zone, therefore is studied in

lake, eustuarine, near shore coastal; suboxic sediments(Slomp et al., 2013, Ruttenberg, 2003, Sivan et al., 2011). In this study, P extraction procedure were not applied for samples, but based on previous findings it would not be wrong to assume the high reactive iron region would have high Fe-bound P pools. The prior works in Cilician Basin mostly focuses on production and its relation with the carbon, nitrogen and phosphorus cycles in eutrophic coastal and oligotrophic open Cilican Basin (Tuğrul et al., 2004, Sağlamtimur, 2007, Akçay, 2015). In Akçay's study(2015) particulate phosphorus is 75-80% of inorganic P in Mersin Bay surface sediment which is closely located in the Seyhan and ETS transects stations of this study. These speciation of detailed P gives hint about iron-bound P, but further studies is needed to asses accurate ratios in basin since iron bound P is referred as highly mobile and and iron oxyhydoxides are strongly linked to P.

The Cilican Basin surface sediment is oxic, however the degree of organic matter accumulation in the seafloor sediments could decide the local redox zonation. To illustrate, high organic matter content, such as wood pieces in seafloor causes the local hyrogen sulfide release, and diverse benthic ecosystem. These kind of local anoxic conditions, and microbial communites are investigated (Yücel et al, 2013). Although Cilician Basin seafloor is oxic, during the sampling, local anoxic conditions could be observable with eye, but sensor measurement to assess degree of hydrogen sulfide concentration, and the determination of fluxes of Fe(II) to the nearby environment and water column require further studies.

5.3 The biogeochemistry of iron in Cilician Basin seafloor.

The seafloor biogeochemical conditions, the amount of reactive iron, the high correlation with organic carbon are global issues studied in diverse oceanographic areas. However, the Cilician Basin reactive iron and its association with other essential elements are given here for the first time. The Cilician Basin is found to be rich in seafloor iron content, with similar ratios for all transects. The origin of organic matter, bottom water nitrate, phosphate and water column biogeochemical parameters differ in each transects but the reactive iron to organic matter relation in the basin is taken attention in this study. To illustrate, the trend of reactive iron and organic carbon in Cilician Basin is a sharp decrease of in both TOC:C and $Fe_R:Fe_T$ may be the evidence of microbial Fe respiration up to 100m depth (Fig. 5.8).
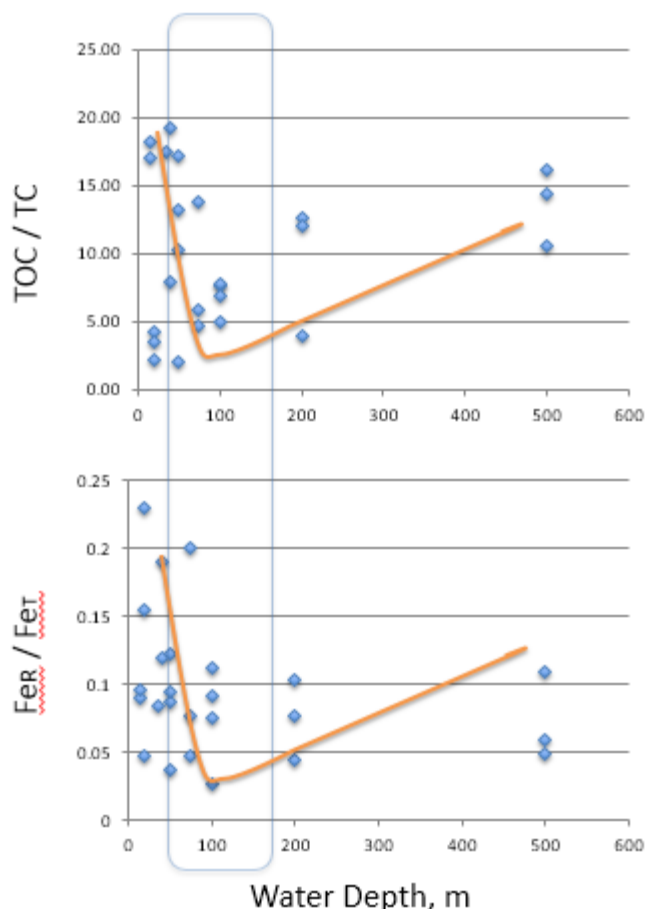

Figure 5.8 The plots of 25 surface sediments TOC/TC(molar ratio/dry g) with water depth, Fe_R/ Fe_T (molar ratio/dry g) with water depth. Brown line shows the decrease in both two molar ratios up to 100m depth.

The oxygen and nitrate could be deficient for organic matter burial until this depth, so the Fe could be used in respiration.

Seyhan river is rich in production in water column and nutrients, also rich in organic carbon and nitrogen. Iron in sediments offshore from the mouth of Seyhan river comes from terrestrial with high correlation of iron to Al. Moreover, the seafloor is muddy, organic carbon and Fe correlates with the % mud.

ETS sediment parameters do not show clear trends in the region. The iron decreases towards the open seafloor, whereas Mn mobilizes to offshore. The interesting result in this transect is very high concentration of Mn in open sea sediments (500) m. Iron shows weak to moderate correlations with organic carbon and grain size.

In the Göksu and Aydıncık transects, the coastal to open biogeochemical discrimination is clearly seen. Total iron and reactive iron decreases with water depth. Vertical accumulation from the sediment and lateral transportation of Mn species towards the open seafloor is observed in these transects. Organic carbon and reactive iron has significant positive correlation (0.81) in Aydıncık transect.

CONCLUSION

The reactive iron in Cilician basin surface sediments is diversely distributed. Cilician Basin has high reactive iron concentration, but each sub-region has own distribution driven by local input (i.e. river input in Goksu-Aydıncık region). Fe_R has significant correlation with organic carbon in Aydıncık transect. Also, organic carbon and % mud show similar trends in the basin.

Highly coupled distributions of reactive iron, organic carbon and grain sizes show evidence for microbial Fe reduction in the 100 m - deep region.

The relative enrichment of reactive Mn in the basin is relatively higher than that of Fe. Reactive iron enrichment decreases with water depth whereas reactive Mn enrichment significantly increases with water depth.

Further studies need to be undertaken in the Basin to detect the redox zonation in the seafloor, reactive iron and organic carbon burial. The microbial communities in Cilician Basin and respiration pathways in the Basin are still completely unexplored. The biogeochemistry of seafloor in Cilician Basin needs to investigated due to its unique characteristic; for instance, the anthropogenic and terrigeneous organic carbon and metal oxide inputs to coastal sites can influence the oligotrophic offshore waters if these material can be transported offshore by wind-driven circulation or via channeling through submarine canyons, now known to be located offshore Göksu Delta. Therefore, the Aydıncık and Göksu transect location seem to be promising model sites to study the fate of river-derived iron and organic carbon across the shelf to the deep-sea.

REFERENCES

Achterberg, E.P., Holland,T.W., Bowie, A.R., Mantoura, R.F.C., Worsfold, P.J., 2001.Determination of iron in seawater, Analytica Chimica Acta, Volume 442, Issue 1,Pages 1-14, ISSN 0003-2670. doi:10.1016/j.gca.2006.05.018.

Akçay, I., 2015. Spatial Variations of Particulate Organic Matter(POM) Composition and Concentrations in Surface Waters and Sediments of the Mersin Bay. M.Sc. Thesis, Institute of Marine Sciences, Middle East Technical University, Mersin, Turkey, 122pp.

Aller RC and Blair NE (2006) Carbon remineralization in the Amazon-Guianas tropical mobile mudbelt: A sedimentary incinerator. Continental Shelf Research 26: 2241–2259.

Aslaner, M.,1973. Goelogy and Petrography of the Ophiolites in the İskenderun Bedforms in the Wave-current-dominated Nearshore Waters of Eastern Mersin Bay (Eastern Mediterranean). Marine Geology, 108,73-93.

Bodur, M.N. and Ergin, M., 1988. Heavy metal concentrations in recent inshore sediments from the Mersin Bay, Turkey, NE-Mediterranean. Rapp. Comm. İnt. Mer Medit., 31(2): 31.

Bodur,M.N., Ergin,M.,1994.Geochemical characteristics of the recent sediments from the

Sea of Marmara.Chem.Geol.,115,73-101.

Boyle, E.A., Edmond, J.M.,1977. Determination of copper, nickel, and cadmium in sea water by apdc chelate coprecipitation and flameless atomic absorption spectrometry. Analytica Chimica Acta, Vol 91, Iss 2, 189-197.

Boyle, E.A., Sclater, F.R. , Edmond; J.M., 1977. The distribution of dissolved copper in the Pacific. Earth and Planetary Science Letters, 37, 38-54.

Breitbarth, E., Achterberg, E. P., Ardelan, M. V., Baker, A. R., Bucciarelli, E., Chever, F., Croot, P. L., Duggen, S., Gledhill, M., Hassellöv, M., Hassler, C., Hoffmann, L. J., Hunter, K. A., Hutchins, D. A., Ingri, J., Jickells, T., Lohan, M. C., Nielsdóttir, M. C., Sarthou, G., Schoemann, V., Trapp, J. M., Turner, D. R., and Ye, Y.: Iron biogeochemistry across marine systems – progress from the past decade, Biogeosciences, 7, 1075-1097, doi:10.5194/bg-7-1075-2010, 2010.

Bruland, K.W. (1983). Trace elements in seawater. In: Chemical oceanography. Riley, J.P. and Chester, R. (Editors), Academic Press London, London. 8: 157-220.

Bruland, K.W., Rue, E.L., Smith, G.J., and DiTullio, G.R., 2005. Iron, macronutrients and diatom blooms in the Peru upwelling regime: brown and blue waters of Peru. Marine Chemistry, 93: 81-103.

Canfield, D.E., 1989. Reactive iron in marine sediments. Geochimica Cosmochimica Acta, 51: 619-632.

Canfield, D.E., Raiswell, R. and Botrell, S., 1992. The reactivity of sedimentary iron minerals towards sulfide. American Journal of Science, 292: 659-683.

Clough, J., P., A., Propato, M.,2016. Modeling the potential effects of sea-level rise on the coast of New York: Integrating mechanistic accretion and stochastic uncertainty, Environmental Modelling & Software, Volume 8, Pages 349-362, ISSN 1364-8152, http://dx.doi.org/10.1016/j.envsoft.2016.06.023.

Collins, M.B. and Banner, F.T. 1979. Secchi disc depths, suspensions and circulation, northeastern Mediterranean Sea. Marine Geology, 31,1-2, M39-M46.

Çağatay, N., Saltoğlu, T., Ged,k, A. 1987. Karadeniz'in Güncel Çökellerinin Jeokimyası(Geochemisrty of the Recent Black Sea Sediments). T.M.M.O.B. Jeol. Müh. Dergisi,30-31, 47-64 pp.

Çağatay, N., 2007. Marmara Denizi Çökel Jeokimyasal Atlası. TÜBİTAK Raporu, No: 103Y053,ITU-Doğu Akdeniz Deniz ve Göl Araştırma Merkezi, 81 pp.

Doğan-Sağlamtimur, N.2007.Seasonal variations of particulate and dissolved fractions of phosphorus and realted hyrdochemical parameters in the Northeastern Mediterranean shelf zone. Ph.D. Thesis, Institute of Marine Sciences, Middle East Technical University, Mersin, Turkey, 260pp.

Doğan-Sağlamtimur, N., Tuğrul, S. 2004. Effect of Riverine Nutrients on Coastal Water Ecosystems: A Case Study from the Northeastern Mediterrean Shelf. Fresenius Environmental Bulletin, 13, p.1288-1294.

Elrod, V. A., W. M. Berelson, K. H. Coale, and K. S. Johnson (2004), The flux of iron from continental shelf sediments: A missing source for global budgets, Geophys. Res. Lett., 31, L12307, doi:10.1029/2004GL020216.

Ediger, V., and Evans, G., 2007. Surficial sediments of the Cilicia Basin-Adan Basin(northeastern Mediterranean) and factors controlling deposition(submitted to Sedimentology in 2007).

Ergin, M., Bodur, M.N., Ediger, V., Yemenicioğlu, S., Okyar, M:, Kubilay, N., 1993. Sources and dispersal of heavy metals in surface sediments along the eastern Aegean shelf.Boll.Oceanol.Teor:App.,11(1):27-44.

Ergin, M., Kazan, B., Ediger, V., 1996. Source and Depositional Controls on Heavy Metal Distribution in Marine Sediments of the Gulf of İskenderun, Eastern Mediterranean.Marine Geology, 133, 223-239.

Fitzsimmons, J.N., et al., Partitioning of dissolved iron and iron isotopes into soluble and colloidal phases along the GA03 GEOTRACES North Atlantic Transect. Deep-Sea Res. II (2015), http://dx.doi.org/10.1016/j.dsr2.2014.11.014i.

Fitzsimmons, J. N., Conway, T. M., Lee, J.-M., Kayser, R., Thyng, K. M., John, S. G. and Boyle, E. A. (2016). Dissolved iron and iron isotopes in the Eastern South Pacific Ocean. Glob. Biogeochem. Cycles. 30 (10). 1372-1395.

Furuya, K., Harada, K., 1995. An automated precise Winkler titration for determining dissolved oxygen on board ship.Journal of Oceanography, 375-383, Vol 51, IS 3, 1573-868X. http://dx.doi.org/10.1007/BF02285173.

Gartman, A., Findlay, A.J., Luther III, G.W.,2014. Nanoparticulate pyrite and other nanoparticles are a widespread component of hydrothermal vent black smoker emissions, Chemical Geology, Volume 366, Pages 32-41, ISSN 0009-2541, http://dx.doi.org/10.1016/j.chemgeo.2013.12.013.

Gogou, A., Sanchez-Vidal, A., Durrieu de Madron, X., Stavrakakis, S., Calafat, A.M., Stabholz, M., Psarra, S., Canals, M., Heussner, S., Stavrakaki, I., Papathanassiou, E., 2014. Carbon flux to the deep in three open sites of the Southern European Seas (SES). J. Mar. Syst. 129, 224–233

Grasshoff, K., Kremling, K., and Ehrhardt, M.: Methods of seawater analysis, Verlag Chemie, Weinheim, 1983.

Guggenberger, G. & Kaiser, K. Dissolved organic matter in soil: challenging the paradigm of sorptive preservation. Geoderma 113, 293–310 (2003).

Haese, R., Schulz R., Horst D., Zabel, Matthias. The Biogeochemistry of Iron, Marine Geochemistry, Pages 241-270, Springer Berlin Heidelberg.

Haese, R.R., Schramm, J., Rutgers van der Loeff, M.M. and Schulz, H.D., 2000. A comparative study of iron and manganese diagenesis in continental slope and deep sea basin sediments off Uruguay (SW Atlantic). International Journal of Earth Sciences, 88: 619-629.

Henrichs SM and Reeburgh WS (1987) Anaerobic mineralization of marine sediment organic-matter-rates and role of anaerobic processes in the oceanic carbon economy. Geomicrobiology Journal 5: 191–237.

Hyacinthe, Christelle, Bonneville, Steeve, Van Cappellen, Philippe. Reactive iron (III) in sediments: chemical versus microbial extractions Geochimica et Cosmochimica Acta, Volume 70, Pages 4166-4180, 2006.

Homoky, William B. John, Seth G. Conway, Tim M. Mills, Rachel A.Distinct iron isotopic signatures and supply from marine sediment dissolution. Nature Communications, 2013/07/19/online, Vol 4, 2143. http://dx.doi.org/10.1038/ncomms3143.

Jensen HS, Mortensen PB, Anderson FO, Rasmussen E, Jensen A (1995).Phosphorus Cycling in a Coastal Marine Sediment, Aarhus Bay, Denmark. Limnol Oceanogr 40: 908–917.

Johnson, K. S., Gordon, R. M., and Coale, K. H. What controls dissolved iron concentrations in the world ocean? Mar. Chem. 57,1997,Pages 137–161. doi:10.1016/S0304-4203(97)00043-1

Jones, D. L. & Edwards, A. C. Influence of sorption on the biological utilization of two simple carbon substrates. Soil Biol. Biochem. 30, 1895–1902 (1998).

Kaiser, K., Guggenberger, G., 2000. The role of DOM sorption to mineral surfaces in the preservation of organic matter in soils. Org. Geochem. 31, 711–725.

Kleint, Charlotte; Hawkes, Jeffrey A; Sander, Sylvia G; Koschinsky, Andrea. Voltammetric investigation of hydrothermal iron speciation. Frontiers in Marine Science,2016, 3, 11 pp, doi:10.3389/fmars.2016.00075.

Kostka, J.E. and Luther, G.W. III, 1994. Partitioning and speciation of solid phase iron in saltmarsh sediments. Geochimica Cosmochimica Acta, 58: 1701-1710.

Kostka, J.E. and Nealson, K.H., 1995. Dissolution and reduction of magnetite by bacteria. Environmental Science and Technology, 29: 2535-2540.

Krom, M.D., Berner, R.A., 1980. Adsorption of phosphate in anoxic marine sediments. Limnology and Oceanography, 25: 797-806.

Lalonde K. , Mucci A., Ouellet A. , Gélinas Y.,2012. Preservation of organic matter in sediments promoted by iron. Nature, 483(7388): 198–200. Published online 2012 Mar 7. doi: 10.1038/nature10855.

Lam, P. J., and J. K. B. Bishop (2008), The continental margin is a key source of iron to the HNLC North Pacific Ocean, Geophys. Res. Lett., 35, L07608, doi:10.1029/2008GL033294.

Liu, X., and Millero, F. J. The solubility of iron in seawater. Mar. Chem. 77,2002, 43–54. doi: 10.1016/S0304-4203(01)00074-3.

Lovley, D.R., 1991. Dissimilatory Fe(III) and Mn(IV) reduction. Microbiological Reviews 55: 259-287.

Maldonado, M. T., and Price, N.M. Reduction and transport of organically bound iron by Thalassiosira Oceanica (Bacillariophyceae). J. Phycol. 37,2001, 298–310. doi: 10.1046/j.1529-8817.2001.037002298.x

Martin JH, Fitzwater SE (1988) Iron deficiency limits phytoplankton growth in the northeast Pacific subarctic. Nature 331:341-343.

Martin JH, Fitzwater SE, Gordon RM (1990a) Iron deficiency limits phytoplankton growth in Antarctic waters. Global Biogeochem Cycles 4: 5-12.

Mason, B., Moore C.B., 1982. Principles of Geochemistry. John Wiley&Sons, New York, 344 p.

Millot, C.: Circulation in the western mediterranean sea, Journal of Marine Systems, 20, 423–442, doi:10.1016/s0924- 7963(98)00078-5, 1999.

Mogollón, J. M., K. Mewes, and S. Kasten (2016), Quantifying manganese and nitrogen cycle coupling in manganese-rich, organic carbon-starved marine sediments: Examples from the Clarion-Clipperton fracture zone, Geophys. Res. Lett., 43, 7114–7123, doi:10.1002/2016GL069117.

Murray, J. W. (1979). Iron oxides. Marine minerals, 6, 47-98.

Niewenhuize, J., Maas, Y. E.M., Middleburg, J.J. 1994. Rapid Analysis od Organic Carbon and Nitrogen in Particulate Materials. Marine Chemistry, 45,217-224.

Özsoy, E., Sözer, A. Forecasting circulation in the Cilician Basin of the Levantine Sea. Ocean Sci. Discuss., 3, 1481–1514, 2006. www.ocean-sci-discuss.net/3/1481/2006/

Pinardi, N., Arneri, E., Crise, A., Ravaioli, M., Zavatarelli, M., 2004. The physical and ecological structure and varialability of shelf areas in the Mediterranean Sea. The Sea, Vol.14, Chapter 32.

Poulton S W, Raiswell R. Chemical and physical characteristics of iron oxides in riverine and glacial meltwater sediments. Chemical Geology 218(3):203-221 · May 2005. DOI: 10.1016/j.chemgeo.2005.01.007.

Poulton, SW; Raiswell, R; Raiswell, R (2005) Chemical and physical characteristics of iron oxides in riverine and glacial meltwater sediments, Chemical Geology, 218, pp.203-221. doi:10.1016/j.chemgeo.2005.01.007.

Poulton, S.W. and Raiswell, R., 2002, The lowtemperature geochemical cycle of iron: from continental fluxes to marine sediment deposition. American Journal of Science, 302: 774-805.

Poulton, S.W., Krom, M.D., and Raiswell, R., 2004. A revised scheme for the reactivity of iron (oxyhydr)oxide minerals towards dissolved sulfide. Geochimica Cosmochimica Acta, 68: 3703-3715.

Raiswell, R., Canfield D. E., 1998. Sources of iron for pyrite formation in marine sediments. Am J Sci , 298:219-245. doi: 10.2475/ajs.298.3.219.

Raiswell, R. and Canfield, D.E., 1996. Rates of reaction between silicate iron and dissolved sulfide in Peru Margin sediments. Geochimica Cosmochimica Acta, 60: 2777-2787.

Raiswell, R., Hawkings, J. R., Benning, L. G., Baker, A. R., Death, R., Albani, S., Mahowald, N., Krom, M. D., Poulton, S. W., Wadham, J., and Tranter, M.: Potentially bioavailable iron delivery by iceberg-hosted sediments and atmospheric dust to the polar oceans, Biogeosciences, 13, 3887-3900, doi:10.5194/bg-13-3887-2016, 2016.

Raiswell, R., Canfield, D.E. and Berner, R.A., 1994. A comparison of iron extraction methods for the determination of degree of pyritisation and the recognition of iron-limited pyrite formation. Chemical Geology, 111: 101-110.

Ramelow, G. J., Tugrul, S., Ozkan, M. A., Tuncel, G., Saydam, C., Balkas, T. I., 1978. The Determination Of Trace Metals In Marine Organisms By Atomic Absorption Spectrometry. International Journal Of Environmental Analytical Chemistry.

Roy,M., McManus, J., Goñi M A., Chase, Z., Borgeld,JZ:, Wheatcroft, R.A., Muratli, J.M.,Megowan, M.R., Mix, A. Reactive iron and manganese distributions in seabed sediments near small mountainous rivers off Oregon and California (USA), Continental Shelf Research, Volume 54, 15 February 2013, Pages 67-79, ISSN 0278-4343, http://dx.doi.org/10.1016/j.csr.2012.12.012.

Rude PD and Aller RC (1991) Fluorine mobility during early diagenesis of carbonate sediment-an indicator of mineral transformations. Geochimica et Cosmochimica Acta 55: 2491–2509.

Ruttenberg, K.C., 1992. Development of a sequential extraction method for different forms of phosphorous in marine sediments. Limnology and Oceanography, 37: 1460-1482.

Ruttenberg KC (2003) The Global Phosphorus Cycle, In: Turekian KK, Holland DJ, editors. Treatise on Geochemistry. Elsevier, 585–643.

Salvadó, J. A., Tesi, T., Andersson, A., Ingri, J., Dudarev, O. V., Semiletov, I. P., and Gustafsson, Ö. (2015), Organic carbon remobilized from thawingpermafrost is resequestered by reactive iron on the Eurasian Arctic Shelf, Geophys. Res. Lett., 42, 8122–8130, doi:10.1002/2015GL066058.

Scholz, F., Severmann, S., McManus, J., Hensen, C., 2014a. Beyond the Black Sea paradigm: the sedimentary fingerprint of an open-marine iron shuttle. Geochim. Cosmochim. Acta 127, 368 380.

Scholz, F., Severmann, S., McManus, J., Noffke, A., Lomnitz, U., Hensen, C., 2014b. On the isotope composition of reactive iron in marine sediments: redox shuttle versus early diagenesis. Chem. Geol. 389, 48–59.

Scholz,F., Severmann, S., McManus, J., Hensen, C. Beyond the Black Sea paradigm: The sedimentary fingerprint of an open-marine iron shuttle, Geochimica et Cosmochimica Acta, Volume 127, 15 February 2014, Pages 368-380, ISSN 0016-7037, http://dx.doi.org/10.1016/j.gca.2013.11.041.

Schmidt, C., S. Behrens, and A. Kappler, 2010, Ecosystemfunctioning from a geomicrobiological perspective—Aconceptual framework for biogeochemical iron cycling:Environmental chemistry,7, 399–405, doi:10.1071/EN10040.

Schulz, H. D., and Zabel, M.,2016, Marine Geochemistry, Springer Berlin.

Schwertmann, U. and Taylor, R.M., 1989. Iron oxides. In: Dinauer, R.C. (ed), Minerals in soil environments, Soil Science Society of America Book Series, 1, Madison, WI, pp. 379-438.

Sert, M.F. 2010. Determination of total nitrogen and total phosphorus in the northeastern Mediterranean water column. M.Sc. Thesis, Institute of Marine Sciences, Middle East Technical University, Mersin, Turkey, 110 pp(in Turkish).

Severmann, S., McManus, J., Berelson, W.M., Hammond, D.E., 2010. The continental shelf benthic iron flux and its isotope composition. Geochim. Cosmochim. Acta 74, 3984–4004.

Sevim, H.E., 1991. Umweltgeochemische und sedimentolog- ische Untersuchungen an Sedimenten der Fltisse Sakarya, Yesilirmak, Ceyhan und Menderes (TtirkeibGeogene/ anthropogene Einflnsse. Heidelb. Geowiss. Abh., 45, 162 pp.

Shaked Y, Lis H. (2012). Disassembling iron availability to phytoplankton. Front Microbiol 3: 1–26.

Shaw,H.F, and Bush, PR, 1978. The mineralogy and geochemistry of the recent surface sediments of the Cilicia Basin, northeastern Mediterranean. Marine Geology, 27, 115-136.

Shields, M. R., T. S. Bianchi, Y. Gélinas, M. A. Allison, and R. R. Twilley (2016), Enhanced terrestrial carbon preservation promoted by reactive iron in deltaic sediments, Geophys. Res. Lett., 43, 1149–1157, doi:10.1002/2015GL067388.

Sivan O, Adler M, Pearson A, Gelman F, Itay B-O, et al. (2011) Geochemical evidence for iron-mediated anaerobic oxidation of methane. Limnol Oceanogr 56: 1536–1544.

Slomp CP, Mort HP, Jilbert T, Reed DC, Gustafsson BG, et al.,2013. Coupled Dynamics of Iron and Phosphorus in Sediments of an Oligotrophic Coastal Basin and the Impact of Anaerobic Oxidation of Methane. PLoS ONE 8(4): e62386. doi:10.1371/journal.pone.0062386.

Slomp, C.P., Van der Gaast, S.J., Van Raaphorst, W., 1996a. Phosphorus binding by poorly crystalline iron oxides in North Sea sediments. Marine Chemistry, 52: 55-73.

Sunda WG, Huntsman SA. (1995). Iron uptake and growth limitation in oceanic and coastal phytoplankton. Mar Chem 50: 189–206.

Strickland JDH, Parsons TR, 1978, A practical handbook of seawater analysis. 2. ed., Ottawa, Canada, Fish. Res. Bd. Can. Bull., 311p.

Talas, E., Duman, M., Küçüksezgin, F.,. Brennan M.L, Nicole A. R. Sedimentology and geochemistry of mud volcanoes in the Anaximander Mountain Region from the Eastern Mediterranean Sea, Marine Pollution Bulletin, Volume 95, Issue 1, 15 June 2015, Pages 63-71, ISSN 0025-326X, http://dx.doi.org/10.1016/j.marpolbul.2015.04.042.

Taylor, S. R., and McLennan, S.M., 1985. The Continental Crust; Its composition and evolution; an examination of the geochemical record preserved in sedimentary rocks. Blackwell, Oxford. 312.

Taylor, S. R., and McLennan, S.M., 1995. The geochemical evolution of the continental crust. Reviews in Geophysics 33:241-265.

Toner B. M., German C. R., Dick G. J. and Breier J. A., 2016. Deciphering the Complex Chemistry of Deep-Ocean Particles Using Complementary Synchrotron X-ray Microscope and Microprobe Instruments. Chemical Research, 49 (1), 128-137. DOI: 10.1021/acs.accounts.5b00282.

Turekian, K.K., Wedepohl, K.H., 1961. Distribution of the Elements in Some Major Units of the Earth's Crust. Geol. Soc. Am. Bull. 72:175-192.

Turekian, K. K.: The fate of metals in the oceans, Geochim. Cosmochim. Acta, 41, 1139–1144, doi:10.1016/0016- 7037(77)90109-0, 1977.

Tunc, S.C. 2008. Geology and Geochemistry of Recent Sediments from the Northeastern Mediterranean Basin. M.Sc.Thesis, METU, Institute of Marine Sciences, Erdemli-İçel, TURKEY, 127 p.

Wagai, R. & Mayer, L. M. Sorptive stabilization of organic matter in soils by hydrous iron oxides. Geochim. Cosmochim. Acta 71, 25–35 (2007)

Wasmund, N., Topp, I., Schories D., 2006. Optimizing the storage and the extraction of chlorophlly samples. Oceanologia, 48(1), pp.125-144.,

Wedepohl, K.H., 1995. The Composition of Continental Crust. Geochimica et Cosmochimica Acta 59:1, 217-1, 239.

Wu, L.L., Couture, R.M., Li, W. Van Cappellen,P. 2015. Iron isotope fractionation in sediments of an oligotrophic freshwater lake, Earth and Planetary Science Letters, Volume 423, Pages 164-172, ISSN 0012-821X, http://dx.doi.org/10.1016/j.epsl.2015.05.010.

Yemenicioglu, S., and Tunc,S..Geology and Geochemistry of Recent Sediments from the Mediterranean Sea: Sediment Texture of Northeastern Mediterranean Basin. Open Journal of Geology, Vol. 3 No. 6, 2013, pp. 371-378. doi: 10.4236/ojg.2013.36042.

Yucel M, Gartman A, Chan CS, Luther GW. Hydrothermal vents as a kinetically stable source of iron-sulphide-bearing nanoparticles to the ocean, Nature Geoscience,Volume 4, 2011, Pages 367-371, ISSN 1752-0894, http://dx.doi.org/10.1038/ngeo1148.

Yılmaz,A., Tuğrul,S., Polat,Ç., Ediger,D., Çoban,Y., and Morkoç,E., On the production, elemental composition (C,N,P) and distribution of photosynthetic organic matter in the southern Black Sea. "Hydrobiologia", 363, (1998), p.141-156.

Yılmaz, A., Tuğrul, S.1998.The effect pf cold-and warm- core eddies on the distribution and stoichiometry of dissolved nutrients in the northeastern Mediterranean. Journal of Marine Systems, 16,253-268.

Yücesoy, F. 1991. Geochemistry of the Heavy Metals in the Surface Sediments from the Southern Black Sea Shlef and Upper Slope. M.Sc.Thesis, METU, Institute of Marine Sciences, Erdemli-İçel, TURKEY, 150 p.

Yücel, M., Konovalov, S. K., Moore T. S. , Janzen C. P., Luther III G.W. Sulfur speciation in the upper Black Sea sediments, Chemical Geology, Volume 269, Issues 3 4,30 January 2010, Pages 364-375, ISSN 0009-2541.

Yücel, M., Gartman, A., Chan, C. S. & Luther, G. W. Hydrothermal vents as a kinetically stable source of iron-sulphide-bearing nanoparticles to the ocean. Nature Geosci. 4, 367– 371 (2011).

Yücel M, Galand PE, Fagervold SK, Contreira-Pereira L, Le Bris N. Sulfide production and consumption in degrading wood in the marine environment. Chemosphere. 2013;90(2):403–9. doi: 10.1016/j.chemosphere.2012.07.036. pmid:22921659.